Universiteit
Leiden
The Netherlands

Therapeutic targeting of immune escaped cancers

Marijt, K.A.

Citation
Marijt, K. A. (2020, February 18). *Therapeutic targeting of immune escaped cancers*. Retrieved from https://hdl.handle.net/1887/85450

Version:	Publisher's Version
License:	Licence agreement concerning inclusion of doctoral thesis in the Institutional Repository of the University of Leiden
Downloaded from:	https://hdl.handle.net/1887/85450

Note: To cite this publication please use the final published version (if applicable).

Cover Page

Universiteit Leiden

The handle http://hdl.handle.net/1887/85450 holds various files of this Leiden University dissertation.

Author: Marijt, K.A.
Title: Therapeutic targeting of immune escaped cancers
Issue Date: 2020-02-18

Therapeutic targeting of immune escaped cancers

Koen Abraham Marijt

The research described in this thesis was performed at the department of medical oncology at the Leiden University Medical Center, the Netherlands. The work discribed in this thesis was funded by a grant of the Dutch Cancer Society (UL 2013-6142)

ISBN: 978-94-028-1919-9

Layout: Koen Marijt

Cover design: Koen Marijt

Thesis printing: Ipskamp printing

All rights reserved. Nothing from this thesis may be reproduced in any form without permission from the author.

Copyright 2020 Koen Marijt

Therapeutic targeting of immune escaped cancers

Proefschrift

ter verkrijging van

de graad van Doctor aan de Universiteit Leiden,

op gezag van Rector Magnificus prof.mr. C.J.J.M. Stolker,

volgens besluit van het College voor Promoties

te verdedigen op

dinsdag 18 februari 2020 klokke 16:15 uur

door

Koen Abraham Marijt

Geboren te Oegstgeest in 1986

Promotor:

Prof. Dr. Sjoerd van der Burg

Co-promotor:

Dr. Thorbald van Hall

Leden promotiecomissie:

Prof. Dr. Jacques (Sjaak) Neefjes (LUMC, Leiden, Nederland)

Prof. Dr. Tanja de Gruijl (Vrije Universiteit Amsterdam, Amsterdam, Nederland)

Dr. Fathia Mami-Chouaib (Institut Gustave Roussy, Villejuif, France)

Table of contents:

	Page:
CHAPTER 1	
General introduction	**7**
CHAPTER 2	
PD-L1 expression on malignant cells is no prerequisite for checkpoint therapy	**19**
CHAPTER 3	
Metabolic stress in cancer cells induces immune escape through an IFN-γ signaling blockade via PI3K pathway	**37**
CHAPTER 4	
TEIPP antigens for T-cell based immunotherapy of immune-edited HLA class I^{low} cancers	**65**
CHAPTER 5	
Identification of non-mutated neoantigens presented by TAP-deficient tumors	**85**
CHAPTER 6	
Dendritic cell vaccination therapy for immune escaped cancers	**117**
CHAPTER 7	
TEIPP peptides: exploration of unTAPped cancer antigens	**137**
CHAPTER 8	
General discussion	**145**
Appendices	
Nederlandse samenvatting	**160**
Dankwoord	**162**
Curriculum Vitae	**165**
List of Publications	**166**

Chapter 1

General introduction

Introduction

Effective immunotherapeutic strategies utilize the immune system of cancer patients to target and eradicate tumors[1,2]. Cancer associated- or cancer specific- antigens, including mutated neo-antigens, are presented in the context of MHC class I (MHC-I) at the surface of cancer cells and recognized by antigen-specific CD8 T cells[3,4]. Consequently, this recognition results in the stimulation of active T cells, to produce pro-inflammatory mediators and the release of cytotoxic granules aiming to kill the cancer cells and to eradicate the tumor[5,6]. However, cancer cells may acquire multiple resistance mechanisms to avoid recognition and killing by CD8 T cells[7,8]. This thesis evaluates how cancers avoid CD8 T cell mediated control, but more importantly, explores strategies to revert or overcome acquired resistance mechanisms which have led to the escape of these cancer cells.

CD8 T cell immunity in cancers

CD8 T cells have been described as the foot soldiers of the immune system in the war against cancer cells[9]. Increased numbers of tumor infiltrating CD8 T cells correlate with better clinical outcome in many cancers, including ovarian carcinoma and melanoma[9-11]. The CD8 T cells go through several developmental stages from thymocytes into mature CD8 T cells. Negative selection, or central tolerance, induces apoptosis of T cells with high affinity to "self" antigens, preventing the release of "self" reactive T cells into the circulation to avoid self-destruction. Premature T cells which have low affinity to "self" antigens, or do not recognize "self" antigens at all, escape central tolerance and enter the circulation as naïve T cells, until they are stimulated by professional antigen presenting cells to become activated and exert their function upon recognition of cells presenting its cognate antigen. T cells with low affinity to "self" antigens can get activated when tumors overexpress the antigen. However, peripheral tolerance for those so-called "shared antigens" is acknowledged as an important problem and limits the efficacy of immunotherapy. Immunotherapies utilizing CD8 T cells specific for "non-self" antigens therefore seem a more promising approach. Cancers with high mutational burden or cancers that have been established through infection with oncogenic viruses, like human papillomavirus or merkel cell virus, results in the presentation of many tumor-specific neoantigens and predicts for better clinical outcome[12,13]. Moreover, clinical efficacy after immune checkpoint blockade therapy is shown to be privileged toward cancers harboring mutation-derived neoantigens[14,15]. This implies that neoantigens specific T cells seem more potent for immunotherapies, and identification of tumor specific neoantigens is therefore a very important objective.

Immune checkpoints

Tight regulation of immune responses are critical for immune homeostasis and survival of the host. Uncontrolled immune responses towards pathogens and cancers can lead to tissue damage and auto-immune diseases. Therefore, immune responses are carefully regulated by stimulatory and inhibitory checkpoint molecules expressed by both immune- and antigen presenting- cells. Indeed, during cancer-associated chronic inflammation many inhibitory checkpoint molecules are upregulated on effector cells to dampen the immune response, stimulating cancer progression. In addition, inhibitory checkpoint molecules, like PD-L1, are concurrently expressed at high levels by cancer infiltrating myeloid cells, such as macrophages, neutrophils, and monocytes[16]. Many inhibitory checkpoint molecules are expressed on effector T cells, including CTLA-4, LAG-3, TIM-3, NKG2A and PD-1. Concomitantly, cancer cells also upregulate the ligands of these inhibitory checkpoint molecules like HLA-E and PD-L1/PD-L2 and bind to NKG2A and PD-1, respectively, to prevent immune activation. Blocking the inhibitory immune checkpoint "axis" using monoclonal antibodies have been very successful in the clinic in a selected group of patients[17,18]. Treatment with Pembrolizumab (anti-PD1) or Nivolumab (anti-PD1) have shown impressive overall response rates up to 57%, and progression free survival of 14.0 months in melanoma patients with high expression of PD-L1[19]. Of note, the amount of CD8 T cell infiltration and mutational load of the tumor is correlated to better efficacy of immune checkpoint blockade therapy, again underscoring the importance for CD8 T cells in this immunotherapeutic modality. Interestingly, PD-L1 negative melanomas had overall response rates of 41.3% with progression free survival of 5.3 months, indicating that blocking PD-L1 on cells other than cancer cells still had beneficial effects for the patients[20]. Understanding which subsets of cells are important to influence the delicate balance towards an active anti-tumor response is pivotal information for patient inclusion and treatment strategy.

T cell epitopes associated with impaired peptide processing

The presentation of antigens in MHC-I molecules depend on the processing of endogenous proteins into short peptides. Proteasomes chop proteins into small peptides which are translocated into the endoplasmic reticulum (ER) lumen through the transporter associated with antigen processing (TAP). TAP is a component of the peptide-loading complex (PLC). The PLC complex consists of beta-2 microglobulin (β2m), calreticulin, ERAAP, TAP, Erp57, tapasin, and MHC-I, and is of utmost importance for the stabilization and loading of empty MHC-I molecules with a peptide. After stable binding with a high affinity peptide, the peptide/MHC-I molecule is transported to the cell surface through the Golgi apparatus[21]. Limiting the supply of peptides transported from the cytosol into the ER lumen

by downregulating the peptide pump TAP strongly reduces the presentation of antigens in MHC-I molecules, and is often observed in cancer cells that escape immune recognition[22-25]. Interestingly, when cancer cells down modulate TAP, a novel subset of non-mutated neoantigens is allowed to be presented in MHC-I molecules. These antigens are called TEIPP (T cell epitopes associated with impaired peptide processing) and are exclusively presented by cancer cells with TAP-deficiency (reviewed in[26]). However, TAP-deficient cancer cells presenting TEIPP antigens usually have poor MHC-I presentation, limiting the endogenous immune responses. Therefore, to exploit TEIPP antigens for immunotherapy, TEIPP specific T cells need to be therapeutically stimulated to fully exploit their potential[27]. Elegant studies have shown the strength of TEIPP targeted immunotherapy in pre-clinical mouse studies[27,28]. A powerful strategy to target TEIPP in a clinical setting is by synthetic long peptide (SLP) vaccination[29] by which TEIPP peptides are administered, processed, and presented by host dendritic cells to induce TEIPP T cell immunity. However, since TEIPP antigens are TAP-independently processed by nature, feeding TAP-proficient host dendritic cells with TEIPP SLPs elongated with flanking sequences might not lead to efficient cross-presentation and consequent T cell activation. Therefore, an optimized dendritic cell vaccination strategy is necessary to fully exploit these tumor specific TEIPP antigens presented on MHC-I^{low} TAP-deficient cancers.

Interferon-gamma signaling pathway

Interferon gamma (IFNγ) is a pro-inflammatory cytokine and is critical for anti-tumor immunity[30-32]. It is the only member of the type II class of interferons[32], and is mainly secreted by NK cells, as well as type 1 CD4 T cells and CD8 T cells when they become activated. The IFNγ pathway is activated through binding of the cytokine with the heterodimic IFNγ receptor (IFNγR1/IFNγR2) and has many consequences for effector cells. Upon activation, phosphorylated JAKs induce the phosphorylation and nuclear translocation of STAT1, followed with binding to Interferon-gamma activated sequences (GAS). Consequently, transcription of many immunoregulatory genes are increased, including interferon regulatory factor-1 (Irf-1), Tap-1/2, and MHC-I[33]. Loss-of-function mutations in the IFNγ signaling pathway have all been associated with impaired therapeutic anti-tumor responses and reduced overall survival after checkpoint therapy. *In vivo* CRISPR-Cas9 studies identified PTPN2 as a negative modulator for the IFNγ signaling pathway by inducing dephosphorylation of STAT1 and JAK1. Additionally, many other genes have been discovered that negatively impact the sensitivity of cancer cells to respond to IFNγ in cancer cells and thereby inhibit the response to immunotherapy[34,35]. These studies underscore the essential role of this signaling pathway for immunotherapy[36-38]. Strategies to increase the responsiveness of cancer cells to IFNγ could lead to increased immunotherapeutic success.

Cancer metabolism and hypoxia

Cells depend on nutrients to sustain viability and to maintain their cellular functions. Two main pathways are involved in the generation of energy for the cell, namely glycolysis and oxidative phosphorylation (OXPHOS). Glucose is transported into the cell through the glucose transporter GLUT-1 where it is catabolized into pyruvate, a molecule important for feeding the TCA cycle. When ample oxygen is available, the metabolites produced in the TCA cycle are utilized in the electron chain transport complexes to generate energy. However, as tumors progress, oxygen becomes a limiting factor and cancer cells start to secrete angiogenic stimuli, including VEGF, to stimulate to growth of new blood vessel. In turn, the development of such highly disorganized vascular network in the tumor microenvironment limits the influx oxygen and ultimately results in severe hypoxia completely restricting OXPHOS metabolism in solid tumors.

Generating energy from glucose through glycolysis can occur without the use of oxygen, although much less efficiently. Interestingly, cancer cells often exploit glucose metabolism, even in the presence of oxygen. This is called the "Warburg effect". Although not exactly known why cancer cells utilize this inefficient energy pathway, data suggests that biomolecules generated when catabolizing glucose, supports the high proliferative capacity of cancer cells and thereby tumor progression. High glucose consumption rates and an inefficient vascular network, ultimately results in a tumor microenvironment which is deprived from both oxygen and glucose.

The harsh metabolic environment limits effector functions of many infiltrating immune cells that depend on glucose as their main source of energy. For example, studies have shown that "unused" GAPDH, as a result of glucose deprivation and inactive glycolysis metabolism, binds to the 3' UTR of the IFNy gene and thereby inhibits transcription of the inflammatory cytokine. In contrast, regulatory T cells survive much better in glucose deprived conditions as they can generate energy from fatty acid metabolism. These changes translate into a highly suppressive metabolic tumor microenvironment and is an important strategy how cancer cells can escape immune recognition.

Scope of this thesis

Great progress has been made in improving clinical responses with immunotherapy. However, it has also led to the increased awareness of the ability of cancer cells to acquire immune-escape mechanisms. It appears that the next challenge in immunotherapy could be the uncovering and understanding of secondary resistance mechanisms. This might result in novel immunotherapeutic strategies to overcome the discouraging results of immunotherapy on patients with immune escaped cancers.

The ligands for several inhibitory checkpoint molecules expressed by T cells can be constitutively or adaptively expressed by both tumor cells and myeloid cells. In **chapter 2**, we dissected the role of PD-L1 expression on either host stromal cells or cancer cells and their effects on clinical outcome during anti-PD-1 therapy in mouse tumor models. To summarize, we first showed that lack of PD-L1 expression on cancer cells greatly delayed cancer outgrowth compared to PD-L1 WT cancer cells. A cumulative anti-tumor effect was observed in mice harboring PD-L1 negative tumor cells and were treated with PD-L1 blocking therapy, suggesting that PD-L1 on host stromal cells contribute to the inhibition of tumor reactive T cells.

Studies have shown that metabolic alternations in the tumor microenvironment creates a harsh environment for immune cells to exert their anti-tumor functions. However, not much is known about how metabolic stress affects the immunogenicity of cancer cells. In **chapter 3** we explored the effects of nutrient deprivation on antigen presentation by cancer cells[39,40]. We found that oxygen- and glucose-deprivation strongly led to reduced MHC-I presentation and abrogated CD8 T cell recognition of cancer cells. Mechanistically, oxygen- and glucose-deprivation decreased the ability of cancer cells to respond to IFNy via increased PI3-kinase pathway signaling with the result that the cancer cells failed to activate the antigen processing pathway. Pharmacological inhibition of the PI3-kinase pathway resulted in restored MHC-I expression and improved CD8 T cell recognition.

In **chapter 4**, we review the current knowledge on the unique aspects of TEIPP cancer antigens, in order to set the stage for our efforts to exploit TEIPP antigen-based immunotherapy in patients. **Chapter 5** describes a hybrid forward-reversed immunological screen to identify human TEIPP antigens. In short, the human proteome was scrutinized for peptide sequences from proteins with high predicted HLA-I binding affinity and an ER-localization. This hit list was matched with a database of peptides which were exclusively eluted from human cancers but not healthy cells. For one lead candidate (p14), we isolated CD8 T cell clones specific for this antigen, which recognized various TAP-deficient cancers, including lymphomas, renal cell carcinomas, colon carcinomas, and melanomas but did not respond

to normal cells.

In **chapter 6**, we describe an approach to apply the SLP vaccination platform for the induction of TEIPP-specific T cells. We were able to induce TAP-dependent processing of the epitope without losing the specificity of the activated TEIPP T cells. This resulted in expansion of TEIPP-specific T cells and efficient immune responses towards TAP-deficient melanomas. An overview how TEIPP targeted immunotherapies may come in the clinic can be read in **chapter 7**.

Collectively, this thesis covers multiple topics about acquired immune resistance mechanisms by cancer cells and how we can counteract them. A general discussion on how therapeutic strategies targeting multiple aspects of these immune resistance mechanisms may lead to improved immunotherapies, can be read in **Chapter 8.**

References

1 Sanmamed, M. F. & Chen, L. A Paradigm Shift in Cancer Immunotherapy: From Enhancement to Normalization. *Cell* **175**, 313-326, doi:10.1016/j.cell.2018.09.035 (2018).

2 Galon, J. & Bruni, D. Approaches to treat immune hot, altered and cold tumours with combination immunotherapies. *Nat Rev Drug Discov* **18**, 197-218, doi:10.1038/s41573-018-0007-y (2019).

3 Verdegaal, E. M. *et al.* Neoantigen landscape dynamics during human melanoma-T cell interactions. *Nature* **536**, 91-95, doi:10.1038/nature18945 (2016).

4 Schumacher, T. N. & Schreiber, R. D. Neoantigens in cancer immunotherapy. *Science* **348**, 69-74, doi:10.1126/science.aaa4971 (2015).

5 Bhat, P., Leggatt, G., Waterhouse, N. & Frazer, I. H. Interferon-gamma derived from cytotoxic lymphocytes directly enhances their motility and cytotoxicity. *Cell Death Dis* **8**, e2836, doi:10.1038/cddis.2017.67 (2017).

6 Nakajima, C. *et al.* A role of interferon-gamma (IFN-gamma) in tumor immunity: T cells with the capacity to reject tumor cells are generated but fail to migrate to tumor sites in IFN-gamma-deficient mice. *Cancer Res* **61**, 3399-3405 (2001).

7 O'Donnell, J. S., Teng, M. W. L. & Smyth, M. J. Cancer immunoediting and resistance to T cell-based immunotherapy. *Nat Rev Clin Oncol* **16**, 151-167, doi:10.1038/s41571-018-0142-8 (2019).

8 Sharma, P., Hu-Lieskovan, S., Wargo, J. A. & Ribas, A. Primary, Adaptive, and Acquired Resistance to Cancer Immunotherapy. *Cell* **168**, 707-723, doi:10.1016/j.cell.2017.01.017 (2017).

9 Zhang, N. & Bevan, M. J. CD8(+) T cells: foot soldiers of the immune system. *Immunity* **35**, 161-168, doi:10.1016/j.immuni.2011.07.010 (2011).

10 Sato, E. *et al.* Intraepithelial CD8+ tumor-infiltrating lymphocytes and a high CD8+/regulatory T cell ratio are associated with favorable prognosis in ovarian cancer. *Proc Natl Acad Sci U S A* **102**, 18538-18543, doi:10.1073/pnas.0509182102 (2005).

11 Erdag, G. *et al.* Immunotype and immunohistologic characteristics of tumor-infiltrating immune cells are associated with clinical outcome in metastatic melanoma. *Cancer Res* **72**, 1070-1080, doi:10.1158/0008-5472.CAN-11-3218 (2012).

12 Samstein, R. M. *et al.* Tumor mutational load predicts survival after immunotherapy across multiple cancer types. *Nat Genet* **51**, 202-206, doi:10.1038/s41588-018-0312-8 (2019).

13 van der Burg, S. H., Arens, R., Ossendorp, F., van Hall, T. & Melief, C. J. Vaccines for established cancer: overcoming the challenges posed by immune evasion. *Nat Rev Cancer* **16**, 219-233, doi:10.1038/nrc.2016.16 (2016).

14 Gubin, M. M. *et al.* Checkpoint blockade cancer immunotherapy targets tumour-specific mutant antigens. *Nature* **515**, 577-581, doi:10.1038/nature13988 (2014).

15 Nghiem, P. T. *et al.* PD-1 Blockade with Pembrolizumab in Advanced Merkel-Cell Carcinoma. *N Engl J Med* **374**, 2542-2552, doi:10.1056/NEJMoa1603702 (2016).

16 Zhang, Y. *et al.* Myeloid cells are required for PD-1/PD-L1 checkpoint activation and the establishment of an immunosuppressive environment in pancreatic cancer. *Gut* **66**, 124-136, doi:10.1136/gutjnl-2016-312078 (2017).

17 Darvin, P., Toor, S. M., Sasidharan Nair, V. & Elkord, E. Immune checkpoint inhibitors: recent progress and potential biomarkers. *Exp Mol Med* **50**, 165, doi:10.1038/s12276-018-0191-1 (2018).

18 van Montfoort, N. *et al.* NKG2A Blockade Potentiates CD8 T Cell Immunity Induced by Cancer Vaccines. *Cell* **175**, 1744-1755 e1715, doi:10.1016/j.cell.2018.10.028 (2018).

19 Brahmer, J. *et al.* Nivolumab versus Docetaxel in Advanced Squamous-Cell Non-Small-Cell Lung Cancer. *N Engl J Med* **373**, 123-135, doi:10.1056/NEJMoa1504627 (2015).

20 Chen, Q., Li, T. & Yue, W. Drug response to PD-1/PD-L1 blockade: based on biomarkers. *Onco Targets Ther* **11**, 4673-4683, doi:10.2147/OTT.S168313 (2018).

21 Blum, J. S., Wearsch, P. A. & Cresswell, P. Pathways of antigen processing. *Annu Rev Immunol* **31**, 443-473, doi:10.1146/annurev-immunol-032712-095910 (2013).

22 Seliger, B. *et al.* Immune escape of melanoma: first evidence of structural alterations in two distinct components of the MHC class I antigen processing pathway. *Cancer Res* **61**, 8647-8650 (2001).

23 Agrawal, S., Reemtsma, K., Bagiella, E., Oluwole, S. F. & Braunstein, N. S. Role of TAP-1 and/or TAP-2 antigen presentation defects in tumorigenicity of mouse melanoma. *Cell Immunol* **228**, 130-137, doi:10.1016/j.cellimm.2004.04.006 (2004).

24 Ling, A. *et al.* TAP1 down-regulation elicits immune escape and poor prognosis in colorectal cancer. *Oncoimmunology* **6**, e1356143, doi:10.1080/2162402X.2017.1356143 (2017).

25 Meissner, M. *et al.* Defects in the human leukocyte antigen class I antigen processing machinery in head and neck squamous cell carcinoma: association with clinical outcome. *Clin Cancer Res* **11**, 2552-2560, doi:10.1158/1078-0432.CCR-04-2146 (2005).

26 Marijt, K. A., Doorduijn, E. M. & van Hall, T. TEIPP antigens for T-cell based immunotherapy of immune-edited HLA class I(low) cancers. *Mol Immunol*, doi:10.1016/j.molimm.2018.03.029 (2018).

27 Doorduijn, E. M. *et al.* T cells specific for a TAP-independent self-peptide remain naive in tumor-bearing mice and are fully exploitable for therapy. *Oncoimmunology* **7**, e1382793, doi:10.1080/2162402X.2017.1382793 (2018).

28 Doorduijn, E. M. *et al.* TAP-independent self-peptides enhance T cell recognition of immune-escaped tumors. *J Clin Invest* **126**, 784-794, doi:10.1172/JCI83671 (2016).

29 Melief, C. J. & van der Burg, S. H. Immunotherapy of established (pre)malignant disease by synthetic long peptide vaccines. *Nat Rev Cancer* **8**, 351-360, doi:10.1038/nrc2373 (2008).

30 Bach, E. A., Aguet, M. & Schreiber, R. D. The IFN gamma receptor: a paradigm for cytokine receptor signaling. *Annu Rev Immunol* **15**, 563-591, doi:10.1146/annurev.immunol.15.1.563 (1997).

31 Brodsky, F. M. & Guagliardi, L. E. The cell biology of antigen processing and presentation. *Annu Rev Immunol* **9**, 707-744, doi:10.1146/annurev.iy.09.040191.003423 (1991).

32 Schroder, K., Hertzog, P. J., Ravasi, T. & Hume, D. A. Interferon-gamma: an overview of signals, mechanisms and functions. *J Leukoc Biol* **75**, 163-189, doi:10.1189/jlb.0603252 (2004).

33 Murray, P. J. The JAK-STAT signaling pathway: input and output integration. *J Immunol* **178**, 2623-2629, doi:10.4049/jimmunol.178.5.2623 (2007).

34 Manguso, R. T. *et al.* In vivo CRISPR screening identifies Ptpn2 as a cancer immunotherapy target. *Nature* **547**, 413-418, doi:10.1038/nature23270 (2017).

35 Patel, S. J. *et al.* Identification of essential genes for cancer immunotherapy. *Nature* **548**, 537-542, doi:10.1038/nature23477 (2017).

36 Shin, D. S. *et al.* Primary Resistance to PD-1 Blockade Mediated by JAK1/2 Mutations. *Cancer Discov* **7**, 188-201, doi:10.1158/2159-8290.CD-16-1223 (2017).

37 Zaretsky, J. M. *et al.* Mutations Associated with Acquired Resistance to PD-1 Blockade in Melanoma. *N Engl J Med* **375**, 819-829, doi:10.1056/NEJMoa1604958 (2016).

38 Gao, J. *et al.* Loss of IFN-gamma Pathway Genes in Tumor Cells as a Mechanism of Resistance to Anti-CTLA-4 Therapy. *Cell* **167**, 397-404 e399, doi:10.1016/j.cell.2016.08.069 (2016).

39 Casciari, J. J., Sotirchos, S. V. & Sutherland, R. M. Variations in tumor cell growth rates and metabolism with oxygen concentration, glucose concentration, and extracellular pH. *J Cell Physiol* **151**, 386-394, doi:10.1002/jcp.1041510220 (1992).

40 Muz, B., de la Puente, P., Azab, F. & Azab, A. K. The role of hypoxia in cancer progression, angiogenesis, metastasis, and resistance to therapy. *Hypoxia (Auckl)* **3**, 83-92, doi:10.2147/HP.S93413 (2015).

Chapter 2

PD-L1 expression on malignant cells is no prerequisite for checkpoint therapy

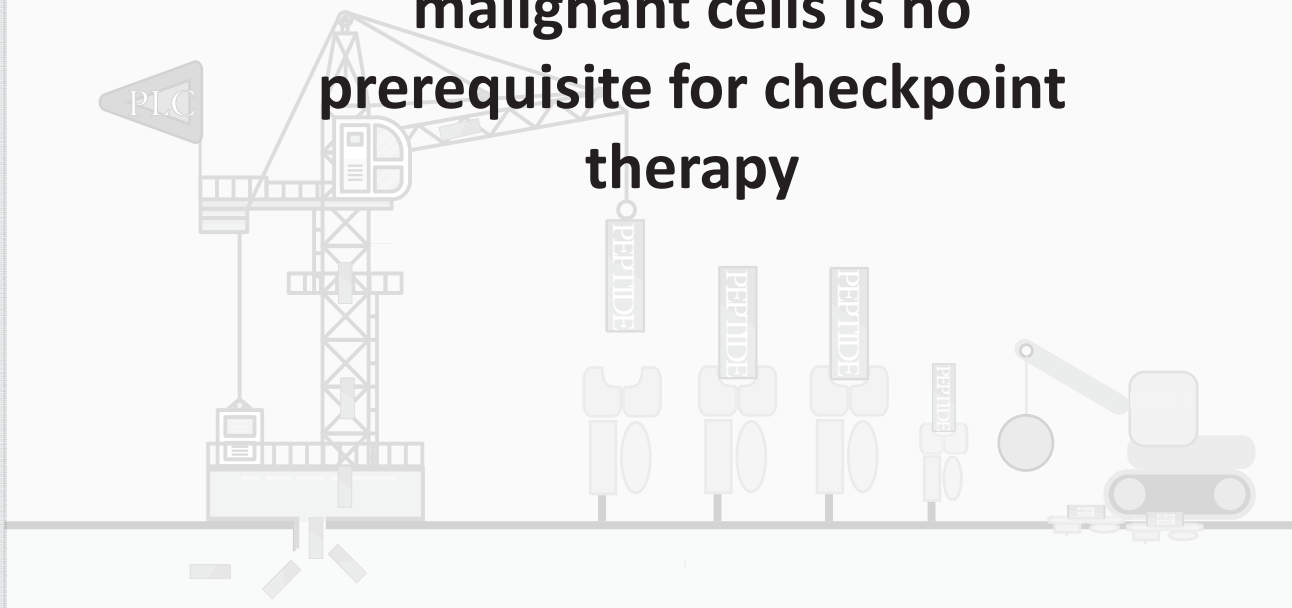

Kleinovink, J. W., ***K. A. Marijt,*** *M. J. A. Schoonderwoerd, T. van Hall, F. Ossendorp and M. F. Fransen*

Oncoimmunology 6(4): e1294299 (2017)

Abstract

Immunotherapy with PD-1/PD-L1 blocking antibodies is clinically effective for several tumor types, but the mechanism is not fully understood. PD-L1 expression on tumor biopsies is generally regarded as an inclusion criterion for this cancer therapy. Here, we describe the PD-L1 blocking therapeutic responses of preclinical tumors in which PD-L1 expression was removed from cancer cells, but not from immune infiltrate. Lack of PD-L1 expression on malignant cells delayed tumor outgrowth in a $CD8^+$ T cell-mediated fashion, showing the importance of this molecule in immune suppression. PD-L1 expression was evident on myeloid infiltrating cells in the microenvironment of these tumors and targeting stromal PD-L1 with blocking antibody therapy had additional anti-tumor effect, demonstrating that PD-L1 on both malignant cells and immune cells is involved in the mechanism of immunotherapeutic antibodies. Importantly, comparable results were obtained with PD-1 blocking therapy. These findings have implications for inclusion of cancer patients in PD-1/PD-L1 blockade immunotherapies.

Introduction

The co-inhibitory receptor PD-1 and its ligand PD-L1 form a well-known immune-inhibiting axis, and engagement of PD-1 on T cells is important for maintaining peripheral tolerance and preventing over-activation of the immune system. PD-L1 expression by tumors is a powerful escape mechanism through which tumors can evade control by T cell immunity.[1,2] The clinical relevance of this immunosuppressive pathway was emphasized by the clinical successes of PD-1 and PD-L1 checkpoint blockade therapies in a range of solid tumors.[3–6] Beneficial outcome of PD-1 and PD-L1 therapy has been correlated with mutational burden of the cancer cells, presence of tumor-infiltrating T cells and PD-L1 expression.[1,2,7,8] Tumor cells may upregulate PD-L1 to counteract immune attack in response to soluble mediators of T cell responses, including interferons and interleukins.[1,2] However, various types of cancer constitutively express PD-L1, either as a result of structural alterations in the regulatory 3' region of the PD-L1 gene,[9] or through activation of the STAT3 and AKT pathways, which are common features of cancer.[10,11]chimeric nucleophosmin (NPM Although several studies have investigated PD-1 and PD-L1 interactions within tumors, the exact cellular mechanisms are not completely elucidated.[1,2] PD-L1 can be expressed by malignant cells, but is also expressed on infiltrating cells within tumors, such as macrophages, neutrophils, endothelial cells and fibroblasts. Currently, arbitrary cut-off values for the percentage of overall PD-L1 staining in the total tumor area are used to classify tumor biopsies as positive or negative for PD-L1 expression. A recent study described a correlation between PD-L1 expression and an improved response to PD-L1 blockade in a clinical trial of multiple types of cancer patients, especially when expression was on tumor-infiltrating cells.[12] However, no convincing proof of the relative importance of tumor-expressed versus stromal-expressed PD-L1 to therapy response exists to date. For future use as a predictive biomarker for therapeutic responsiveness, it is essential to understand the relevance of the expression pattern of PD-L1 within the tumor area. To evaluate this topic, we made use of two mouse tumor models (MC38 and CT26) on two different genetic backgrounds in which the PD-L1 gene in the cancer cells was knocked out with CRISPR-Cas9 technology. We show here that PD-L1 expressed on cancerous cells is not exclusively responsible for the therapeutic effect of PD-1/PD-L1 checkpoint blockade and that PD-L1 on infiltrating (mostly myeloid) cells contributes significantly. Our data indicate that PD-L1 expression on malignant cells is not required for successful PD-1/PD-L1 blocking therapy, which has important clinical implications regarding patient inclusion strategies for immune checkpoint blockade.

Results and discussion

PD-L1 is expressed on tumor cells and immune infiltrating cells

PD-L1 expression was determined in MC38 and CT26 tumors, two widely used murine colon carcinoma models that are responsive to several types of immunotherapy including PD-L1 blockade, and are known to have a high mutational load leading to neo-antigen presentation.[13,14] After staining sections of excised MC38 and CT26 tumors with PD-L1 antibody, we observed heterogeneous PD-L1 expression throughout the tumor, with faint expression on some cells and strong expression on clusters of other cells (**Fig. 1a**). Several correlation studies have been done on PD-L1 expression and prognosis, however, many are fraught with practical problems including heterogeneous expression patterns and antibody variability.[15–17] Unlike the majority of clinical PD-L1 biomarker assays, one assay distinguishes expression on malignant cells versus tumor-infiltrating immune cells.[12] To dissect the role of PD-L1 expression on tumor versus non-tumor cells, we created PD-L1-deficient variants of MC38 and CT26 tumor cells using CRISPR-Cas9 technology. Complete PD-L1 knockdown was confirmed by flow cytometry after interferon-gamma (IFN-γ) stimulation *in vitro* (**Fig. 1b**). In order to specify which cells in MC38 and CT26 tumors express PD-L1, we inoculated mice with WT and PD-L1^{KO} tumor cells and analyzed the cell suspensions of excised tumors by flow cytometry. We determined that in WT tumors, PD-L1 expression was present on CD45-negative tumor cells, but also strongly on CD45+ immune infiltrate (**Fig. 1c**). PD-L1^{KO} tumors still contained this strong PD-L1 expression on CD45+ immune cells (**Fig. 1d**). A recent study in other mouse tumor models reported that PD-L1 deficiency affected tumor cell viability and proliferation.[18]but the basis for their effects remains unclear, leaving a gap in the understanding of how to rationally leverage therapeutic activity. PD-L1 is widely expressed in tumor cells, but its contributions to tumor pathogenicity are incompletely understood. In this study, we evaluated the hypothesis that PD-L1 exerts tumor cell-intrinsic signals that are critical for pathogenesis. Using RNAi methodology, we attenuated PD-L1 in the murine ovarian cell line ID8agg and the melanoma cell line B16 (termed PD-L1(lo However, the absence of PD-L1 on MC38 and CT26 tumor cells did not hamper *in vitro* proliferation (**Supplementary Fig. S1**).

PD-L1 on cancer cells suppresses CD8^{+} mediated immune control

In order to determine whether the lack of PD-L1 expression on tumor cells alters tumor growth characteristics in vivo, we injected immunocompetent mice with either WT or PD-L1^{KO} tumor cells. Although both WT and PD-L1^{KO} tumor cells formed established tumors within one week after inoculation, subsequent outgrowth of PD-L1^{KO} MC38 tumors was significantly slower compared to WT MC38 tumors (**Fig. 2a**). A similar delay in tumor out

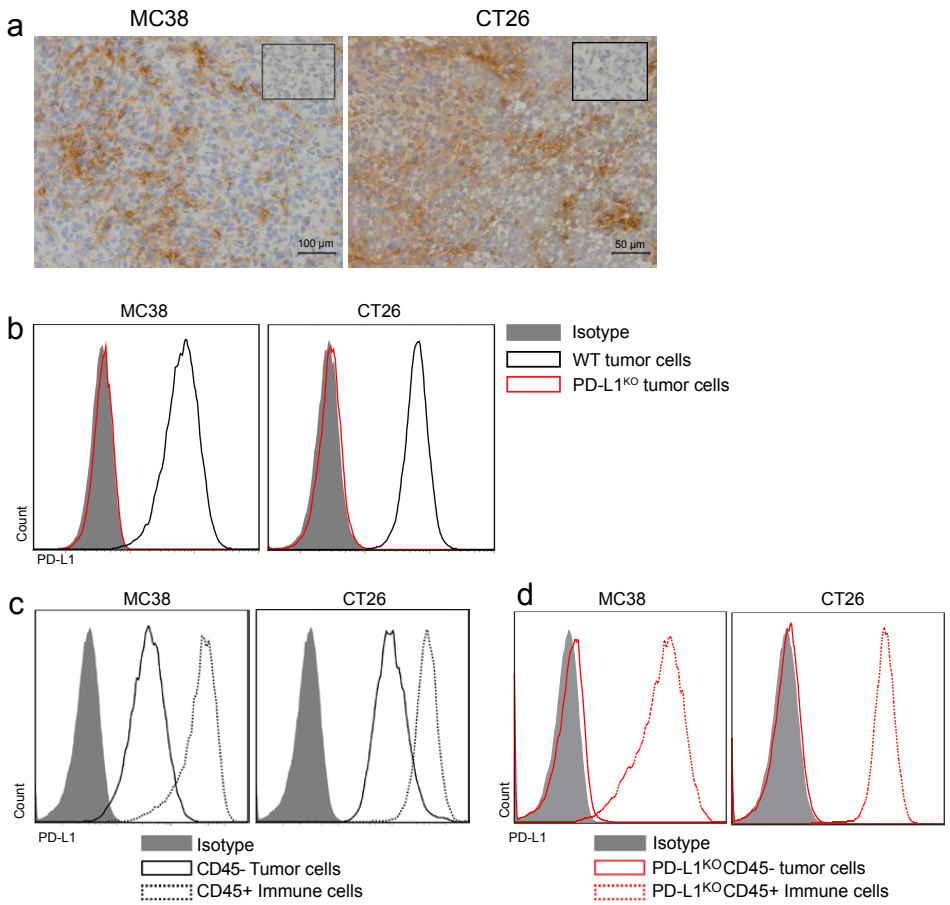

Figure 1. PD-L1 is expressed on tumor cells and infiltrating immune cells. (A) Immunohistochemistry for PD-L1 expression in MC38 (left) and CT26 (right) tumors. Cryosections of snap-frozen excised tumors were made 10 days after tumor inoculation and stained for PD-L1 expression (brown). Scale bars are provided in the bottom right corner. Insert shows control staining with secondary antibody only. Representative images of n=3 tumors. **(B)** Flow cytometry histograms showing PD-L1 expression of MC38 tumors cells (left plot) or CT26 tumor cells (right plot). WT tumor cells (black) or PD-L1^{KO} tumor cells (red) were incubated for 48h with IFN-γ and stained for PD-L1 expression (PE-conjugated antibody) for flow cytometry analysis, using isotype-PE stained cells (grey) as controls. **(C)** Flow cytometry histograms for PD-L1 expression (X-axis, PE-conjugated antibody) of excised MC38 (left) or CT26 (right) tumors. Both tumors express PD-L1 on both tumor cells (solid black line) and on tumor-infiltrating immune cells (dotted black line). **(D)** Flow cytometry histograms for PD-L1 expression of excised PD-L1^{KO} MC38 (left) or CT26 (right) tumors showing lack of PD-L1 expression on PD-L1^{KO} tumor cells (solid red line) compared to infiltrating immune cells from PD-L1^{KO} tumors retained high PD-L1 expression (dotted red line).

growth was observed for PD-L1^{KO} CT26 tumor cells versus WT CT26 cells after injection in immunocompetent BALB/c mice, albeit less pronounced than in the MC38 model (**Fig. 2b**). Our observation of identical growth rates in culture but delayed outgrowth of PD-L1^{KO} cells in mice suggested that the immune system inhibited growth of PD-L1^{KO} tumors. To test this, we treated mice bearing PD-L1 proficient or deficient MC38 tumors with CD4- or CD8-depleting antibodies and followed tumor outgrowth. Depletion of CD8^{+} T cells or depletion of both CD8^{+} and CD4^{+} T cells completely abrogated the delayed outgrowth of PD-L1^{KO} tumors, confirming our hypothesis on the tumor-eradicating effector function of cytotoxic T cells in this model (**Fig. 2c**). In contrast, depletion of only CD4^{+} T cells enhanced tumor clearance, suggesting that CD4 T cells in this model most likely represent regulatory T cells, as has been published in several settings (**Fig. 2c**).[1,2] These findings of T cell-dependent retardation of tumor outgrowth of PD-L1^{KO} cancer cells suggest active control by CD8^{+} T cells, which are inhibited by PD-L1 expressed on tumor cells.

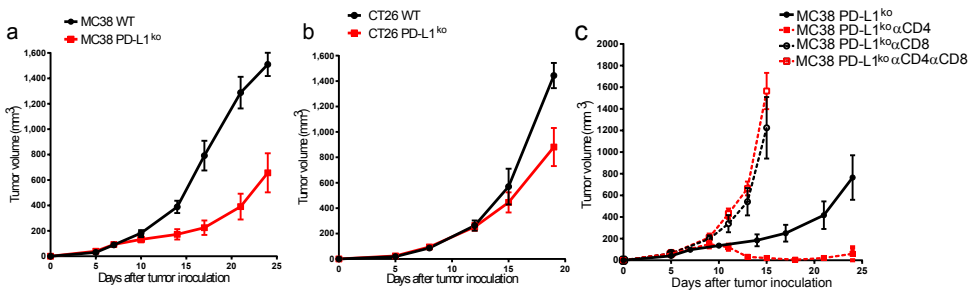

Figure 2. PD-L1 on cancer cells suppresses CD8^{+} T cell-mediated immune control. Tumor outgrowth curves of **(A)** MC38 and **(B)** CT26 tumors growing in B6 and BALB/c mice, respectively. Mice were inoculated with either WT tumor cells (black circles) or PD-L1^{KO} tumor cells (red squares) on day 0, and tumor volume was followed in time. The graphs show the group average tumor volume and contain pooled data from 3 independent experiments with 20-22 mice (MC38) or 2 independent experiments with 12-15 mice (CT26). Volumes of mice that had to be killed due to local ethical guidelines of maximal tolerated tumor size were afterwards counted as last measured volume. Line was stopped when more than 50% of mice in group had died due to tumor burden. By Student's T test, differences in WT versus PD-L1KO MC38 tumor volumes are statistically significant on day 14 ($p<0.01$) and days 17, 21 and 24 ($p<0.001$). Differences in WT versus PD-L1^{KO} CT26 tumor volumes are statistically significant on day 19 ($p<0.01$). **(C)** Tumor outgrowth curves of PD-L1^{KO} MC38 tumors either without treatment (solid black line), with CD4-depleting antibody (solid red line, closed squares), with CD8-depleting antibody (dotted black line, open circles) or with both CD4- and CD8-depleting antibodies (dotted red line, open squares). Tumors were inoculated on day 0, depleting antibodies were injected periodically from day 5 on, and tumor volume was followed in time. Volumes of mice that had to be killed due to local ethical guidelines of maximal tolerated tumor size were afterwards counted as last measured volume. Line was stopped when more than 50% of mice in group had died due to tumor burden. Differences in tumor volume compared to untreated PD-L1^{KO} MC38 tumors are statistically significant ($p<0.05$, Student's T test) for αCD4 treatment on days 13 through 25 (all $p<0.01$), for αCD8 treatment on days 13 ($p<0.05$) and 15 ($p<0.01$), and for αCD4+ αCD8 treatment on days 11, 13 and 15 (all $p<0.001$).

Tumor microenvironment is not altered by PD-L1 deficiency of cancer cells

We observed high levels of PD-L1 expression on immune cells in WT tumors, which may further contribute to the $CD8^+$ T cell mediated control of tumor outgrowth (**Fig. 1b).** It has recently been published that tumor-infiltrating T cells can have a profound effect on the myeloid composition of the tumor microenvironment.[19,20]metastasis formation, and suppression of Th1-type immune responses. Here, we show that successful treatment of cervical carcinoma in mouse models with synthetic long peptide (SLP Therefore, we analyzed the immune infiltrate composition in WT versus PD-$L1^{KO}$ tumors in the MC38 and CT26 model. Surprisingly, no significant quantitative differences in T cell infiltrate of WT versus PD-$L1^{KO}$ tumors were found (**Fig. 3a**). Furthermore, total $CD11b^+$ myeloid infiltrate was not altered, nor were the $Ly6C^+$ and $Ly6C^-$ macrophages and neutrophils. Moreover, PD-L1 expression levels on tumor-infiltrating myeloid cells were not significantly altered by the lack of PD-L1 expression on the malignant cells in either tumor model (**Fig. 3b**). These results indicate that the composition of the myeloid immune infiltrate is not strongly influenced by PD-L1 expression on the malignant cells.

PD-L1 blockade is still effective against PD-$L1^{KO}$ tumors

To test whether the therapeutic efficacy of PD-L1 blockade is solely based on alleviating immune suppression by PD-L1 expression on cancer cells, we examine treatment efficacy with PD-L1 blocking antibody in mice carrying WT or PD-$L1^{KO}$ tumors. Remarkably, outgrowth of PD-$L1^{KO}$ MC38 tumors was even further decreased by therapeutic PD-L1 blockade, leading to complete eradication of most tumors and long-term survival of nearly 90% of animals (**Fig. 4a and Supplementary Fig. S2** for individual tumor growth curves). A less striking but similar additional effect of PD-L1 blockade in PD-$L1^{KO}$ tumors was found in the CT26 model (**Fig. 4b and Supplementary Fig. S3** for individual tumor growth curves). These data indicate that PD-L1 expression on non-tumor cells also contribute to immune evasion and thereby tumor outgrowth. Depletion of $CD8^+$ T cells during PD-L1 blockade of PD-$L1^{KO}$ MC38 tumors returned tumor growth rates to the level of untreated WT tumors, showing that non-tumor cell expression of PD-L1 contributes to the inhibition of effector $CD8^+$ T cell responses (**Fig. 4c**). A similar effect was observed with therapy with a different PD-L1 blocking antibody clone (data not shown). To test whether the absence of PD-L1 on cancer cells also influenced the therapeutic efficacy of PD-1 blockade, we treated mice bearing WT or PD-$L1^{KO}$ MC38 tumors with PD-1 blocking antibody. Again, there was an additional strong treatment effect by PD-1 blockade of PD-$L1^{KO}$ tumors, showing that the treatment effect was effectively mediated through blocking the inhibiting PD-1/PD-L1 interactions on non-tumor cells (**Fig. 4d**).

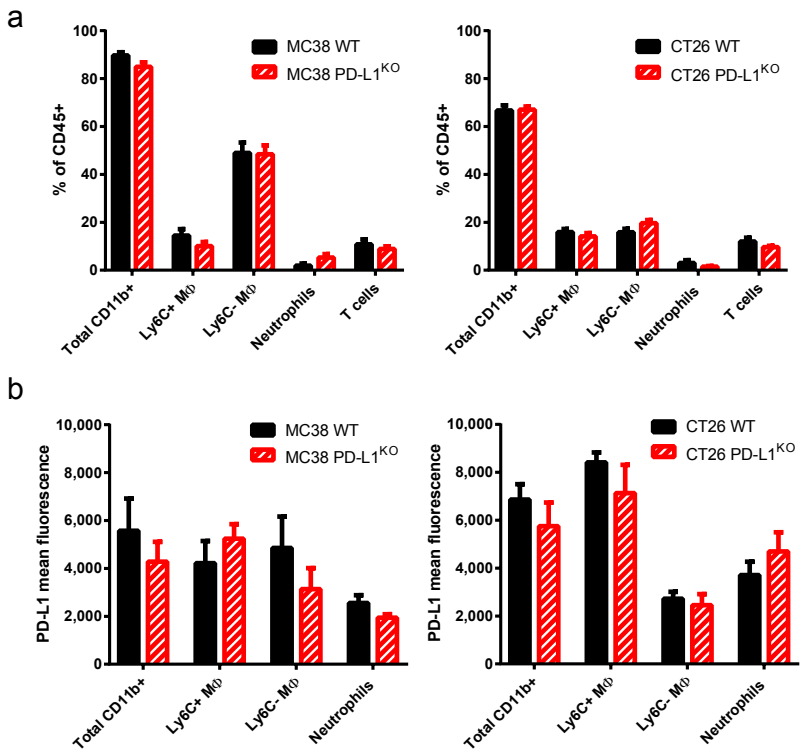

Figure 3. Tumor microenvironment is not altered by PD-L1 deficiency of cancer cells. (A) Bargraphs showing the percentages of immune cell subsets infiltrating MC38 tumors (left) or CT26 tumors (right) comparing WT tumors (black bars) with PD-L1^{KO} tumors (red bars). Established tumors were excised and processed for flow cytometry analysis, using 7-AAD to exclude dead cells. Gating strategies are as follows; Total CD11b = CD45$^+$ CD11b$^+$ cells; Ly6C+ MΦ = CD45$^+$ CD11b$^+$ F4-80$^+$ Ly6G$^-$ Ly6C$^+$; Ly6C- MΦ = CD45$^+$ CD11b$^+$ F4-80$^+$ Ly6G$^-$ Ly6C$^-$; Neutrophils = CD45$^+$ CD11b$^+$ Ly6G$^+$ and T cells: CD45$^+$ CD11b$^-$ CD3$^-$. None of the differences are statistically significant. **(B)** Bargraphs showing the geometric mean fluorescence for PD-L1 expression (PE-conjugated antibody) on the myeloid immune subsets described in (A). None of the differences are statistically significant according to the Student's T test.

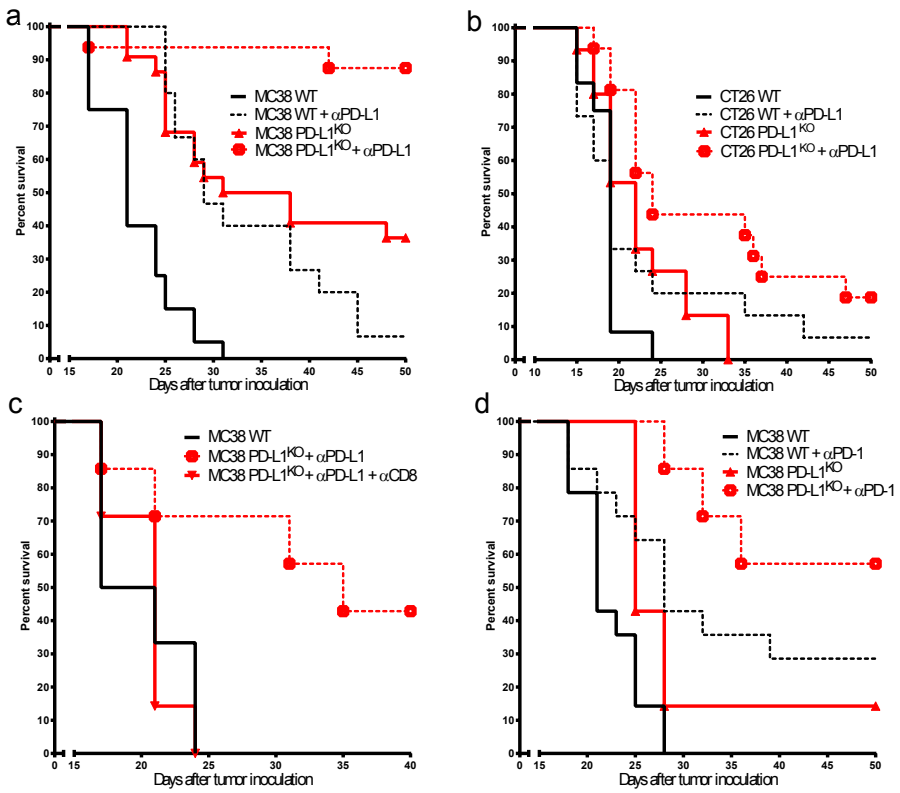

Figure 4. PD-L1 blockade is still effective against PD-L1^{KO} tumors. Survival curves of mice bearing **(A)** MC38 or **(B)** CT26 tumors either left untreated (solid lines) or treated with PD-L1 blocking antibody (dotted lines), comparing WT tumors (black lines) to PD-L1^{KO} tumors (red lines). Antibodies were given on days 5, 8 and 11. For both tumor models, tumor outgrowth curves of individual mice are provided in Supplemental Figures 2 and 3. In both tumor models, Log-rank analysis shows statistically significant differences ($p<0.05$) between survival of each group compared to the others. **(C)** Survival curves of B6 mice bearing untreated WT MC38 tumors (solid black line), αPD-L1 treated PD-L1^{KO} MC38 tumors (dotted red line), or αPD-L1 treated PD-L1^{KO} MC38 tumors with CD8 depletion (solid red line). The effect of CD8 depletion on the survival of αPD-L1 treated PD-L1^{KO} MC38 tumor bearing mice is statistically significant ($p<0.05$) using the Log-rank test. **(D)** Survival curves of B6 mice bearing WT (black lines) or PD-L1^{KO} (red lines) MC38 tumors, either left untreated (solid lines) or treated with PD-1 blocking antibody on days 5, 8 and 11 (dotted lines). Log-rank analysis shows statistically significant ($p<0.05$) differences in survival between untreated and PD-1 blockade treated mice for both WT and PD-L1^{KO} tumors. In all graphs, survival refers to the time before reaching the maximally allowed tumor volume of 2000 mm^3.

In parallel with a recently published study by Noguchi *et al*,[21] our findings concur with the clinical study by Herbst *et al*.,[12] which describes that patients with PD-L1 expression on tumor cells and/or immune infiltrate have a more favorable outcome of therapeutic PD-L1 blockade. Our experimental models provide a mechanistic basis underlying these clinical observations, by showing that PD-L1 expression on both tumor cells and on tumor-infiltrating immune cells inhibits $CD8^+$ T cell responses against the tumor. Complete responses were found in many, but not all animals. This can probably be explained by the fact that PD-1/PD-L1 is only one of several immune-inhibiting mechanisms. PD-1 also binds to PD-L2, but its expression is less pronounced than PD-L1 expression.[22] Several other compensatory interactions, such as upregulation of LAG3, TIM-3 and other immune checkpoint molecules have been found in tumors, indicating the diversity and flexibility of the tumor-immune cell interactions.[1] Therefore, combinatorial therapies with immune-modulating antibodies, based on multiple molecular interactions within the tumors, have more potential.[1,2] Nonetheless, the great efficacy of PD-1/PD-L1 axis blockade as monotherapy in curing mice from aggressive tumors indicates a dominant role. Altogether, our work shows that malignant cells and tumor-infiltrating immune cells jointly suppress $CD8^+$ T cell responses by PD-L1 expression, and that tumors lacking PD-L1 expression on malignant cells can be efficiently treated by PD-1/PD-L1 axis blockade therapy.

Material and methods

Mice and cell lines

C57BL/6 mice were obtained from Harlan Laboratories - ENVIGO (The Netherlands) and BALB/c mice were purchased from Charles River (France) and housed under specified pathogen-free conditions in animal facilities of the Leiden University Medical Center. All animal experimentations were approved by and according to guidelines of the Dutch Animal Ethical committee. MC38 and CT26 cells (kindly provided by Mario Colombo) were cultured in IMDM medium (Lonza) containing 8% Fetal Calf Serum (Greiner), 100 IU/mL penicillin/streptomycin (Gibco), 2 mM glutamin (Gibco) and 25 µM 2-mercaptoethanol. Cell lines were mycoplasma and MAP-tested before the start of experiments.

Tumor inoculation and Immunohistochemistry

Tumors were inoculated by subcutaneous injection in the right flank of 500,000 MC38 cells or 100,000 CT26 cells in 100 µL PBS. Tumor outgrowth was measured by caliper in three dimensions, until mice had to be sacrificed due to tumor burden, according to local ethical guidelines. For immunohistochemistry, established tumors were excised on day 10 and 5 µm frozen sections were fixed using ice-cold acetone and blocked in 0.3% hydrogen

peroxidase (MERCK) in methanol. Next, slides were stained for PD-L1 (clone 10F.9G2, BioLegend), secondary biotin-conjugated rabbit anti-rat IgG (Boster Biological Technology) and Vectastain complex (Vector labs). Color was developed using DAB+ reagent (DAKO) and nuclei were counterstained with Myers Haematoxylin (Merck). Slides were mounted using Entellan (Merck). Photos were taken using an Olympus DX51 light microscope and Olympus cellSens software.

CRISPR/Cas9

For CRISPR/Cas9-knockout of PD-L1, an online CRISPR Design Tool (crispr.mit.edu) was used to design two gRNA sequences for exon 1 of the mouse *cd274* gene encoding the PD-L1 protein (gRNA #1 = GTATGGCAGCAACGTCACGA, gRNA #2 = GCTTGCGTTAGTGGTGTACT) and each gRNA was cloned into a gRNA cloning vector (Addgene 41824). Next, MC38 or CT26 tumor cells were transfected with these two gRNA plasmids (2 µg/plasmid) and with Cas9 WT (Addgene 41815), using the Lipofectamine 2000 protocol (ThermoFisher). Cells were then stimulated for 48h with 20 IU/mL interferon-gamma to upregulate PD-L1 on WT cells and stained with PE-labeled PD-L1 antibody for FACS-sorting of PD-L1^{KO} cells.

In vitro proliferation assay

3,000 cells of each tumor cell line were seeded, and after 24, 48 or 72 hours cells were pulsed with 1 µM ^{3}H and analyzed 15 hours later.

Treatments

Tumor-bearing mice were treated on day 5, 8 and 11 after tumor inoculation by intraperitoneal injection of 200 µg PD-L1 blocking antibody (clone 10F.9G2, BioXCell) or peritumoral subcutaneous injection of 50 µg PD-1 blocking antibody (clone RMP1-14, BioXCell). T cells were depleted by intraperitoneal injection of 50 µg depleting antibody (clone 2.43 for CD8, clone GK1.5 for CD4, both in-house production) on day 5 after tumor inoculation. Complete depletion was confirmed on the following day in peripheral blood by flow cytometry, and mice were screened periodically and re-injected when T cell populations started returning in peripheral blood.

Flow cytometry

Cell surface staining was performed using the following antibodies: CD8α (clone 53-6.7), CD4 (clone L3T4), CD3ε (clone 145-2c11), CD11b (clone M1/70), F4-80 (clone BM8), CD45.2 (clone 104), Ly6G (clone 1A8), Ly6C (clone HK1.4), PD-L1 (clone MIH5). For analysis of the tumor microenvironment, tumor-bearing mice were sacrificed, and perfused with 20 mL of PBS/EDTA (2 mM) to eliminate blood contamination of tumor material. Tumors were

cut into small pieces with scalpels, incubated with 2.5 mg/mL Liberase TL (Roche) for 20 minutes at 37°C and single-cell suspensions were made using 70-µm cell strainers (BD Biosciences). Fc-Receptors were blocked with 10% normal mouse serum before antibody staining. dead cells were excluded based on 7-AAD (Invitrogen). Samples were analyzed with LSRII cytometer (BD) using FacsDIVA software (BD) and FlowJo software (Tree Star).

Statistical analysis

GraphPad Prism 7 software was used for all statistical analyses. The means of two groups were compared using the Student's T test, and survival differences in Kaplan-Meier curves were analyzed by Log-rank test. Differences were considered statistically significant at $p<0.05$.

Acknowledgements

The authors would like to thank Eveline S. M. de Jonge-Muller for technical assistance and the Animal Facility of the LUMC for excellent care.

References

1. Baumeister, S. H., Freeman, G. J., Dranoff, G. & Sharpe, A. H. Coinhibitory Pathways in Immunotherapy for Cancer. *Annu. Rev. Immunol.* **34,** 539–573 (2016).

2. Zou, W., Wolchok, J. D. & Chen, L. PD-L1 (B7-H1) and PD-1 pathway blockade for cancer therapy: Mechanisms, response biomarkers, and combinations. *Sci. Transl. Med.* **8,** 328rv4-328rv4 (2016).

3. Postow, M. A., Callahan, M. K. & Wolchok, J. D. Immune Checkpoint Blockade in Cancer Therapy. *J. Clin. Oncol.* **33,** 1974–1982 (2015).

4. Fehrenbacher, L. *et al.* Atezolizumab versus docetaxel for patients with previously treated non-small-cell lung cancer (POPLAR): a multicentre, open-label, phase 2 randomised controlled trial. *Lancet* **387,** 1837–1846 (2016).

5. Rosenberg, J. E. *et al.* Atezolizumab in patients with locally advanced and metastatic urothelial carcinoma who have progressed following treatment with platinum-based chemotherapy: a single-arm, multicentre, phase 2 trial. *Lancet* **387,** 1909–1920 (2016).

6. Zitvogel, L. & Kroemer, G. Targeting PD-1/PD-L1 interactions for cancer immunotherapy. *Oncoimmunology* **1,** 1223 (2012).

7. Gubin, M. M. *et al.* Checkpoint blockade cancer immunotherapy targets tumour-specific mutant antigens. *Nature* **515,** 577–581 (2014).

8. Taube, J. M. *et al.* Colocalization of Inflammatory Response with B7-H1 Expression in Human Melanocytic Lesions Supports an Adaptive Resistance Mechanism of Immune Escape. *Sci. Transl. Med.* **4,** 127ra37-127ra37 (2012).

9. Kataoka, K. *et al.* Aberrant PD-L1 expression through 3'-UTR disruption in multiple cancers. *Nature* **534,** 402–406 (2016).

10. Marzec, M. *et al.* Oncogenic kinase NPM/ALK induces through STAT3 expression of immunosuppressive protein CD274 (PD-L1, B7-H1). *Proc. Natl. Acad. Sci.* **105,** 20852–20857 (2008).

11. Parsa, A. T. *et al.* Loss of tumor suppressor PTEN function increases B7-H1 expression and immunoresistance in glioma. *Nat. Med.* **13,** 84–88 (2007).

12. Herbst, R. S. *et al.* Predictive correlates of response to the anti-PD-L1 antibody MPDL3280A in cancer patients. *Nature* **515,** 563–567 (2014).

13. Yadav, M. *et al.* Predicting immunogenic tumour mutations by combining mass spectrometry and exome sequencing. *Nature* **515,** 572–576 (2014).

14. Castle, J. C. *et al.* Immunomic, genomic and transcriptomic characterization of CT26 colorectal carcinoma. *BMC Genomics* **15,** 190 (2014).

15. Mahoney, K. M. *et al.* PD-L1 Antibodies to Its Cytoplasmic Domain Most Clearly Delineate Cell Membranes in Immunohistochemical Staining of Tumor Cells. *Cancer Immunol. Res.* **3,** (2015).

16. Ilie, M. *et al.* Comparative study of the PD-L1 status between surgically resected specimens and matched biopsies of NSCLC patients reveal major discordances: a potential issue for anti-PD-L1 therapeutic strategies. *Ann. Oncol.* **27,** 147–153 (2016).

17. Schats, K. A. *et al.* Validated programmed cell death ligand 1 immunohistochemistry assays (E1L3N and SP142) reveal similar immune cell staining patterns in melanoma when using the same sensitive detection system. *Histopathology* **70,** 253–263 (2017).

18. Clark, C. A. *et al.* Tumor-Intrinsic PD-L1 Signals Regulate Cell Growth, Pathogenesis, and Autophagy in Ovarian Cancer and Melanoma. *Cancer Res.* **76,** 6964–6974 (2016).

19. van der Sluis, T. C. *et al.* Therapeutic Peptide Vaccine-Induced CD8 T Cells Strongly Modulate Intratumoral Macrophages Required for Tumor Regression. *Cancer Immunol. Res.* **3,** 1042–1051 (2015).

20. Marigo, I. *et al.* T Cell Cancer Therapy Requires CD40-CD40L Activation of Tumor Necrosis Factor and Inducible Nitric-Oxide-Synthase-Producing Dendritic Cells. *Cancer Cell* **30,** 377–390 (2016).

21. Noguchi, T. *et al.* Temporally Distinct PD-L1 Expression by Tumor and Host Cells Contributes to Immune Escape. *Cancer Immunol. Res.* **5,** (2017).

22. Latchman, Y. *et al.* PD-L2 is a second ligand for PD-1 and inhibits T cell activation. *Nat. Immunol.* **2,** 261–268 (2001).

Supplementary figures

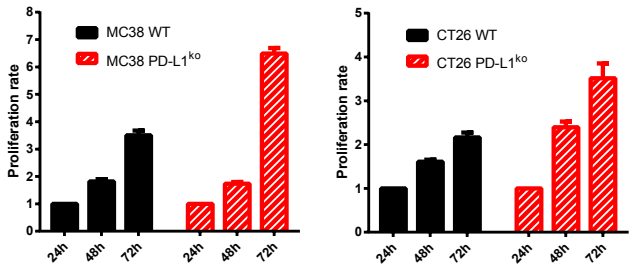

Supplementary Figure S1. In vitro proliferation plots of MC38 (left) and CT26 (right) tumor cells, either WT (black) or PD-L1^{KO} (red), based on the 3H incorporation assay. Cells were seeded and pulsed with ^{3}H at 24, 48 or 72 hours and analyzed 15h later.

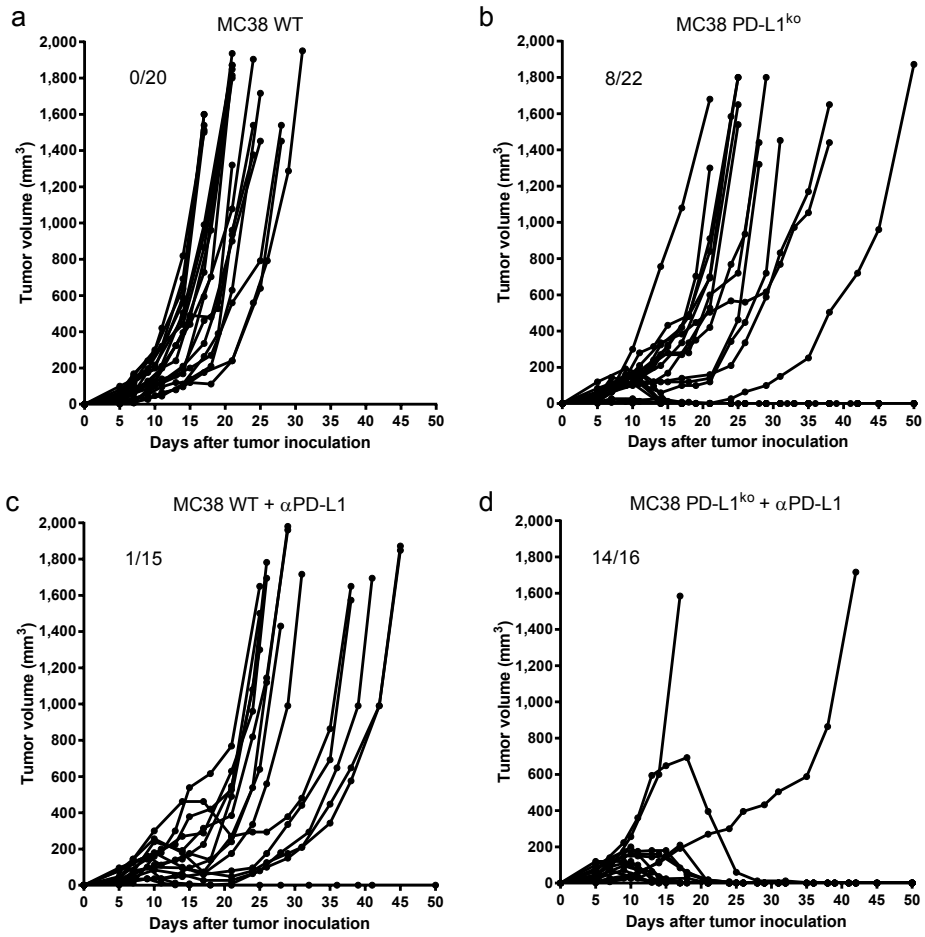

Supplementary Figure S2. MC38 tumor outgrowth curves of individual B6 mice bearing **(A)** untreated WT tumors, **(B)** untreated PD-L1^{KO} tumors, **(C)** WT tumors treated with PD-L1 blockade or **(D)** PD-L1^{KO} tumors treated with PD-L1 blockade. Graphs correspond to survival curves in Figure 4A. Each line represents the tumor of an individual mouse. The fraction of mice that fully cleared the tumor is indicated in the graph.

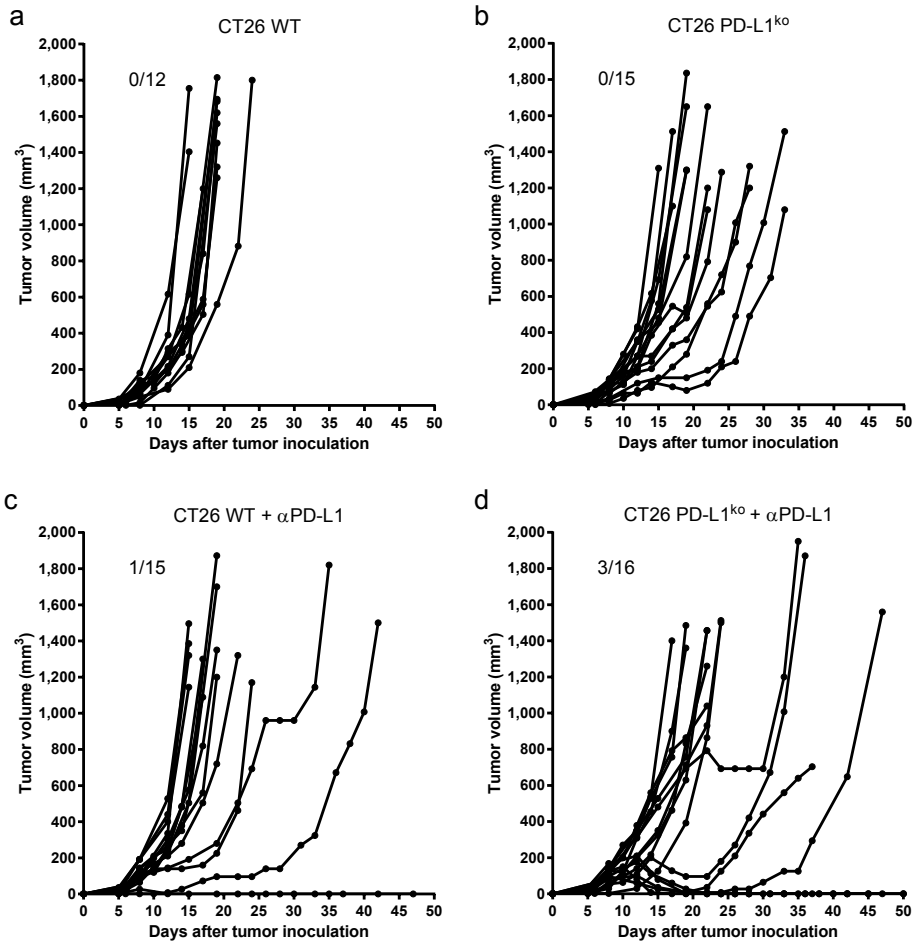

Supplementary Figure S3. CT26 tumor outgrowth curves of individual B6 mice bearing **(A)** untreated WT tumors, **(B)** untreated PD-L1^{KO} tumors, **(C)** WT tumors treated with PD-L1 blockade or (D) PD-L1^{KO} tumors treated with PD-L1 blockade. Graphs correspond to survival curves in Figure 4B. Each line represents the tumor of an individual mouse. The fraction of mice that fully cleared the tumor is indicated in the graph.

Chapter 3

Metabolic stress in cancer cells induces immune escape through an IFN-γ signaling blockade via PI3K pathway

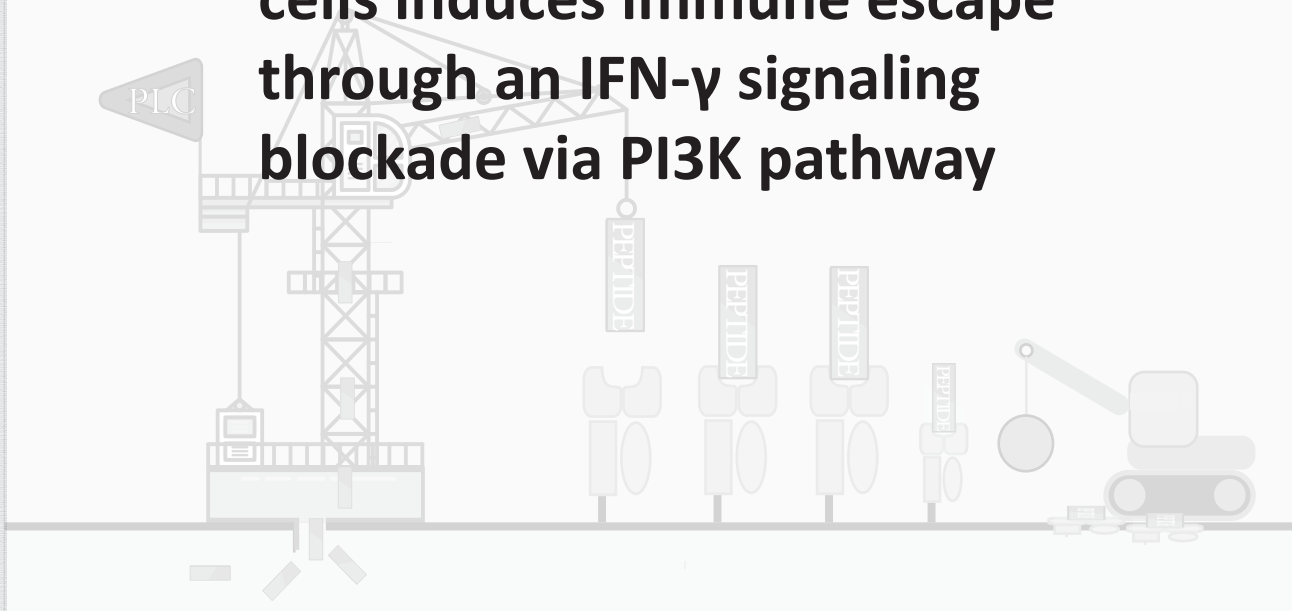

K. A. Marijt*, *M. Sluijter, L. Blijleven, S. H. Tolmeijer, F. A. Scheeren, S. H. van der Burg and T. van Hall*

* Corresponding author

Journal of Immunotherapy of Cancer 7(1): 152 (2019)

Abstract

Background:

T-cell mediated immunotherapy brought clinical success for many cancer patients. Nonetheless, downregulation of MHC class I antigen presentation, frequently occurring in solid cancers, limits the efficacy of these therapies. Unraveling the mechanisms underlying this type of immune escape is therefore of great importance. We here investigated the immunological effects of metabolic stress in cancer cells as a result of nutrient deprivation.

Methods:

TC1 and B16F10 tumor cell lines were cultured under oxygen- and glucose-deprivation conditions that mimicked the tumor microenvironment of solid tumors. Presentation of peptide antigens by MHC class I molecules was measured by flow cytometry and via activation of tumor-specific CD8 T cell clones. The proficiency of the IFNy-STAT1 pathway was investigated by Western blots on phosphorylated proteins, transfection of constitutive active STAT1 constructs and qPCR of downstream targets. Kinase inhibitors for PI3K were used to examine its role in IFNy receptor signal transduction.

Results:

Combination of oxygen- and glucose-deprivation resulted in decreased presentation of MHC class I antigens on cancer cells, even in the presence of the stimulatory cytokine IFNy. This unresponsiveness to IFNy was the result of failure to phosphorylate the signal transducer STAT1. Forced expression of constitutive active STAT1 fully rescued the MHC class I presentation. Furthermore, oxygen- and glucose-deprivation increased PI3K activity in tumor cells. Pharmacological inhibition of this pathway not only restored signal transduction through IFNy-STAT1 but also improved MHC class I presentation. Importantly, PI3K inhibitors also rendered tumor cells sensitive for recognition by CD8 T cells in culture conditions of metabolic stress.

Conclusions:

These data revealed a strong impact of metabolic stress on the presentation of tumor antigens by MHC class I and suggest that this type of tumor escape takes place at hypoxic areas even during times of active T cell immunity and IFNy release.

Keywords: cancer metabolism, tumor microenvironment, immune-escape

Background

Recent advances in immunotherapy have led to great clinical successes in multiple cancer types, especially advanced melanoma and non-small cell lung carcinoma. T cell based immunotherapy, like checkpoint blockade therapy, adoptive T cell transfer, and DC vaccination all rely on the surface presentation of tumor-associated or tumor-specific (neo-) antigens on cancer cells by major histocompatibility complex class I (MHC-I) molecules[1,2]. Type II interferon-y (IFNy) is a major regulator of MHC-I gene expression and, in addition, also upregulates the expression of processing associated genes, like immunoproteasome subunits and the peptide transporter TAP[3]. Therefore, proficient IFNy signaling in the local tumor microenvironment (TME) is of utmost importance for immune-surveillance by the adaptive immune system and scrutiny of intracellular tumor antigens. Many cancer types downregulate MHC-I surface display as primary or acquired immunological resistance through molecular mechanisms affecting IFNy signaling, including loss-of-function mutations in the Janus kinase (JAK) signal transducers, mutations in the IFNy receptor, and alterations in APLNR and PTPN2 genes that control IFNy sensing[4-8]. However, the impact of tumor microenvironmental metabolic cues on IFNy receptor signaling and immune recognition of cancer cells is a largely unexplored area of research.

Due to unregulated tumor growth and uncontrolled angiogenesis, human solid cancers often contain a dysfunctional vascular system, restricting the availability of essential nutrients like oxygen and glucose, triggering metabolic stress in the tumor cells[9,10]. Oxygen levels in solid cancers often drop to levels between 0.3% and 4.2% (2-32 mmHg) with most below 2%[11-15]. When cells experience hypoxic stress, HIF1a degradation is prevented via prolyl hydroxylases (PHDs) inhibition, leading to induced expression of transcription factors responsible for modulating energy metabolism by activation of the glycolysis and glutaminolysis pathway, including upregulation of the glucose transporter GLUT-1[16] as well as the glycolytic enzymes Hexokinase-1 (HK-1), Hexokinase-2 (HK-2), and Phosphoglycerate kinase-1 (PKG1)[17-20]. Enhanced glycolysis leads to increased consumption of glucose by cancer cells, draining glucose from the interstitial fluid, resulting in very limited glucose concentrations in the TME. Glucose concentrations in the interstitial fluid of two mouse melanomas reported *in situ* glucose levels of approximately 0.6 mM compared to 9mM in the spleen and blood[21], similar to observations reported for other tumor types[22,23]. Importantly, these microenvironmental nutrient limitations correlate with poor patient survival[24]. Several studies investigated the effects of nutrient limiting conditions on immune cells infiltrating the TME[21,25]. However, the effects of nutrient deprivation on cancer immunogenicity remain poorly understood.

In this study, we examined the impact of limited oxygen- and glucose- levels as found in the TME, on MHC-I presentation by cancer cells. Under these circumstances cancer cells lose their sensitivity to IFNγ by disrupting the IFNγ-STAT1 signaling pathway and consequently antigen presentation via MHC-I molecules. Mechanistically, this was related to the activation of the PI3K pathway and pharmacological inhibition of PI3K, using small molecule inhibitors, restored functional MHC-I antigen presentation under oxygen- and glucose-deprived conditions. Our findings describe a novel immune escape mechanism how cancer cells can acquire resistance for immunotherapy.

Material and methods

Cell culture

Tumor cells were seeded in 6-well plates and cultured overnight until fully attached (t_0). Next, tumor cells were cultured under normal (21% oxygen, 25mM glucose), glucose deprivation (GD, 21% oxygen, 0.5mM glucose), oxygen deprivation (OD, 1% oxygen, 25mM glucose), or oxygen and glucose deprivation (OGD, 1% oxygen, 0.5mM glucose) conditions with, our without IFNγ (20U/mL) for 24 hours. Tumor cell medium (TCM) contained IMDM media (Invitrogen) supplemented with 100ug/mL streptomycin, 100 U/mL penicillin, 2mM L-glutamine (Invitrogen) and 10% FCS (Gibco). Tumor cells were maintained in humidified air at 37°C and with 5% CO_2. Pharmacological inhibition of PI3K was done by adding LY294002 or wortmannin (Seleckchem) at timepoint t_0 for 24h.

T cell medium contained IMDM media (Invitrogen) and 10% FCS (Greiner), 0.2% β2ME, 100ug/mL streptomycin, 100 U/mL penicillin, 2mM L-glutamine (Invitrogen), and 10 IU/mL recombinant human IL-2 (Novartis). B16F10 specific CD8 T cells (CTL clone LP9[26]) were stimulated once a week with irradiated B16F10-B7 tumor cells and splenocytes from C57BL/6 mice. TC1 specific CD8 T cells (CTL clone 9.5c3[27]) were stimulated once a week with irradiated TC1-B7 tumor cells and splenocytes from C57BL/6 mice.

Functional T cells assays

B16F10 specific (CTL clone LP9, K^b-binding $TRP2_{180-188}$)[26] or TC1 specific (CTL clone 9.5C3, D^b-binding $HPV16/E7_{49-57}$)[27] T cells were co-cultured overnight under normal culture conditions, with either B16F10 or TC1 tumor cells collected from normal, OD, GD, or OGD conditions of which MHC-I antigen presentation was fixated using 1ug/mL GolgiPlug (BD Biosciences). T cells were incubated with 1ug/mL TRP2 peptide and used as positive control. After 24h incubation T cells were fixed, permeabilized, and stained for IFNγ and analyzed by flow cytometry.

RNA isolation & cDNA synthesis

Tumor cells were washed with cold PBS followed by total RNA isolation using the RNeasy Plus Mini Kit (Qiagen). 1000 ng of RNA was used for cDNA synthesis using a High Capacity RNA-to-cDNA kit (Applied Biosystems).

qPCR gene expression analysis

qPCRs were performed using the CFX96TM Real Time System (Biorad) with SYBR® Green Supermix (Biorad). The cycling conditions were set at 95°C for 3 min, followed by 40 cycles of 15 s at 95°C, 30 s at 60°C and 30 s at 72°C. Measurements were performed in triplicates. Ct-values were normalized to the expression of the housekeeping gene UBC. Primer sequence overview can be found in supplemental table 1.

Flow cytometry

Tumor cells were stained with H-2D^{b} (28-14-8), or H-2K^{b} (AF6-88.5) antibodies for 30min at 4˚C. T cell activation was quantified by measuring intracellular IFNγ (XMF1.2, Biolegend) production using an ICS kit (BioLegend) according to manufactures protocol. Cells were acquired on a Fortessa flowcytometer (BD Biosciences) and analyzed using FlowJo software (Tree Star).

Microscopy

An Olympus DX51 light microscope and Olympus cellSens software was used to capture images of tumor cells cultured under normal, OD, GD, or OGD conditions.

Western Blot

Cellular protein extracts were isolated by directly adding Laemmli sample buffer containing 5% beta mercaptoethanol to the cells. Protein concentrations were measured using Bradford protein assay. Equal amounts of protein extracts (50ug) were separated by Mini Protean precast gels TGX (Biorad). Afterwards, protein extracts were transferred to nitrocellulose membrane using a Trans-Blot® TurboTM transfer Pack (biorad) and Biorad semi-dry Transfer System. Membranes were blocked for 1h in 5mL 5% BSA/0.1% Tween/TBS and probed overnight with primary antibody for pSTAT1 Y701 (Cell Signaling #9167), pSTAT1 S727 (Cell Signaling #9177), Total-STAT1 (Cell Signaling #9172), IRF-1 (Cell Signaling #14028), Phospho-AKT (Cell Signaling #9271) or beta-actin (Cell Signaling #3700). membranes were washed 3 times with 5mL 0.1% Tween/TBS and incubated with anti-rabbit IgG or anti-mouse IgG with HPR-linked antibody (Cell signaling #7074, #7075) for 1h. Membranes were developed using 1X SignalFireTM ECL Reagent (Cell signaling) and analyzed with a compatible imager. Western-blots were quantified by measuring protein band in-

tensity using imageJ software. Samples were normalized with beta-actin band intensity.

Statistical analysis

All data are presented as means and SD. Statistical analysis was done using a paired Student's t test (two-tailed) with welch correction to determine the statistical significance of the differences. A minimum of three replicates were used in all experiments. Differences were considered statistically significant at $p < 0.05$. (* $p<0.05$, ** $p<0.01$, *** $p<0.001$).

Results

Oxygen- and glucose-deprived conditions downmodulate MHC-I surface expression on tumor cells resulting in immune escape from CD8 T cells

Here we set out to investigate the role of metabolic stress on MHC-I expression levels on tumor cells. Therefore, we cultured the HPV16 E6 and E7 transformed TC1 cancer line and the B16F10 melanoma line under nutrient proficient (normal), oxygen deprived (OD) (1% oxygen), glucose deprived (GD) (0.5mM), or the combination of oxygen- and glucose-deprived (OGD) conditions, simulating the physiological levels measured in the microenvironment of solid cancers[11,21-23]. These nutrient limiting conditions resulted in altered expression of several metabolism-associated genes and an increase of the unfolded protein response (UPR), witnessing a metabolic stress response (supplemental figure 1a-d)[28-30]. Of note, these conditions did not affect the viability of these two tumor cell lines (supplemental figure 1e-f). Strikingly, MHC-I surface display was strongly repressed in OGD cultured TC1 tumor cells (figure 1a-d). This effect was more pronounced in both tumor lines when the cells were stimulated with IFNy, a strong inducer of MHC-I antigen processing. Importantly, cells cultured under OD or GD conditions only did not repress MHC-I expression, indicating that the combination of both nutrients created a unique metabolic signature in tumor cells leading to repression of MHC-I. IFNy treatment did not affect this metabolic signature in the tumor cells as measured by the induction of metabolism-associated gene expression (supplemental figure 2a-b). The OGD-mediated resistance to IFNy was reversible as tumor cells transferred to normal nutrient-rich culture conditions restored the responsiveness to IFNy within 24 hours (figure 1e and h).

To determine whether the decrease of MHC-I molecules was specific for IFNy signaling and not merely reflect a general reduction of surface proteins, we measured the expression levels of the cell surface glycoprotein CD44, and Tyrosinase-related protein-1 (TRP1). The expression of these two molecules was not downregulated, but rather somewhat upregulated under low-glucose conditions (supplemental figure 3a-c), excluding the possibility that OGD conditions led to a general reduction of cell surface protein expression.

To assess the functional impact of repressed MHC-I expression on tumor cells, we co-cultured the tumor cells with CD8 T cell clones specific for TC1 (CTL clone 9.5C3)[27] or B16F10 (CTL clone LP9)[26] tumor cells and measured T cell activation. The recognition by tumor-specific T cells was clearly reduced when OGD cultured tumor cells were used as targets, compared to normal or single-deprived culture conditions for either glucose or oxygen (figure 1f-g and h-i).

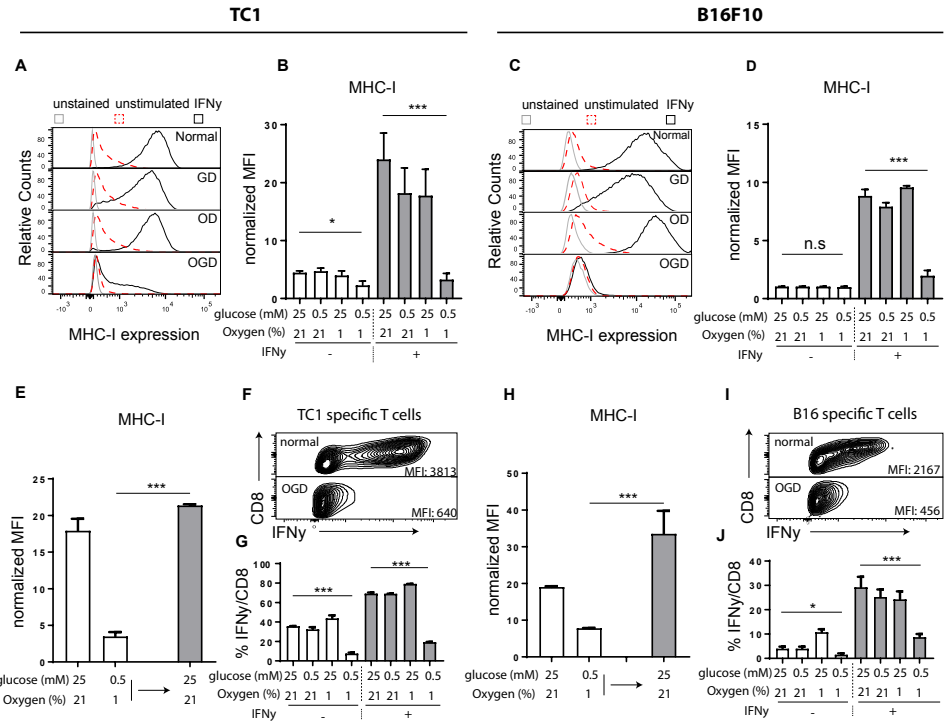

Figure 1: OGD culture conditions impairs IFNy response and leads to abrogated tumor recognition by CD8 T cells

(A, C) Histogram plots of MHC-I expression of TC1 (A) and B16F10 (C) when cultured under different nutrient limiting conditions with our without stimulation of IFNy for 24h. (B, D) Quantification of MHC-I expression of TC1 (B) and B16F10 (D) tumor cells of three independently performed experiments. Data is shown as normalized Mean Fluorescence Intensity (MFI) by dividing the MFI of the stained sample by the MFI of negative control. (E, H) B16F10 (E) or TC1 (H) tumor cells were cultured under normal or OGD conditions for 24h with IFNy (white bars). OGD cultured tumor cells were cultured an additional 24h under nutrient repleted conditions (gray bars). MHC-I surface expression of tumor cells was measured by flow cytometry. Quantitative data of three independent experiments is shown as normalized MFI. (F, I) Density plots of IFNy production of TC1 (F) or B16F10 (I) specific CD8 T cells upon tumor recognition measured by flow cytometry. MFI, mean fluorescence intensity. (G, J) Quantified data of F and I. Data is shown as mean +- SD. Unpaired t test was used to calculate significance; n.s., not significant *, p<0.05, **, p<0.01, ***, p<0.001.

In addition to the reduced frequency of T cells responding to the tumor targets, the degree of cytokine production was also strongly repressed. When the tumor targets were pre-incubated with IFNy to stimulate MHC-I levels[3] (figure 1b and d), the differences between the four culture conditions was even more pronounced, especially for the B16F10 tumor line (figure 1g and j). Taken together, these data indicated that tumor cells in a OGD environment repressed MHC-I surface expression, even after stimulation with IFNy, leading to strongly decreased immune recognition by CD8 T cells.

Unresponsiveness to IFNy is mostly regulated via blockade of STAT1 phosphorylation

Our results indicate that the IFNy-STAT1 signal transduction pathway was impaired in OGD cultured tumor cells. This prompted us to determine the proficiency of the several components of IFNy-STAT1 signaling pathway of tumor cells under nutrient limiting conditions. In response to IFNy receptor (IFNyR) signaling, JAK1 and JAK2 are phosphorylated and subsequently STAT1 is phosphorylated at multiple residues, allowing dimerization, nuclear translocation and activation of interferon stimulated genes (ISGs)[31]. IFNyR surface expression on TC1 and B16F10 tumor cells and *Jak1* and *Jak2* expression was similar in all culture conditions (supplemental figure 4a-b and figure 2a-b, respectively). Strikingly, IFNy-mediated upregulation of *Stat1* expression levels were significantly inhibited in both TC1 and B16F10 tumor cells under OGD conditions (figure 2c-d). Moreover, the expression levels of *Interferon regulatory factor (Irf)-1*, and its downstream targets *Tap1* and *H2-D^b* (one of the MHC-I *genes)* were consequently also strongly inhibited in both tumor cell lines in OGD conditions (figure 2c-f).

We then analyzed the IFNy-STAT1 signaling pathway at the protein level by Western-blot. IFNy stimulation greatly induced total STAT1 expression in normal, OG, and DG conditions in both tumor cell lines. When the tumor cells were cultured under OGD conditions, the upregulation of total STAT1 protein expression was inhibited, corroborating the qPCR results (figure 3a-b, c and e). More prominently, activation of STAT1 via tyrosine and serine phosphorylation was strongly repressed in OGD conditions upon IFNy stimulation (figure 3a-b, d and f, g and i). Consequently, protein expression of IRF-1 was virtually absent in tumor cells cultured under OGD conditions (figure 3a-b, h and j). Together these data show that OGD conditions affect the IFNy responsiveness of tumor cells, which is associated with strongly decreased STAT1 activation.

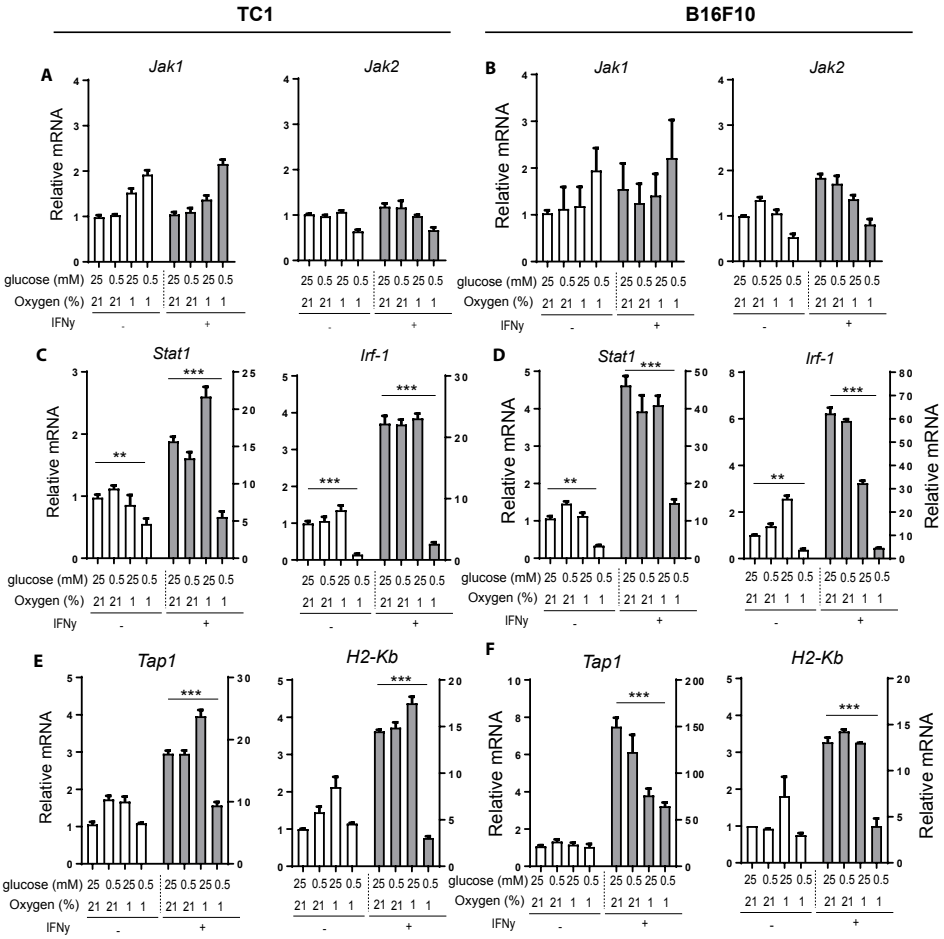

Figure 2: Gene transcription levels of IFNy-STAT1 relevant genes of tumor cells

Tumor cells were cultured under several nutrient limiting conditions for 24h with or without IFNy. (A, B) *Jak1* and *Jak2* gene expression levels of TC1 (A) and B16F10 tumor cells (B) measured by qPCR. (C, D) *Stat1* and *Irf-1* gene expression levels of TC1 (C) and B16F10 tumor cells (D) measured by qPCR. (E, F) *Tap1* and *H2-k*^{b} (MHC-I) gene expression levels of TC1 (E) and B16F10 tumor cells (F) measured by qPCR. Relative mRNA expression is shown compared to normal culture conditions without IFNy stimulation and normalized to *UBC* housekeeping gene expression. Representative data is shown as mean +- SD (n=3). Unpaired t test was used to calculate significance; n.s., not significant *, p<0.05, **, p<0.01, ***, p<0.001.

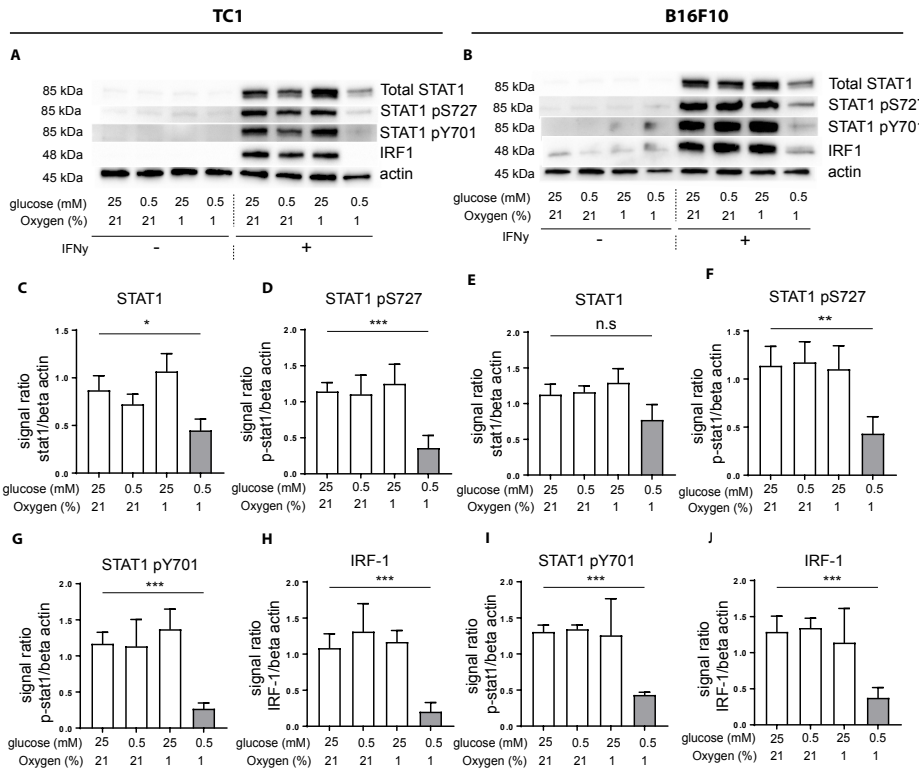

Figure 3: Impaired phosphorylation of STAT1 responsible for impaired MHC-I upregulation

Tumor cells were cultured for 24h under several nutrient limiting conditions with or without IFNy. (A, B) Western-blots of TC1 (A) and B16F10 tumor cells (B). Representative data out of three experiments is shown. (C, E) Quantification of western-blot results of total STAT1 protein expression of TC1 (C) and B16F10 (E). (D, F) Quantification of western-blot results of phosphorylated STAT1 at Y701 and S727 of TC1 (D) and B16F10 (F). (G, H) Quantification of western-blot results of IRF-1 protein expression of TC1 (G) and B16F10 (H). Data was quantified by calculating signal ratio between protein of interest and beta-actin. Unpaired t test was used to calculate significance; n.s., not significant *, p<0.05, **, p<0.01, ***, p<0.001.

Constitutive active STAT1 but not wild-type STAT1, rescues MHC-I expression in OGD culture conditions

STAT1 activation through phosphorylation is essential for downstream IFNyR signaling. We, thus, set out to determine the importance of STAT1 activation for the MHC-I presentation in OGD condition. Two different STAT1 constructs were introduced, one encoding the wild-type sequence of the gene ('STAT1-WT') and another with constitutive active STAT1 ('STAT1-cc') comprising point mutations in the src homology 2 (SH2)-homodimerization domain. This STAT1-cc mutant results in a IFNy hypersensitive variant of STAT1[32]. Transient overexpression of STAT1-wt in B16F10 tumor cells that were cultured in OGD conditions

led to strong increase in STAT1 protein levels (figure 4a), but failed to restore MHC-I expression (figure 4b-c). However, transient overexpression of the constitutive active STAT1-cc mutant restored MHC-I expression on B16F10 tumor cells cultured under OGD to levels, comparable to those of B16F10 cells cultured under normal conditions (figure 4b-c). These results implied that the OGD-mediated repression of MHC-I is mediated by inhibited phosphorylation of STAT1 affecting its downstream functions.

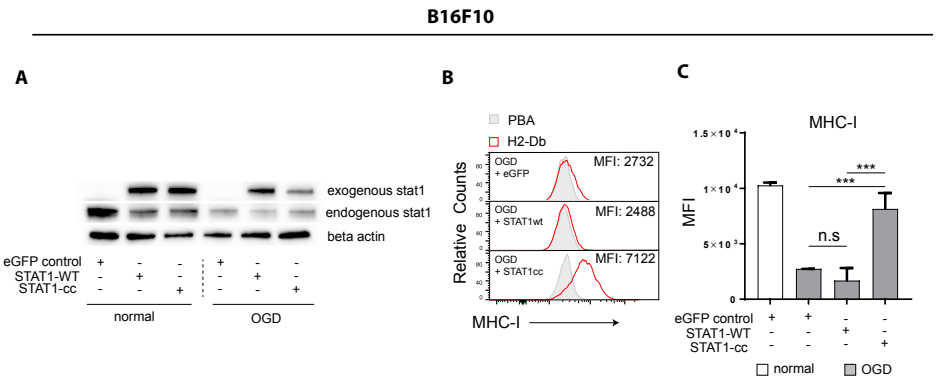

Figure 4: Transient expression of constitutive active STAT1 restores MHC-I expression on OGD stressed tumor cells

B16F10 tumor cells were transiently overexpressed with STAT1-WT or STAT1-cc using e-GFP as a control, prior to culturing the cells under normal or OGD culture conditions for 24h with IFNγ stimulation. (A) Western-blot results of endogenous STAT1 expression and exogenous STAT1 overexpression after transfection of STAT1-WT, STAT1-cc, or control. (B) Histogram illustrating MHC-I surface expression of B16F10 tumor cells cultured under normal or OGD conditions measured by flow cytometry. Representative data is shown as mean +- SD (n=3). (C) Quantified data of B is shown as normalized MFI. Unpaired t test was used to calculate significance; n.s., not significant *, p<0.05, **, p<0.01, ***, p<0.001.

OGD conditions activate AKT/PKB and chemical inhibitors for the upstream PI3K restored IFNγ responsiveness of tumor cells

We then investigated the mechanism by which OGD cultured tumor cells reduced their capacity to respond to IFNγ, resulting in impaired STAT1 phosphorylation. Phosphoinositide 3-kinases (PI3Ks) play pivotal roles in the regulation of cellular metabolism[33,34] and its downstream effector AKT/PKB mediates survival of tumor cells under hypoxia[35] and protects cells from death induced by glucose deprivation[36]. This involvement of PI3K in orchestrating metabolism prompted us to examine its role in IFNγ responsiveness under OGD conditions. Phosphorylation levels of the PI3K effector, AKT/PKB, in TC1 and B16F10 tumor cells were assessed by Western-blot and we indeed observed a strong upregulation of phospho-AKT (pAKT) under GD, OD and especially OGD conditions in the TC1 tumor cell line (figure 5a-b). A similar pattern was observed in the B16F10 tumor line, but less pronounced (figure 5c-d). These results showed that the PI3K pathway

was activated under OGD conditions. To assess if upregulation of activated PI3K was responsible for the OGD-associated effects on IFNγ signaling we tested whether pharmacological inhibition of PI3K could restore the sensitivity of the tumor cells to respond to IFNγ. The common PI3K inhibitor LY294002 prevented phosphorylation of AKT induced by OGD conditions in both tumor cell lines, demonstrating functional inhibition of this pathway (figure 5e-h). Importantly, inhibition of PI3K signaling restored STAT1 Y701 phosphorylation and recovered protein expression of IRF-1 in TC1 cells (figure 5i-j, m) and B16F10 cells (figure 5k-l, n). In addition, pharmacological inhibition also restored total STAT1 protein levels in TC1 cells, but not in B16F10, most likely due to higher constitutive pAKT levels in these cells (supplemental figure 5a-d). We concluded that OGD culture conditions induced the activation of the PI3K/AKT pathway in tumor cells and thereby blocks IFNγ responsiveness.

MHC-I surface display and CD8 T cell recognition are restored by inhibitors of PI3K

Then, we investigated the impact of the PI3K inhibitors on MHC-I expression on tumor cells cultured under OGD conditions and compared this to tumor cells cultured under normal conditions (figure 6a-d). An almost complete rescue of cell surface MHC-I expression was observed on both cell lines. To corroborate these findings, we repeated this experiment with another PI3K inhibitor, Wortmannin and similar dose-response effects were observed (supplemental figure 5e-f), implying that the OGD-induced repression of MHC-I could be counteracted by inhibition of PI3K activity. Finally, we tested if the restored MHC-I levels led to full stimulation of tumor-specific CD8 T cells (figure 6e-h). Indeed, blockade of PI3K activity by LY294002 (L) or Wortmannin (W) significantly improved tumor cell recognition by both tumor-specific CD8 T cells.

Together, our data demonstrate that metabolic stress induces a PI3K-dependent response signature which inhibits the IFNγ responsiveness of tumor cells. Consequently, tumor cell recognition by CD8 T cells is strongly impaired allowing tumor cells to escape immune control. These findings highlight the influence of nutrient availability in the tumor microenvironment on immunoregulation.

Discussion

We showed that the combination of hypoxia and glucose deprivation of tumor cells, often found in microenvironments of solid tumors, results in lower tumor immunogenicity reflected by an impaired IFNγ responsiveness, lowered MHC-I surface expression, and decreased recognition by tumor-specific CD8 T cells. This was caused by disruption of IFNγ-mediated activation of the STAT1 signaling pathway, restricting the activation of

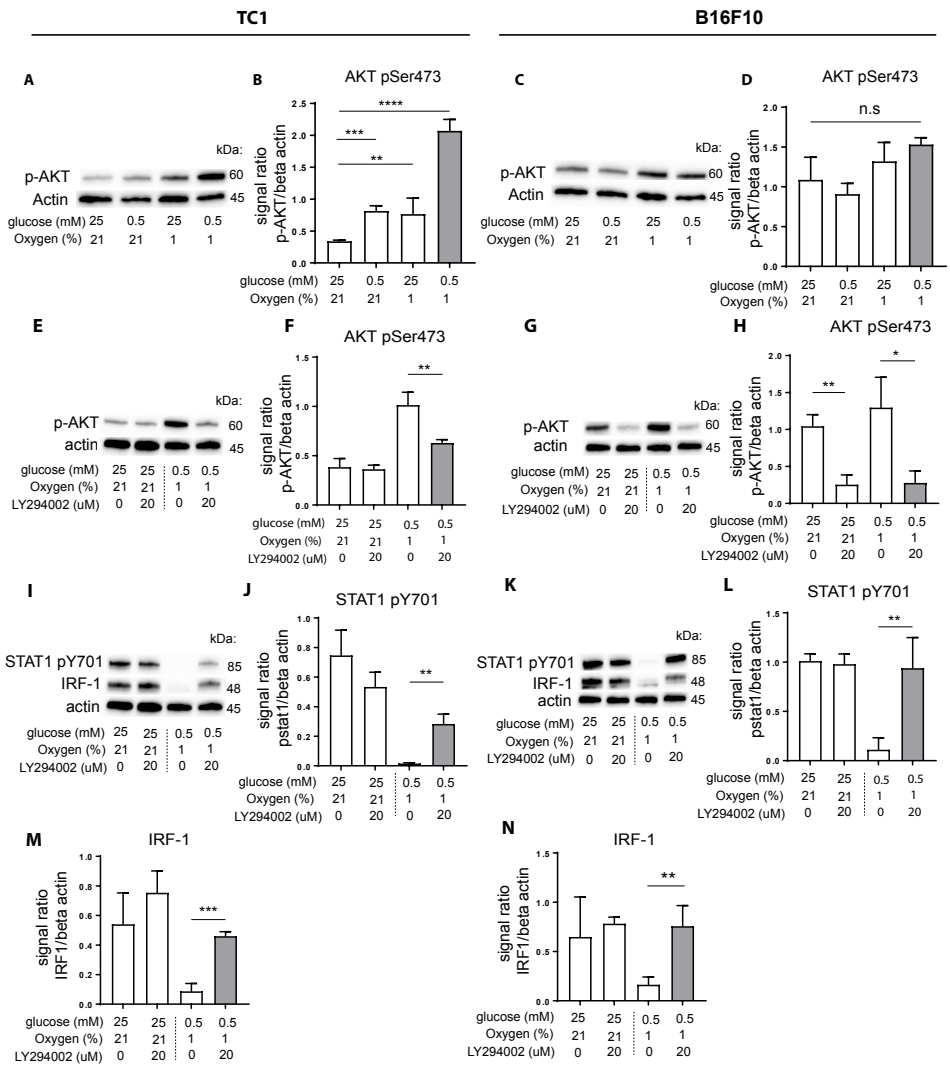

Figure 5: IFNy responsiveness of metabolically stressed tumor cells can be restored by PI3K inhibition

Tumor cells were cultured under normal, GD, OD, or OGD conditions together with IFNy for 24h. (A, C) Western-blots of TC1 (A) and B16F10 (C) tumor cells. Representative data out of three experiments is shown. (B, D) Quantification of western-blot results of phospho-AKT expression in TC1 (B) and B16F10 (D) tumor cells. (E, G) TC1 (E) and B16F10 (G) tumor cells were cultured under normal or OGD conditions with or without LY294002 for 24h. Representative western-blot results out of three experiments is shown. (F, H) Quantification of western-blot results of phospho-AKT expression in TC1 (F) and B16F10 (H) tumor cells. (I, K) Western-blots of TC1 (I) and B16F10 (K). Phospho-STAT1 and IRF-1 expression levels are shown. (J, L, M, N) Quantified data of I and K. Data was quantified by calculating signal ratio between protein of interest and beta-actin. Unpaired t test was used to calculate significance; n.s., not significant *, p<0.05, **, p<0.01, ***, p<0.001.

its downstream target molecules, including IRF-1, TAP-1, and MHC-I. As a result, tumors failed to efficiently present tumor antigens to CD8 T cells and consequently may escape from immunosurveillance or immunotherapy. Mechanistical studies suggested that metabolic stress-induced activation of the PI3K/AKT pathway was the underlying cause since the chemical inhibitors of the PI3K pathway, LY294002 and Wortmannin, relieved the inhibition of the IFNy-STAT1 signaling pathway, resulting in restored antigen presentation, and restored CD8 T cell recognition of the tumor cells. These data suggest an important interplay between STAT1 and PI3K, linking cancer metabolism with immunity. Our results furthermore indicate that immunotherapy-induced recruitment of tumor-specific CD8 T cells and local production of IFNy might not suffice for an effective tumor killing response.

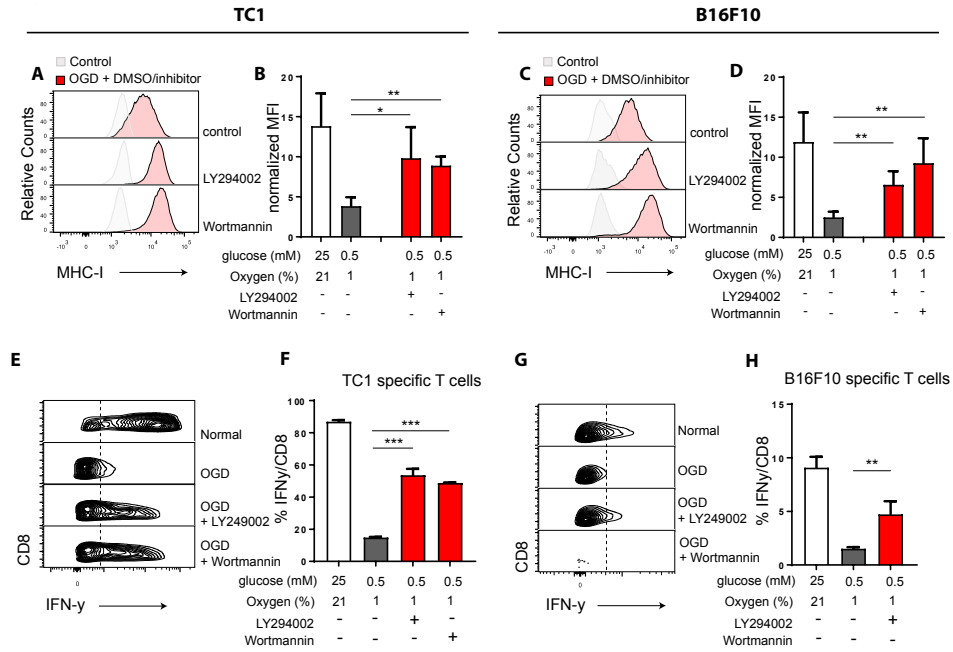

Figure 6: Improved tumor cell recognition by CD8 T cells after PI3K inhibition

Tumor cells were cultured under several nutrient limiting conditions stimulated with IFNy for 24h with or without LY294002 or Wortmannin using DMSO as a control. (A, C) Histogram plot of MHC-I expression of TC1 (A) or B16F10 (C) tumor cells measured by flow cytometry. Representative data of three experiments is shown. (B, D) Quantified data of A and C, shown as normalized MFI. (E,G) Density plots of IFNy production of TC1 (E) or B16F10 (G) specific T cells upon tumor cell recognition measured by flow cytometry. (F, H) Quantified data of E and G. Representative data is shown as mean +- SD (n=3). Unpaired t test was used to calculate significance; n.s., not significant *, p<0.05, **, p<0.01, ***, p<0.001.

Genetic alterations in metabolism pathways or insufficient oxygen levels often dictates cancer cells to utilize anaerobic glycolysis instead of OXPHOS. *Charni et al.* showed that forcing glycolytic cancer cells to utilize OXPHOS by DCA (dichloroacetate) treatment, results in upregulation of MHC-I through activation of the ERK5/MAPK pathway[37]. Similar findings were reported by *Catalan et al.*, showing a correlation between the loss of ERK5 expression and reduced MHC-I expression in glycolytic leukemia cells and transformed fibroblasts[38]. MHC-I presentation was also altered upon activation of an UPR response. *Almeida et al.*, showed that overexpression of UPR signaling transcription factors ATF6 (nATF6) and XBP-1 (sXBP-1) in hek293T cells results in reduced MHC-I presentation[39]. Importantly, only surface expression of MHC-I was inhibited, as total MHC-I expression was not altered. This can be explained by limited peptide availability for MHC-I binding as a result of repressed protein synthesis[40,41]. Interestingly, in addition with our observations that metabolic stress reduces the responsiveness of tumor cells to IFNy and thereby leads to reduced MHC-I expression, these studies describe a mechanism that directly inhibit basal levels of MHC-I surface expression. Together, it shows that metabolic alternations of cancer cells and its impact on the TME can directly or indirectly modulate the MHC-I presentation through different pathways.

The interplay between the PI3K and STAT1 pathways is not extensively studied and only a limited number of studies reported on interactions and crosstalk of the two pathways. Nguyen *et al.* showed that phosphorylation of STAT1 at serine 727 after IFNy stimulation is required for activation of PI3K and AKT in T98G glioblastoma cells[42], whereas Mounayar *et al.* reported a study on PI3Kα-dependent activation of STAT1 phosphorylation at serine 727, resulting in regulation of human mesenchymal stem cell immune polarization[43]. However, we observed that metabolic stress-induced increase of PI3K activity results in impaired STAT1 phosphorylation. To the best of our knowledge, no reports implicate PI3K activation as a negative regulator for STAT1 signaling. These contradicting findings about the crosstalk between PI3K and STAT1 might be explained by the fact that we investigated the role of PI3K as a metabolic regulator upon nutrient deficiency, while others concluded that STAT1 serine-727 phosphorylation is affected by a kinase downstream of PI3K under nutrient proficient conditions. Together, these findings suggest a complex interplay between PI3K signaling and STAT1 expression.

Nutrient deprivation, such as low oxygen and glucose levels, activates AMPK[44], which suppresses biosynthetic processes in cells[45]. This regulator of metabolic stress responses dampens anabolic cell growth through inhibition of mTOR, the coordinator of metabolism, via diverse mechanisms among which TSC2. These pathways promote cell survival by preventing apoptosis in times of limited nutrient availability[46]. AMPK is also a key player in the homeostasis of cellular acetyl-CoA by inhibiting acetyl-CoA carboxylase (ACC) activity,

responsible for the conversion of acetyl-CoA to malonyl-CoA[47]. Acetyl-CoA is a key metabolite that links metabolism with cell signaling and transcription[48]. In addition, acetyl-CoA is the universal donor for acetylation reactions[49], and cellular availability of this metabolite can affect histone- and protein-acetylation in both nucleus and cytoplasm[47,50]. Interestingly, Krämer *et al.* revealed a link between acetylation and STAT1 signaling in that it counteracts IFNy induced STAT1 phosphorylation[51]. Although beyond the scope of this study, we speculate that AMPK activation may alter STAT1 protein acetylation as a result of cellular acetyl-CoA accumulation and, consequently, reduces the IFNy responsiveness through inhibition of STAT1 phosphorylation. However, the exact mechanism and the involvement of PI3K activity in this pathway remains elusive and is subject of further research.

The failure of cancer cells to respond to IFNy caused by acquired mutations in the IFNy-STAT1 signaling pathway is an important predictor for cancer progression and patient survival[5,52-54]. Whole exome sequencing of refractory melanoma tumor lesions of patients initially responding to anti–programmed death 1 (PD-1) therapy revealed loss-of-function mutations in the IFNyR-associated genes Janus kinase 1 (JAK1) and Janus kinase 2 (JAK2). This type of acquired resistance led to failure to respond to IFNy and lack of HLA class I antigen presentation. In parallel, evaluation of primary resistance to anti-CTLA therapy in a cohort of 16 melanoma patients also revealed mutations in genes associated with IFNy signaling pathway in 12 patients, confirming that defects in the IFNy-STAT1 pathway provide resistance to immunotherapy[4]. Moreover, recent CRISPR/CAS9 screening studies implicated other genes involved in regulating IFNy sensitivity as a cancer immunotherapy target, namely, tyrosine-protein phosphatase non-receptor type 2 (PTPN2) and apelin receptor (APLNR)[6,7]. They showed in preclinical models that altering the expression of these genes resulted in altered IFNy responsiveness and reduced efficacy of anti-CTLA4 blockade therapy *in vivo*. These studies emphasize the importance of IFNy signal transduction for immunotherapeutic success in cancer therapy. In our study, we showed soft-wired alterations in this pathway which were induced by limited nutrient availability in the tumor microenvironment. This highlights that acquired resistance to IFNy is not only caused by loss-of-function mutations but can also be acquired through common features in the tumor microenvironment, like oxygen- and glucose-deprivation. This cancer cell extrinsic determinant of nutrient limitation might therefore impact the efficacy of immunotherapy. This suggests that improving the influx of nutrients by normalization of the tumor vasculature[55] or reducing the glucose consumption by targeting cancer metabolism could potentially greatly improve immunotherapeutic success.

Abbreviations

MHC-I: Major Histocompatibility Complex-I

MFI: Mean Fluorescence Index

IFNy: Interferon-gamma

TME: Tumor Microenvironment

OD: Oxygen Deprivation

GD: Glucose Deprivation

OGD: Oxygen and Glucose Deprivation

UPR: Unfolded Protein Response

Declarations

Ethics approval and consent to participate:

Not applicable

Consent for publication:

Not applicable

Availability of data and material:

Experimental data is available upon request

Competing interests:

The authors declare that they have no competing interests.

Funding:

Dutch Cancer Society (grant 2013-6142 to SvdB and TvH).

Authors' contributions:

TvH and KM designed the project and experiments. MS, ST, LB, and KM performed experiments. FS, ST, TvH and KM interpreted the results of the experiments. TvH and KM wrote the manuscript. FS and SvB contributed toward editing and finalizing the manuscript.

Acknowledgements:

The authors thank Ramon Arens for his contribution in reading the manuscript and useful suggestions. We also thank Febe Smits for the technical assistance.

References

1 Hu, Z., Ott, P. A. & Wu, C. J. Towards personalized, tumour-specific, therapeutic vaccines for cancer. *Nat Rev Immunol* **18**, 168-182, doi:10.1038/nri.2017.131 (2018).

2 Ribas, A. & Wolchok, J. D. Cancer immunotherapy using checkpoint blockade. *Science* **359**, 1350-1355, doi:10.1126/science.aar4060 (2018).

3 Zhou, F. Molecular mechanisms of IFN-gamma to up-regulate MHC class I antigen processing and presentation. *Int Rev Immunol* **28**, 239-260, doi:10.1080/08830180902978120 (2009).

4 Gao, J. *et al.* Loss of IFN-gamma Pathway Genes in Tumor Cells as a Mechanism of Resistance to Anti-CTLA-4 Therapy. *Cell* **167**, 397-404 e399, doi:10.1016/j.cell.2016.08.069 (2016).

5 Shin, D. S. *et al.* Primary Resistance to PD-1 Blockade Mediated by JAK1/2 Mutations. *Cancer Discov* **7**, 188-201, doi:10.1158/2159-8290.CD-16-1223 (2017).

6 Patel, S. J. *et al.* Identification of essential genes for cancer immunotherapy. *Nature* **548**, 537-542, doi:10.1038/nature23477 (2017).

7 Manguso, R. T. *et al.* In vivo CRISPR screening identifies Ptpn2 as a cancer immunotherapy target. *Nature* **547**, 413-418, doi:10.1038/nature23270 (2017).

8 Sharma, P., Hu-Lieskovan, S., Wargo, J. A. & Ribas, A. Primary, Adaptive, and Acquired Resistance to Cancer Immunotherapy. *Cell* **168**, 707-723, doi:10.1016/j.cell.2017.01.017 (2017).

9 Siemann, D. W. The unique characteristics of tumor vasculature and preclinical evidence for its selective disruption by Tumor-Vascular Disrupting Agents. *Cancer Treat Rev* **37**, 63-74, doi:10.1016/j.ctrv.2010.05.001 (2011).

10 Bertout, J. A., Patel, S. A. & Simon, M. C. The impact of O2 availability on human cancer. *Nat Rev Cancer* **8**, 967-975, doi:10.1038/nrc2540 (2008).

11 McKeown, S. R. Defining normoxia, physoxia and hypoxia in tumours-implications for treatment response. *Br J Radiol* **87**, 20130676, doi:10.1259/bjr.20130676 (2014).

12 Becker, A. *et al.* Oxygenation of squamous cell carcinoma of the head and neck: comparison of primary tumors, neck node metastases, and normal tissue. *Int J Radiat Oncol Biol Phys* **42**, 35-41 (1998).

13 Lartigau, E. *et al.* Intratumoral oxygen tension in metastatic melanoma. *Melanoma Res* **7**, 400-406 (1997).

14 Lawrentschuk, N. *et al.* Assessing regional hypoxia in human renal tumours using 18F-fluoromisonidazole positron emission tomography. *BJU Int* **96**, 540-546, doi:10.1111/j.1464-410X.2005.05681.x (2005).

15 Nordsmark, M., Bentzen, S. M. & Overgaard, J. Measurement of human tumour oxygenation status by a polarographic needle electrode. An analysis of inter- and intratumour heterogeneity. *Acta Oncol* **33**, 383-389 (1994).

16 Sun, R. C. & Denko, N. C. Hypoxic regulation of glutamine metabolism through HIF1 and SIAH2 supports lipid synthesis that is necessary for tumor growth. *Cell Metab* **19**, 285-292, doi:10.1016/j.cmet.2013.11.022 (2014).

17 Buzzai, M. *et al.* The glucose dependence of Akt-transformed cells can be reversed by pharmacologic activation of fatty acid beta-oxidation. *Oncogene* **24**, 4165-4173, doi:10.1038/sj.onc.1208622 (2005).

18 Elstrom, R. L. *et al.* Akt stimulates aerobic glycolysis in cancer cells. *Cancer Res* **64**, 3892-3899, doi:10.1158/0008-5472.CAN-03-2904 (2004).

19 Rathmell, J. C. *et al.* Akt-directed glucose metabolism can prevent Bax conformation change and promote growth factor-independent survival. *Mol Cell Biol* **23**, 7315-7328 (2003).

20 Ebert, B. L., Firth, J. D. & Ratcliffe, P. J. Hypoxia and mitochondrial inhibitors regulate expression of glucose transporter-1 via distinct Cis-acting sequences. *J Biol Chem* **270**, 29083-29089 (1995).

21 Ho, P. C. *et al.* Phosphoenolpyruvate Is a Metabolic Checkpoint of Anti-tumor T Cell Responses. *Cell* **162**, 1217-1228, doi:10.1016/j.cell.2015.08.012 (2015).

22 Hirayama, A. *et al.* Quantitative metabolome profiling of colon and stomach cancer microenvironment by capillary electrophoresis time-of-flight mass spectrometry. *Cancer Res* **69**, 4918-4925, doi:10.1158/0008-5472.CAN-08-4806 (2009).

23 Gullino, P. M., Clark, S. H. & Grantham, F. H. The Interstitial Fluid of Solid Tumors. *Cancer Res* **24**, 780-794 (1964).

24 Le, Q. T. *et al.* An evaluation of tumor oxygenation and gene expression in patients with early stage non-small cell lung cancers. *Clin Cancer Res* **12**, 1507-1514, doi:10.1158/1078-0432.CCR-05-2049 (2006).

25 Chang, C. H. *et al.* Metabolic Competition in the Tumor Microenvironment Is a Driver of Cancer Progression. *Cell* **162**, 1229-1241, doi:10.1016/j.cell.2015.08.016 (2015).

26 Schreurs, M. W. *et al.* Dendritic cells break tolerance and induce protective immunity against a melanocyte differentiation antigen in an autologous melanoma model. *Cancer Res* **60**, 6995-7001 (2000).

27 Feltkamp, M. C. *et al.* Vaccination with cytotoxic T lymphocyte epitope-containing peptide protects against a tumor induced by human papillomavirus type 16-transformed cells. *Eur J Immunol* **23**, 2242-2249, doi:10.1002/eji.1830230929 (1993).

28 McDonald, P. C. & Dedhar, S. Carbonic anhydrase IX (CAIX) as a mediator of hypoxia-induced stress response in cancer cells. *Subcell Biochem* **75**, 255-269, doi:10.1007/978-94-007-7359-2_13 (2014).

29 Vavilis, T. *et al.* Oxygen-Glucose Deprivation (OGD) Modulates the Unfolded Protein Response (UPR) and Inflicts Autophagy in a PC12 Hypoxia Cell Line Model. *Cell Mol Neurobiol* **36**, 701-712, doi:10.1007/s10571-015-0250-2 (2016).

30 Tsuru, A., Imai, Y., Saito, M. & Kohno, K. Novel mechanism of enhancing IRE1alpha-XBP1 signalling via the PERK-ATF4 pathway. *Sci Rep* **6**, 24217, doi:10.1038/srep24217 (2016).

31 Bach, E. A., Aguet, M. & Schreiber, R. D. The IFN gamma receptor: a paradigm for cytokine receptor signaling. *Annu Rev Immunol* **15**, 563-591, doi:10.1146/annurev.immunol.15.1.563 (1997).

32 Zhang, Y. *et al.* Modification of the Stat1 SH2 domain broadly improves interferon efficacy in proportion to p300/CREB-binding protein coactivator recruitment. *J Biol Chem* **280**, 34306-34315, doi:10.1074/jbc.M503263200 (2005).

33 Fruman, D. A. *et al.* The PI3K Pathway in Human Disease. *Cell* **170**, 605-635, doi:10.1016/j.cell.2017.07.029 (2017).

34 Engelman, J. A., Luo, J. & Cantley, L. C. The evolution of phosphatidylinositol 3-kinases as regulators of growth and metabolism. *Nat Rev Genet* **7**, 606-619, doi:10.1038/nrg1879 (2006).

35 Stegeman, H. *et al.* Interaction between hypoxia, AKT and HIF-1 signaling in HNSCC and NSCLC: implications for future treatment strategies. *Future Sci OA* **2**, FSO84, doi:10.4155/fso.15.84 (2016).

36 Gao, M. *et al.* Site-specific activation of AKT protects cells from death induced by glucose deprivation. *Oncogene* **33**, 745-755, doi:10.1038/onc.2013.2 (2014).

37 Charni, S. *et al.* Oxidative phosphorylation induces de novo expression of the MHC class I in tumor cells through the ERK5 pathway. *J Immunol* **185**, 3498-3503, doi:10.4049/jimmunol.1001250 (2010).

38 Catalan, E. *et al.* MHC-I modulation due to changes in tumor cell metabolism regulates tumor sensitivity to CTL and NK cells. *Oncoimmunology* **4**, e985924, doi:10.4161/2162402X.2014.985924 (2015).

39 de Almeida, S. F., Fleming, J. V., Azevedo, J. E., Carmo-Fonseca, M. & de Sousa, M. Stimulation of an unfolded protein response impairs MHC class I expression. *J Immunol* **178**, 3612-3619 (2007).

40 Granados, D. P. *et al.* ER stress affects processing of MHC class I-associated peptides. *BMC Immunol* **10**, 10, doi:10.1186/1471-2172-10-10 (2009).

41 Qian, S. B. *et al.* Tight linkage between translation and MHC class I peptide ligand generation implies specialized antigen processing for defective ribosomal products. *J Immunol* **177**, 227-233 (2006).

42 Nguyen, H., Ramana, C. V., Bayes, J. & Stark, G. R. Roles of phosphatidylinositol 3-kinase in interferon-gamma-dependent phosphorylation of STAT1 on serine 727 and activation of gene expression. *J Biol Chem* **276**, 33361-33368, doi:10.1074/jbc.M105070200 (2001).

43 Mounayar, M. *et al.* PI3kalpha and STAT1 Interplay Regulates Human Mesenchymal Stem Cell Immune Polarization. *Stem Cells* **33**, 1892-1901, doi:10.1002/stem.1986 (2015).

44 Laderoute, K. R. *et al.* 5'-AMP-activated protein kinase (AMPK) is induced by low-oxygen and glucose deprivation conditions found in solid-tumor microenvironments. *Mol Cell Biol* **26**, 5336-5347, doi:10.1128/MCB.00166-06 (2006).

45 Saxton, R. A. & Sabatini, D. M. mTOR Signaling in Growth, Metabolism, and Disease. *Cell* **168**, 960-976, doi:10.1016/j.cell.2017.02.004 (2017).

46 Edinger, A. L. & Thompson, C. B. Akt maintains cell size and survival by increasing mTOR-dependent nutrient uptake. *Mol Biol Cell* **13**, 2276-2288, doi:10.1091/mbc.01-12-0584 (2002).

47 Galdieri, L., Gatla, H., Vancurova, I. & Vancura, A. Activation of AMP-activated Protein Kinase by Metformin Induces Protein Acetylation in Prostate and Ovarian Cancer Cells. *J Biol Chem* **291**, 25154-25166, doi:10.1074/jbc.M116.742247 (2016).

48 Martinez-Reyes, I. & Chandel, N. S. Acetyl-CoA-directed gene transcription in cancer cells. *Genes Dev* **32**, 463-465, doi:10.1101/gad.315168.118 (2018).

49 Pietrocola, F., Galluzzi, L., Bravo-San Pedro, J. M., Madeo, F. & Kroemer, G. Acetyl coenzyme A: a central metabolite and second messenger. *Cell Metab* **21**, 805-821, doi:10.1016/j.cmet.2015.05.014 (2015).

50 Rios Garcia, M. *et al.* Acetyl-CoA Carboxylase 1-Dependent Protein Acetylation Controls Breast Cancer Metastasis and Recurrence. *Cell Metab* **26**, 842-855 e845, doi:10.1016/j.cmet.2017.09.018 (2017).

51 Kramer, O. H. *et al.* A phosphorylation-acetylation switch regulates STAT1 signaling. *Genes Dev* **23**, 223-235, doi:10.1101/gad.479209 (2009).

52 Mandai, M. *et al.* Dual Faces of IFNgamma in Cancer Progression: A Role of PD-L1 Induction in the Determination of Pro- and Antitumor Immunity. *Clin Cancer Res* **22**, 2329-2334, doi:10.1158/1078-0432.CCR-16-0224 (2016).

53 Karachaliou, N. *et al.* Interferon gamma, an important marker of response to immune checkpoint blockade in non-small cell lung cancer and melanoma patients. *Ther Adv Med Oncol* **10**, 1758834017749748, doi:10.1177/1758834017749748 (2018).

54 Zaretsky, J. M. *et al.* Mutations Associated with Acquired Resistance to PD-1 Blockade in Melanoma. *N Engl J Med* **375**, 819-829, doi:10.1056/NEJMoa1604958 (2016).

55 Jain, R. K. Normalization of tumor vasculature: an emerging concept in antiangiogenic therapy. *Science* **307**, 58-62, doi:10.1126/science.1104819 (2005).

Supplementary figures

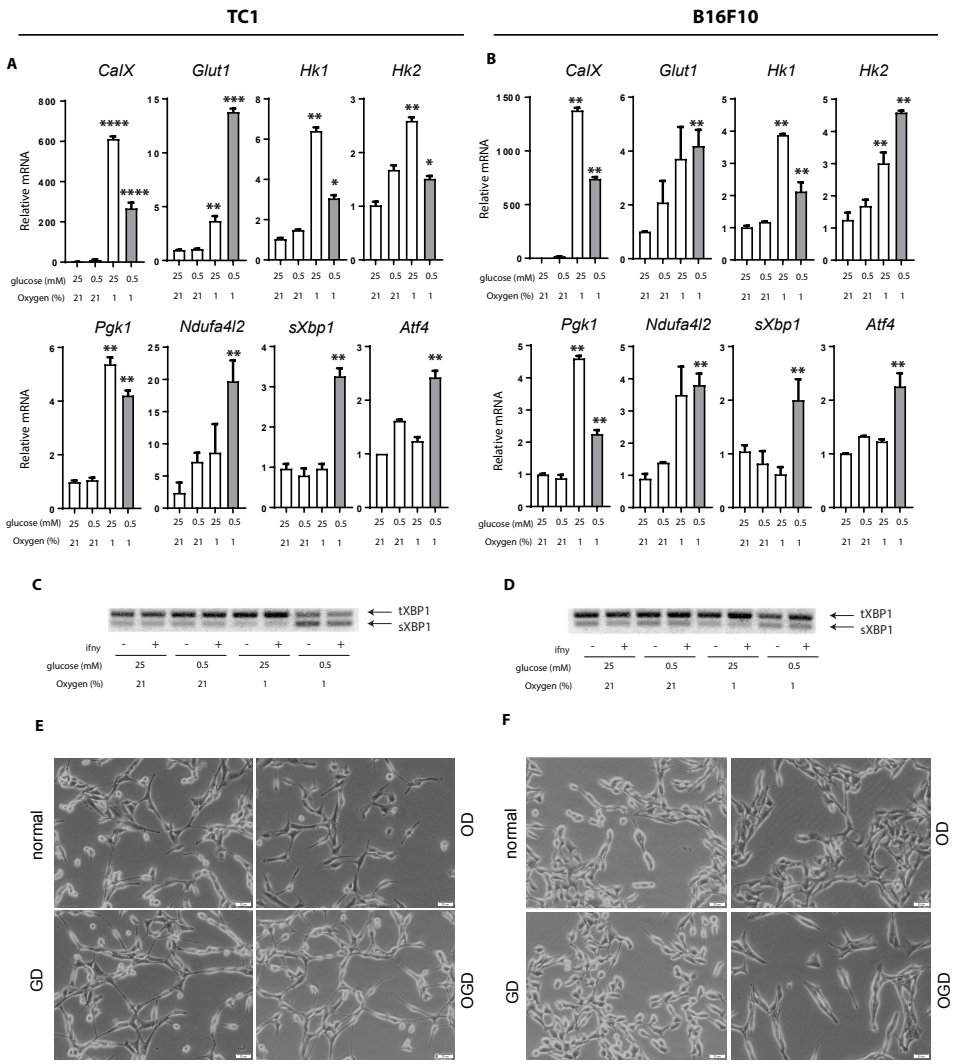

Supplemental figure 1: Cellular adaptions to oxygen and/or glucose deprivation

(A, B) mRNA expression of genes associated with glycolysis, OXPHOS and UPR response regulation in TC1 (A) and B16F10 (B) tumor cells. (C, D) PCR fragments of *total Xbp1* and *spliced Xbp1* by agarose separation and ethidium bromide visualization of TC1 (C) and B16F10 (D) tumor cells with or without stimulation with IFNy for 24h. (E, F) Microscopic images of TC1 (E) and B16F10 tumor cells (F) cultured for 24h under normal, OD, GD, or OGD conditions. Magnification 100x. All data is shown as mean of triplicates with +/-SD (n=3). Unpaired t test was used to calculate significance; n.s., not significant; *, p<0.05, **; p<0.01; ***, p<0.001.

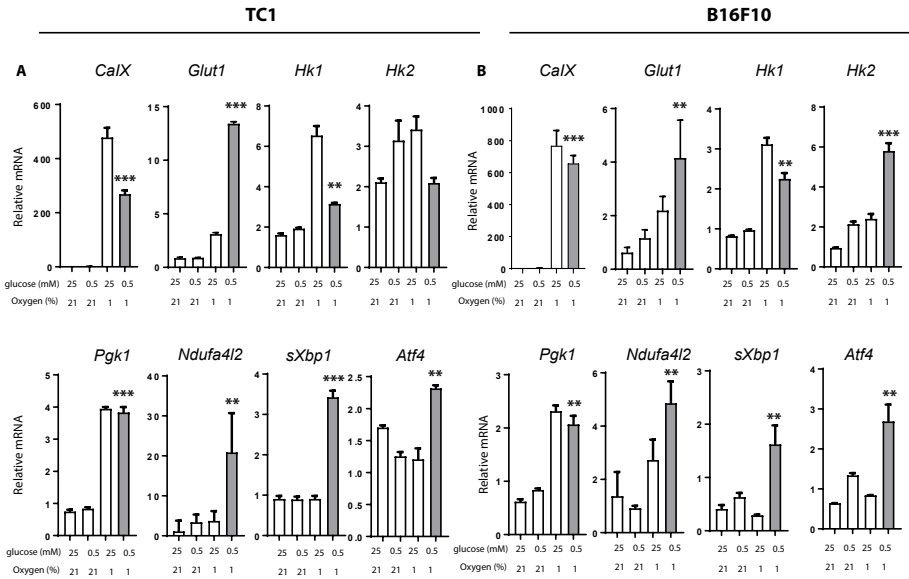

Supplemental figure 2:

Tumor cells were cultured under normal, OD, GD, or OGD conditions and stimulated with IFNγ for 24h. (A, B) mRNA expression of genes associated with glycolysis, OXPHOS and UPR response regulation in TC1 (A) and B16F10 (B) tumor cells. Representative data is shown as mean of triplicates with +/-SD (n=3). Unpaired t test was used to calculate significance; n.s., not significant *, p<0.05, **, p<0.01, ***, p<0.001.

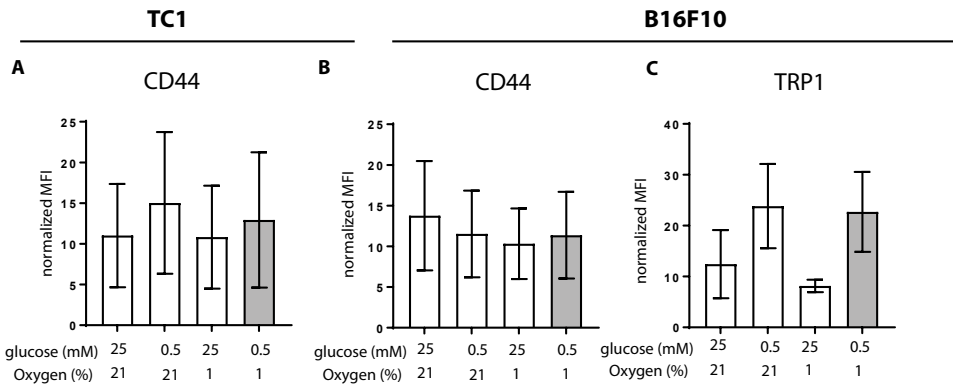

Supplemental figure 3:

Tumor cells were cultured under normal, OD, GD, or OGD conditions and stimulated with IFNy for 24h. (A, B) CD44 surface expression on TC1 (A) and B16F10 (B) tumor cells measured by flow cytometry. (C) TRP1 surface expression on B16F10 tumor cells measured by flow cytometry. Data is shown as mean with +/-SD of normalized MFI (n=3).

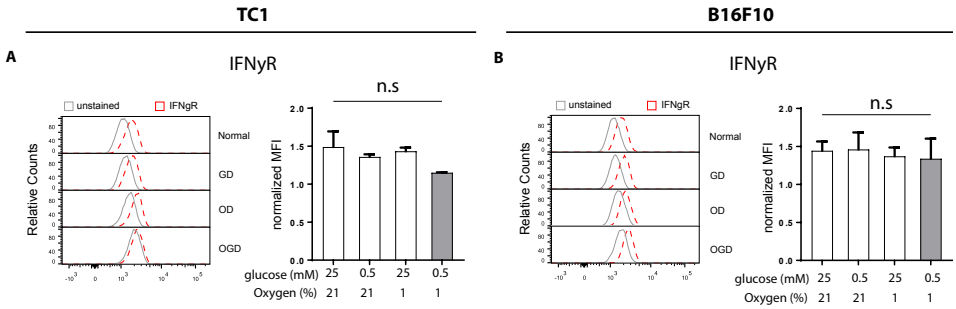

Supplemental figure 4:

Tumor cells were cultured under normal, OD, GD, or OGD conditions and stimulated with IFNy for 24h. (A, B) Histogram plot and quantification of IFNyR expression of TC1 (A) and B16F10 (B) tumor cells measured by flow cytometry. Quantified data is shown as normalized MFI (n=3). Unpaired t test was used to calculate significance; n.s., not significant.

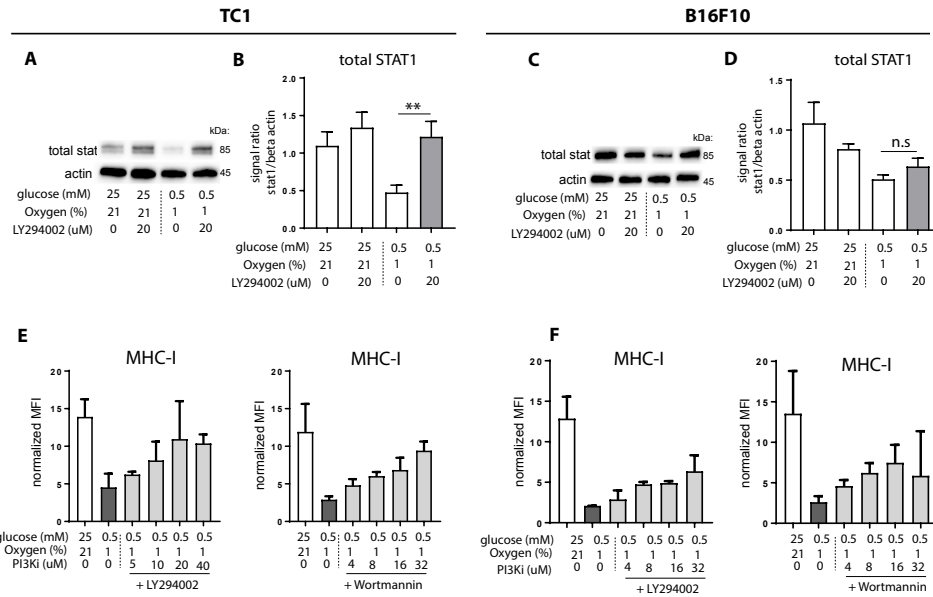

Supplemental figure 5:

(A, C) Western-blots of total STAT1 protein expression in TC1 (A) and B16F10 (C) when cultured under normal, OG, DG, and OGD conditions with IFNγ stimulation for 24h. Representative data of three experiments is shown (B, D) Quantified data of Western-blot results of A and C. Data was quantified by calculating signal ratio between protein of interest and beta-actin. (E, F) Dose-response effect of restored MHC-I expression on OGD cultured tumor cells treated with increasing concentrations of LY294002 or wortmannin in TC1 (E) or B16F10 (F) tumor cells (n=3). Data is shown as normalized MFI. Unpaired t test was used to calculate significance; n.s., not significant *, $p<0.05$, **, $p<0.01$, ***, $p<0.001$.

Supplementary table 1. Primers used for qPCR.

Primer name	Primer sequence forward (5'-3')	Primer sequence reverse (3'-5')
Ubc	GCCCAGTGTTACCACCAAGA	CCCATCACACCCAAGAACA
Stat1	CCCCATGGAAATCAGACAGT	GAGAAAAGCGGCTGTACTGG
Tap1	ATGCCTTCGCTATCAGTTA	GAGAATCAAGAGAACCAGAAC
$H2k^b$	GGAAGGAGCAGTATTACAC	CAAGGACAACCAGAACAG
$H2d^b$	ATCTCTGTCGGCTATGTG	TTGGCTTTCTGTGTTTCC
IFNyR	TTGAACCCTGTCGTATGCTG	TCAGAAATGTTGGTGCAGGA
CaIX	CACAGTCATTGGAGCTATGGAG	GCTGGAGCTCATAACCCAGA
Glut1	GCAGTTCGGCTATAACACTGG	AACAAAGAGGCCGACAGAGA
Hk1	AGATGCTGCCAACCTTTGTC	ACGATGTTCTCTGGGGTGTC
Hk2	GAAGATGCTGCCCACCTTT	TTCTCCATCTCCACCCTCTG
Pgk1	TAGAGCCAGTTGCTGCTGAA	GCATCTTTTCCCTTCCCTTC
Irf1	ACCCTGGCTAGAGATGCAGA	AGGCATCCTTGTTGATGTCC
Ndufa4l2	TGATTGGCTTCATCTGCTTG	ACTGGTCATTGGGACTCAGG
Atf4	GCCGGTTTAAGTTGTGTGCT	CTGGATTCGAGGAATGTGCT
sXbp1	GAGAACCAGGAGTTAAGAACACG	GAAGATGTTCTGGGGAGGTGAC
tXbp1	GAATGGACACGCTGGATCCT	GCCACCAGCCTTACTCCACTC

Overview of primer sequences used for qPCR analysis.

Chapter 4

TEIPP antigens for T-cell based immunotherapy of immune-edited HLA class I^{low} cancers

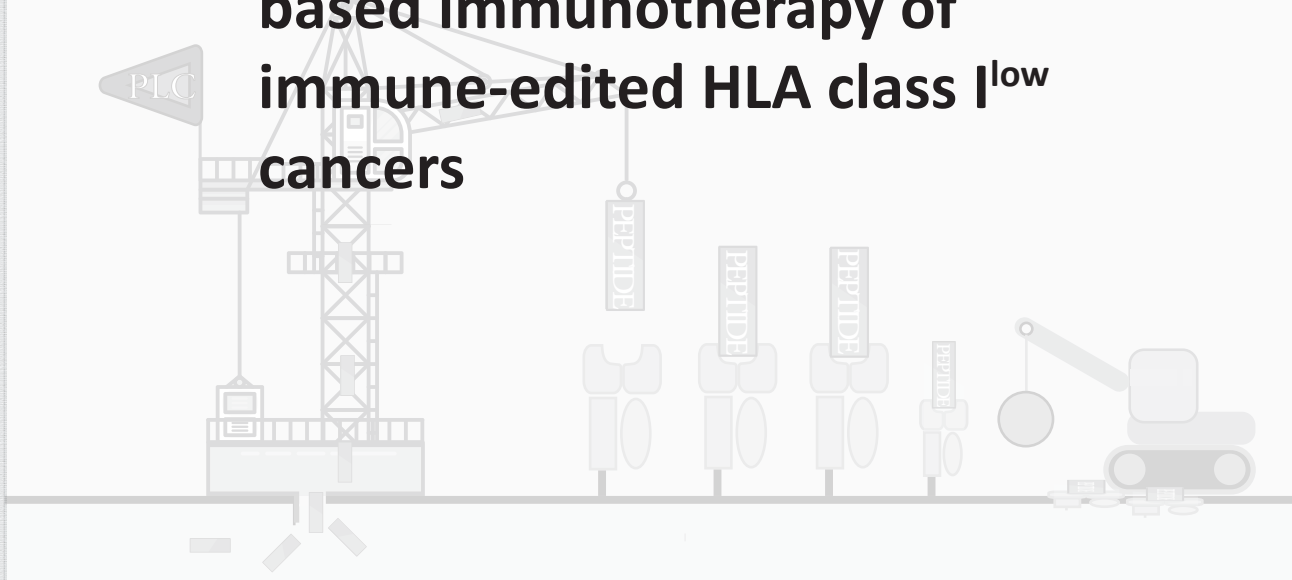

K. A. Marijt, *E. M. Doorduijn, and T. van Hall*

Molecular Immunology. pii: S0161-5890(18)30108-1.
doi: 10.1016/j.molimm.2018.03.029 (2018)

Abstract

T-cell based immunotherapies through checkpoint blockade or adoptive transfer are effective treatments for a wide range of cancers like melanomas and lung carcinomas that harbor a high mutational load. The HLA class I and class II (HLA-I and HLA-II) presented neoantigens arise from genetic mutations in the cancerous cells and are ideal non-self targets for the T cell-based treatments. Although some cancer patients responded with complete regression, many others are irresponsive to checkpoint blockade treatments, or relapse after initial success. One of the mechanisms by which tumors evade T cell recognition is by acquiring deficiencies in the HLA-I antigen-processing pathway, leading to downregulation of HLA-I molecules at the cell surface and thereby creating an 'invisible' tumor phenotype. Interestingly, an alternative antigen repertoire arises on these HLA-I^{low} cancer cells. We refer to this alternative antigen repertoire as TEIPP: T cell epitopes associated with impaired peptide processing. TEIPP antigens are curious non-mutated peptides from housekeeping proteins that are not presented in homeostasis. In this review, for the first time we recapitulate all our published work on TEIPP antigens, including our recent understanding of the CD8 T cell repertoire. We are convinced that TEIPP-directed T cells will be valuable resources to target immune-edited tumors that have acquired resistance to checkpoint blockade therapy.

Introduction

Great progress has been made in using the host's immune system to fight cancers and T-cell based immunotherapies have shown to be successful in treating patients with many different human cancers, including melanomas, lung- and renal cell carcinomas and lymphomas. Especially immune checkpoint inhibition therapies with blocking antibodies to PD-1, PDL-1, and CTLA4 proved to be effective in many patients[1-4]. Interestingly, patients who, after an initial response, become refractory to checkpoint blockade therapy have been shown to carry tumors with mutations in the interferon-γ signal transduction pathway[5,6]. Inactivating mutations in the JAK1/2-STAT1 cascade effectively renders tumors 'deaf' for interferons and thereby tumor cells acquire resistance to its anti-proliferative signals. In addition, these mutations were shown to strongly hamper the capacity of tumor cells to present endogenous antigens by HLA-I molecules[7,8]. As a result, the checkpoint-induced T cell attack becomes futile. Genetic mutations or epigenetic silencing of HLA-I molecules or components of the intracellular processing machinery, like the peptide transporter TAP, similarly result in immune-edited HLA-I^{low} tumors[9,10].

Nearly a decade ago, we published a first report on a new category of tumor antigens that arises on such immune-escaped tumors and refer to them as TEIPP[11]. TEIPP-specific T cells are able to selectively recognize TAP-deficient, HLA-I^{low} tumors, whereas conventional T cells were unable to do so. TEIPP antigens are non-mutated self-antigens and derive from housekeeping proteins. Since then we examined why TEIPP antigens are not presented on normal cells; how safe the exploitation of TEIPP antigens is; if TEIPP T cells are hampered by central tolerance in the thymus; if they actually exhibit similar T cell functions as conventional T cells; and the ultimate question: if TEIPP T cells can effectively be used for immune-edited cancers.

TEIPP as a new category of tumor antigens

Antigen-specific T cells are able to recognize peptide/MHC complexes on the surface of almost all nucleated cells. The peptides loaded into these MHC-I molecules are degradation products of intracellular proteins. Aged and misfolded proteins, or defective ribosomal products (DRIPs) are degraded by the multicatalytic proteasome in the cytosol[12]. The generated peptides are then translocated into the endoplasmic reticulum (ER) by the peptide transporter TAP where they have access to MHC-I in the peptide loading complex (PLC), consisting of chaperones like tapasin, ERp57 and calreticulin and trimming enzymes like ERAAP[13]. Subsequently, the stabilized peptide:MHC-I complexes egress to the cell surface and can be recognized by surveilling CD8 T cells.

The first tumor antigens that were exploited for immune therapy belong to the subset of commonly expressed proteins called tumor-associated antigens (TAA). TAAs are often non-mutated antigens that are (ectopically) overexpressed in cancers. Until now most therapies have focused on TAAs like the melanoma differentiation antigens MART-1, tyrosinase and gp100. Unfortunately, most clinical trials targeting TAAs failed to show success, possibly due to central and peripheral immune tolerance mechanisms resulting in less potent T cells[14]. Another category of tumor-associated antigens are cancer testis antigens (CTA). CTAs belong to a group of tumor antigens expressed on tumors and in the testis, which include MAGE-1 and NY-ESO. However, many CTAs are only expressed on a restricted number of tumor types and it is now known that presentation of CTAs is also found in low levels on healthy cells, making them less favorable to use in a therapeutic setting[15].

Tumor-specific antigens (TSA) are a subset of highly immunogenic tumor antigens specific for transformed cancerous cells. This includes peptides derived from oncogenic viruses, like the human papilloma virus (HPV), which can cause head- and neck carcinomas or cervical neoplasms. These HPV-transformed cancer cells present virus-derived E6 and E7 peptides on the surface and therapeutic vaccination against E6 and E7 antigens has shown great successes in pre-malignant lesions[16]. Another important category of TSAs are neoantigens derived from the accumulation of genetic mutations in cancer cells. Personalized designed vaccination against neoantigens showed great responses in melanoma patients[17,18] and checkpoint therapy-induced immune responses are frequently directed towards these personal point-mutated antigens[19-21]. Therefore this category of unique and tumor-specific T cell epitopes are at the forefront of scientific interest at the moment.

HLA class I downregulation

The vast majority of the tumor antigens described above require proteasome activity and peptide transport by TAP[22]. However, most tumors eventually develop resistance and evade immune recognition[23-25]. Immunotherapy resistance can be described by 3 categories, namely, “primary resistance”, “adaptive resistance”, and “acquired resistance”[24]. It has become clear that tumors can develop resistance against immune recognition by downregulation of HLA-I levels and thereby resist T cell immunity and checkpoint therapy[7,26]. HLA-I down modulation in cancers is frequently found, in 50% of the primary prostate carcinomas, 43% of the primary breast carcinoma, and approximately 30% of the primary lung, colon, and cervical carcinomas[27]. In metastatic prostate lesions, HLA-I downregulation occurred in 70% of the investigated samples, whereas 50% of the analyzed metastatic melanoma, breast, and cervical lesions had downregulation of HLA class I expression[26,27]. Many components of the peptide processing machinery were lost in human cancer cell lines including LMP-2, LMP-7 as well as the peptide transporter TAP1[28].

Histological protein expression analysis of the peptide transporter chain TAP1 on different tumor types showed downregulation in 6% of the head and neck carcinoma up to 56% in melanomas[26,27]. Remarkably, more than 80% of the metastatic melanoma lesions and metastatic cervical carcinomas showed down regulated TAP1 expression[26,27]. But also patients who initially respond to immune-therapy can relapse over time due to shutdown of antigen presentation. In melanoma patients approximately one forth to one third of the patients who responded to anti-CTLA4 of anti-PD1 therapy will relapse over time[29]. The cancer cells "acquire" mechanisms to resist therapy. Two recent studies showed that tumors from patients relapsing ("acquired resistance") or not responding to checkpoint inhibitor therapy ("primary resistance") had mutations in genes encoding the IFN-γ pathway, including JAK/STAT signaling[5,6]. The failure of these tumors to respond to IFN- γ signaling rendered them, among other effects, resistant to up-regulation of HLA-I expression and consequently less targetable for tumor-specific T cells. Several other studies recently revealed the dominance of acquired IFN-γ resistance during immunotherapy[7,8,30]. Additionally, in another case of late acquired resistance to anti-PD1 therapy the resistant cells had a homozygous truncation mutation in β2M leading to absence of HLA-I molecules on the cell surface[6]. Finally, acquired resistance has also been reported in a patient with metastatic colorectal carcinoma who initially responded to TIL therapy recognizing mutated KRAS G12D presented by HLA-C*08:02[31]. The refractory tumors showed loss of HLA-C*08:02 by mutations in chromosome 6. These examples illustrate that defects in the peptide-processing pathway are an often adopted strategy of "immune resistance" where a cancer is initially recognized by the immune system but edited to evade T cell recognition (see Fig 1). Any defect in the TAP-dependent antigen processing pathway or HLA-I gene expression will lead to failure to present conventional tumor antigens and turns these tumors 'invisible' for T-cell immunity.

TEIPP: tumor antigens on immune-edited cancers

Interestingly, defects in the antigen processing machinery can give rise to the presentation of a new category of tumor antigens called TEIPP: T-cell epitopes associated with impaired peptide processing. TEIPP antigens are non-mutated tumor antigens that have an alternative antigen-processing route and are only presented on tumor cells with defects in the conventional proteasome-TAP-mediated peptide-processing pathway. Presentation of this alternative peptide repertoire has been shown on cells deficient for TAP, as well as cells deficient for the ER-resident amino peptidase ERAAP[11,32]. Targeting TEIPP antigens offers an opportunity for immune-therapy on tumor cells that adopted a resistance mechanism to evade the immune system (see Fig 1).

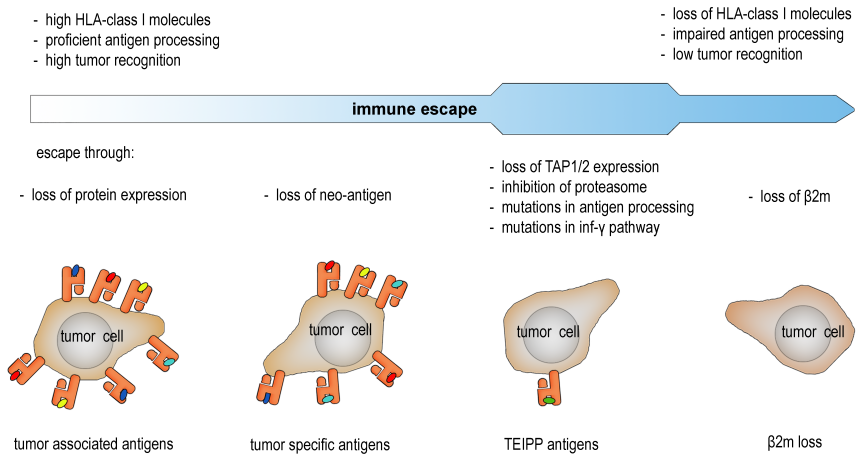

Figure 1. Tumor immune-editing and immune defense strategies.

Cancers develop several escape mechanisms under selective pressure of T cell immunity. Tumor cells with immunogenic neo-antigens can lose their mutated epitope to evade T cell recognition. Alternatively, tumor cells can down regulate the overall expression of HLA class I molecules so immunogenic epitopes are not "visible" anymore for surveilling T cells. It has been described that 35-90% of tumors down modulate HLA class I expression. Interestingly, those HLA class I^{low} tumors present a new set of tumor antigens, known as 'T cell epitopes associated with impaired peptide processing' (TEIPP). Tumor cells with complete loss of HLA class I might therapeutically be targeted by natural killer cells. This figure is adopted from reference[74].

The first identified mouse TEIPP tumor antigen is derived from the Trh4 protein, a ceramide synthase and fatty acid regulator that spans the ER membrane multiple times[11]. TEIPP-specific CD8 T cells were established by immunizing syngeneic mice with TAP-deficient RMA-S tumor cells expressing the co-stimulatory molecule CD80, followed by *in vitro* re-stimulations. Several T cell clones were isolated specific for the TAP-deficient RMA-S tumor cells and cross-reacted to non-transformed TAP-deficient B cell blasts, but not the TAP-proficient counterparts. T cells had different MHC-I restrictions. Some recognized peptide antigens when presented by the classical MHC class I molecules H-2D^b or H-2K^b as well as the conserved non-classical Qa-1^b, showing a broad T cell repertoire[11]. Using a T-cell Receptor (TCR)-transgenic mouse based on the Trh4-specific T cell clone, we showed that activated TEIPP-specific T cells could control outgrowth of MHC class I^{low} tumors [33,34]. Importantly, no signs of adverse autoimmune reactivity was observed using these T cells, as expected since the TEIPP antigen presentation is restricted to TAP-deficient tumor cells.

Alternative antigen processing pathways

TAP-independent processing pathways are able to partly compensate for the loading of peptides in HLA class I molecules[35]. Although not all processing pathways of TEIPP peptides are known, several alternative peptide-processing routes have been described. Of these, the processing of signal peptides is best known. Proteins intended for cell surface display or extracellular secretion contain a signal peptide, an address code that directs their translocation into the ER lipid bilayer via the Sec61 protein-conducting channel[36]. After insertion into the protein-conducting channel, most signal peptides are cleaved from the preprotein by the proteolytic enzyme signal peptidase (SP)[37]. Subsequently, the signal peptide peptidase (SPP) is responsible for the intramembranous cleavage of the signal peptide stump that is trapped in the ER-membrane, which is thereby released from its intramembrane location[38]. Peptide fragments fall into the ER lumen where they can bind HLA-I molecules[39]. Biochemical analysis of the peptide repertoire of TAP-deficient T2 cells confirmed that signal sequence-derived peptides are efficiently processed and presented at the cell surface of TAP-negative cells[40-42]. The signal peptide of the human calcitonin protein encoded by the CALCA gene is an example of how peptides can be TAP-independently processed and are able to elicit an T cell immune response[43]. Interestingly, SPP-mediated liberation of peptides is not limited to signal peptides. We discovered that the prototypic TEIPP antigen in our mouse model of which the epitope is located at the very C-terminus of the protein is also cleaved by this proteolytic enzyme[44].

A second mechanism that enables peptides to be loaded into MHC-I without functional TAP is operated by members of the protein convertase family, like furin[45-47]. Amino acids located at the C-terminal end of secreted proteins can be cleaved by furin in the Golgi and subsequently gain access to HLA-I molecules. In our research on TEIPP antigens, we found T cell epitopes that were liberated by the proteasome, but gained access to MHC-I molecules in a TAP-independent pathway in the vesicular system[48]. Interestingly, a surprising dominant role for metalloproteinases was found for the TAP-independent route[48,49]. Clearly, there are multiple roads that lead to Rome and in the absence of conventional antigen processing, an alternative peptide repertoire becomes exposed on tumor cells in the context of HLA[50]. These novel antigens and their specific T cells are therefore suitable candidates for the treatment of tumors that have escaped from conventional T-cell based immunotherapies.

Why are TEIPP antigens not presented by normal cells?

TEIPP antigens are derived from housekeeping proteins, expressed by all cells. But why are TEIPP antigens then only presented by TAP-deficient cells and not their TAP-proficient counterparts? Our main hypothesis is that TEIPP peptides are outcompeted in the ER by

the overwhelming quantities of TAP-imported peptides. This hypothesis is supported by the fact that TAP-imported peptides are normally chaperoned into the MHC class I molecules due to the peptide loading complex (PLC). The TAP transporter is physically linked to MHC-I in the PLC via tapasin and thereby bridges these protein complexes[12]. Thus, TAP-independent peptides that found their way into the ER via alternative mechanisms will have difficulty to find empty HLA-I molecules. In the absence of TAP, more HLA-I molecules are available for binding TEIPP peptides without the competition of the massive number of the normal peptide repertoire. We tested this notion in two systems, using the molecularly characterized mouse TEIPP derived from the Trh4 protein and human TEIPP derived from the calcitonin protein[51,52]. We found that overexpression of the proteins that comprise TEIPP peptides in TAP-proficient cells resulted in MHC-I surface display of the respective TEIPP peptides, indicating that higher availability of TEIPPs in the ER successfully overcomes the peptide competition. In addition, gradual increase of TAP expression led to paralleled surface display of TEIPP, implying that the peptide transporter functions as a lever of control for the competing peptide repertoires[51,52]. The alternative hypothesis that TEIPP peptides are weak binders and fail to bind HLA class I molecules in the presence of the normal repertoire was abandoned, since the Trh4 peptide is a stable and high affinity peptide that was superior to all other tested peptides[51]. Not much is known yet on the broadness of the TEIPP repertoire, but biochemical characterization of peptides eluted from TAP-deficient cells showed a significant number of non-mutated peptides with binding affinities from high to intermediate[40].

Determination of the TEIPP Trh4/H2-D^b structure

The Trh4 peptide in the context of the H-2D^b was crystallized in order to determine its structure[53]. Nearly all identified T-cell epitopes presented on H-2D^b have an asparagine at position 5 and an aliphatic amino acid at the C-terminal position, acting as main anchor positions[54,55]. Interestingly, the peptide sequence of the Trh4 epitope does not follow this conventional H-2D^b binding motif, but instead has several sulfur-containing amino acids: methionines at positions 1, 5, and 9 and a cysteine at position 2. This resulted in a slightly modified positioning in the peptide-binding groove, which was found to be essential for T cell recognition. Replacement of position 5 with the traditional asparagine led to an altered binding configuration and failure of T cell activation[53]. Since this is the first crystal of a TEIPP antigen, its general implications remain elusive.

Thymic development of TEIPP T cells

T cells development takes place in the thymus and self MHC molecules shape a personalized repertoire of T cells that egress to the periphery[56,57]. In the outer cortex of the thymus the immature thymocytes interact with MHC-I and -II molecules. Thymocytes that fail to interact to self MHC molecules die by neglect and those binding with a too high avidity are deleted by apoptosis to prevent the development of self-reactive T cells. Positive selection occurs by intermediate avidity interaction of thymocytes with peptide:MHC complexes. Since TEIPP antigens constitute non-mutated peptides derived from housekeeping proteins, the question arises whether the TEIPP-specific CD8 T cell repertoire is hampered by central tolerance in the thymus. Analysis of different thymic cell populations showed that indeed the Trh4 gene transcripts are expressed by medullary thymus epithelial cells (mTECs), dendritic cells as well as macrophages[51], as expected from a housekeeping gene. However, thymus cells of wild type, TAP-proficient mice were not recognized by the TEIPP-specific T cell clone, showing that the epitope is not presented at the surface of these cells[51]. In agreement with this finding, we observed that a transgenic TCR efficiently mediated positive selection in the thymus of wild type mice, in contrast to the thymus of TAP-deficient mice[33] (see Fig 2). Strong and efficient thymus deletion was observed in the TEIPP-presenting latter mice.

In vitro and *in vivo* analysis of these TCR-transgenic T cells revealed that TEIPP T cells remained "untouched": they were naïve in the periphery and did not proliferate when transferred into wild type mice, even under inflammatory conditions[33]. Importantly, the CD8 T cells exhibited full effector functions when transferred into TAP-deficient mice or when stimulated by peptide vaccination with either short or long Trh4 peptide[33]. These data show that in a normal, TAP-proficient environment, TEIPP-specific T cells do not become activated, unless they are specifically activated by a vaccine. Collectively, we showed that the TEIPP T cell repertoire is efficiently selected in the thymus and emerges in the periphery in a naïve state, even though the housekeeping proteins that comprise the TEIPP antigens are widely expressed. The critical step of surface display in MHC-I molecules is induced by defects in the processing pathway, like TAP-deficiency, and results in full blown activation of the T cells. Thus, TEIPP antigens are strong neoantigens, although they derive from non-mutated self-proteins.

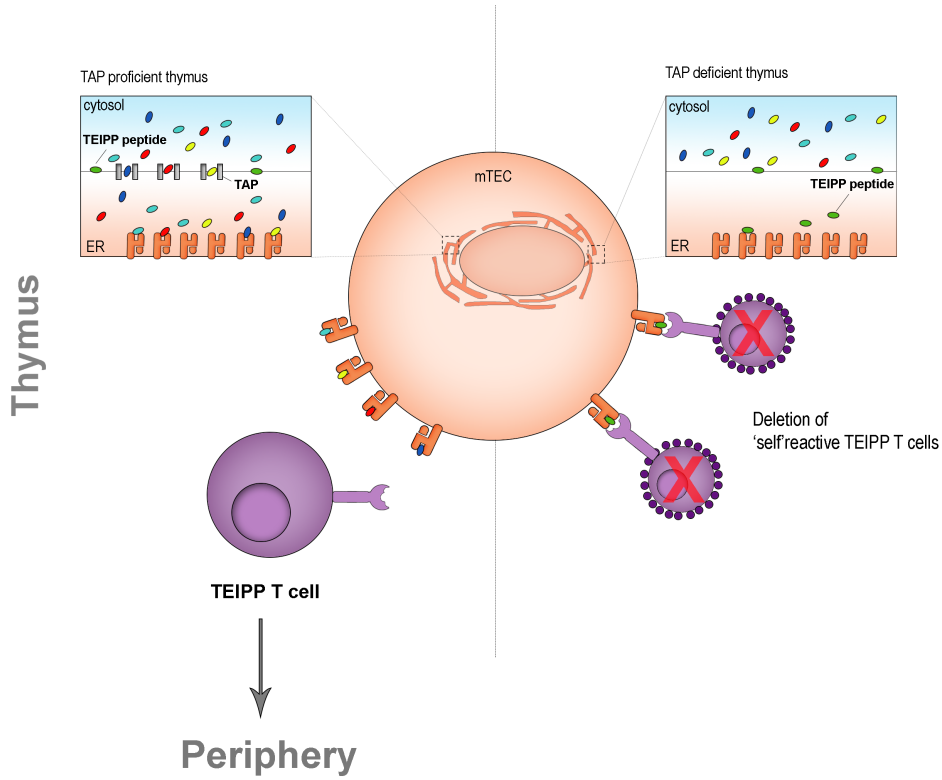

Figure 2. Thymus selection of TEIPP T cells

TEIPP antigens are peptides from normal non-mutated self-proteins, but selectively presented in MHC class I of cell with defects in the antigen processing machinery. TEIPP epitopes are therefore not presented at the surface of medullary thymus epithelial cells and TEIPP T cells are not deleted (left side of the figure), unless the peptide transporter TAP is deleted (right side of the figure). Consequently, TEIPP-specific T cells are efficiently selected in the thymus and arrive in the periphery in a naïve state. Results of these studies were published in reference[33].

Behavior of TEIPP-specific T cells in the presence of immune-edited tumors

How do TEIPP-specific T cells behave in tumor-bearing mice and how can we exploit TEIPP antigens in a therapeutic setting? One of the unique characteristics of TEIPP antigens is that they are presented on MHC-I^{low} cells, whereas the professional antigen-presenting host cells, responsible for the induction of CD8 T cell responses, have optimal processing and presentation capacities for antigens. We therefore transferred naïve TCR-transgenic TEIPP T cells in mice bearing MHC class I^{low} tumors and investigated their fate[34]. Interestingly, the T cells still remained naïve and tumors grew progressively. How is it possible that

TAP-deficient tumors did not activate TEIPP T cells? This is probably due to the fact that TEIPP peptides are poorly cross-presented by host dendritic cells due to their alternative processing. Signal peptides of proteins are co-translationally chopped off and thus might easily be lost in the tumor debris. An elegant study demonstrated that signal peptides indeed poorly gain access to host dendritic cells and fail to induce T cell responses[58]. Moreover, direct priming of T cells by the tumors did also not happen because of the very low levels of MHC class I. In our recent study, we showed that enhanced expression of MHC-I molecules on the surface of tumor cells in combination with increased levels of the TEIPP tumor antigen or artificial introduction of co-stimulatory molecules resulted in efficient priming of TEIPP T cells via direct priming[34]. Alternatively, TEIPP T cells can be activated by peptide vaccination, which is much easier to translate to the clinic[33]. Once activated, TEIPP T cells potently infiltrated MHC-I^{low} tumors and efficiently controlled their outgrowth. In that sense, the continued naïve status of this T cell subset is an advantage, because tumor-induced suppressive mechanisms do not hold a grip on them. On the other hand, their therapeutic exploitation firstly requires priming and activation of TEIPP T cells. Due to the high specificity of TEIPP antigens on cancer cells, adoptive T cell transfer, peptide vaccination, or TCR gene transfer are all potentially effective methods to reach a safe recruitment of these immune cells.

Do TEIPP T cells also exist in human?

Most of our results have been obtained in mouse tumor models and, thus far, much less is known on TEIPP antigens in humans. The first molecularly identified TEIPP antigen in humans originates from the signal peptide of the CALCA gene[43,52]. Several CD8 T cell clones recognizing autologous tumor cells were isolated from a lung cancer patient and the peptide-epitope of one clone was derived from the non-mutated signal peptide of the preprocalcitonin protein. Treatment of the autologous tumor cells with the proteasome inhibitor epoxomicin had no effect on the recognition and inhibition of TAP resulted in better presentation of this peptide by HLA-A2[52]. Conventional CD8 T cells recognizing the same lung carcinoma displayed a complete opposite reactivity pattern, showing that these two T cell clones represented complementary specificities. As far as we know, this is the first described human TEIPP antigen.

In our efforts to disclose additional human TEIPP antigens, we first utilized an approach in which dendritic cells were rendered TAP deficient by introduction of viral immune evasion proteins and incubated them with autologous T cells. Several herpes viruses encode dedicated molecules to shutdown MHC-I presentation in order to evade T cell recognition and elimination. The peptide transporter TAP is the bottleneck in the pathway and therefore an ideal target for these chronic viruses. Currently, four herpes viral genes have been

described that are able to inhibit human TAP function[59,60]. The Human Cytomegalo Virus (HCMV) US6 protein prevents ATP binding to TAP and thereby inhibits peptide translocation to the ER. ICP47 is encoded by the Herpes Simplex Virus (HSV) and prevents peptide translocation by physically obstructing the peptide-binding site of TAP. UL49.5 protein synthesized by the Bovine Herpes Virus 1 (BoHV-1) inhibits TAP by preventing structural rearrangements required for peptide transport and mediates degradation of the protein. Finally, BNLF2a encoded by Epstein Barr Virus (EBV) prevents both peptide and ATP binding to TAP.

After introduction of UL49.5 in human dendritic cells and co-culture with autologous CD8 T cells, we were able to generate TEIPP-specific T cells from all tested PBMC of healthy individuals[61]. All characterized T cell clones were reactive to target cells expressing either of the four TAP-inhibitors and were restricted by different HLA-I molecules, revealing a diverse repertoire of TEIPP antigens. The TEIPP epitopes were, however, not identified at the molecular level. In order to uncover the identity of human TEIPP we recently started a bioinformatics-based approach in which we predicted TEIPP antigens from the complete human proteome. We were able to identify 15 new TEIPP antigens presented by HLA-A2 and recognized by CD8 T cells (K.A. Marijt, unpublished data). Preliminary results revealed that some of these TEIPP-specific T cells were present in the naïve T cell repertoire, as expected based on our findings in mouse models, but others were isolated from the antigen-experienced memory pool of T cells. This could be explained by the fact that herpes viruses like EBV and HCMV cause latent infections and are never cleared in humans. In the active episodes of infections, these viruses express their TAP-inhibiting proteins and might thereby induce TEIPP-specific T cells. However, this remains speculation at the moment and further investigation is necessary.

TEIPP tumor antigens and HLA-E

HLA-E and its mouse homologue Qa-1^{b} are non-classical MHC class I molecules and are expressed on almost all nucleated cells[62]. The unique feature of HLA-E is its extremely conserved nature in the human population and across species. In contrast to the polymorphic classical class I molecules, only two functional alleles exist in humans(E*0101 and E*0103), which vary in one amino acid at a position outside the peptide-binding groove[63]. HLA-E has a function in natural killer (NK)-cell biology as it is the ligand of the inhibitory receptor NKG2A/CD94. The monomorphic and conserved peptides bound in the groove of HLA-E are derived from other HLA-I molecules, thereby serving as a sensor for integrity of the antigen processing pathway. Defects in ERAAP, tapasin, proteasome and TAP all result in the failure to present the dominant monomorphic peptide[62]. Therefore, inhibition of the antigen processing machinery does not only affect the expression of classical MHC-I mole-

cules, but also strongly affects the non-classical HLA-E[64]. Instead of a monomorphic peptide, a wide array of alternative peptides emerges in HLA-E when the TAP peptide transporter is abrogated[65]. A similar alternative peptide repertoire was demonstrated in the mouse Qa-1^b in TAP-deficient tumor cells[66]. Interestingly, these Qa-1^b presented TEIPP peptides were immunogenic and served as neoantigens [66,67]. T cells engaging these TEIPP peptides bound Qa-1^b molecules revealed unique TCR composition of a shared Vα chain with a variety of Vβ chains (van Hall et al., 2018). Of note, inhibition of the ER-resident amino peptidase ERAAP also results in presentation of neoantigens by $Qa1^b$, which triggered a strong CD8+ T cell response[68]. The conserved nature of HLA-E in the human population and the very monomorphic peptide repertoire in homeostasis renders this molecule an ideal TEIPP target for future investigations.

Conclusions and perspectives

Overall, our studies in both mice and man on TEIPP antigens and their cognate CD8 T cells reveal a potent and specific branch of immunity to cancers, predominantly those with defects in the antigen processing machinery (see Fig 1). These deficiencies are rather common in human cancers and are a witness of close interactions with and selective pressure by conventional T cell immunity. TEIPP antigens are a very interesting complementary player for immunotherapy of cancer in order to include immune-edited tumors[69,70]. Cancers with a complete loss of HLA class I molecules, e.g. through loss of β2m, are not sensitive for CD8 T cells at all and need to be targeted by naturel killer cells (see Fig 1). Compared to other categories of tumor antigens, TEIPP antigens are ideal targets: they are tumor specific, immunogenic and shared (see Table I). TEIPP antigens presented by the conserved HLA-E molecule might represent the ultimate holy grail, especially since this class I is often upregulated by tumors[71-73]. However, we still lack detailed knowledge of HLA-E restricted T cells and it is difficult to predict if this repertoire behaves like conventional CD8 T cells. How will we translate this concept to clinical practice? Activation and recruitment of the TEIPP T cell subset can be reached by vaccination with synthetic peptides or one could transfer cloned TEIPP TCRs. However, we would prefer to exploit the full breadth of the TEIPP antigens instead of single epitopes, and RNA-based strategies that silence TAP in host dendritic cells might be successful in reaching this goal.

Acknowledgements

Koen A. Marijt and Elien M. Doorduijn were funded by grants of the Dutch Cancer Society (UL 2013-6142 and UL 2010-4785, respectively).

References

1 Larkin, J., Hodi, F. S. & Wolchok, J. D. Combined Nivolumab and Ipilimumab or Monotherapy in Untreated Melanoma. *The New England journal of medicine* **373**, 1270-1271, doi:10.1056/NEJMc1509660 (2015).

2 Dranoff, G. Immunotherapy at large: Balancing tumor immunity and inflammatory pathology. *Nature medicine* **19**, 1100-1101, doi:10.1038/nm.3335 (2013).

3 Delamarre, L., Mellman, I. & Yadav, M. Cancer immunotherapy. Neo approaches to cancer vaccines. *Science* **348**, 760-761, doi:10.1126/science.aab3465 (2015).

4 Chen, D. S. & Mellman, I. Elements of cancer immunity and the cancer-immune set point. *Nature* **541**, 321-330, doi:10.1038/nature21349 (2017).

5 Gao, J. *et al.* Loss of IFN-gamma Pathway Genes in Tumor Cells as a Mechanism of Resistance to Anti-CTLA-4 Therapy. *Cell* **167**, 397-404 e399, doi:10.1016/j.cell.2016.08.069 (2016).

6 Zaretsky, J. M. *et al.* Mutations Associated with Acquired Resistance to PD-1 Blockade in Melanoma. *N Engl J Med* **375**, 819-829, doi:10.1056/NEJMoa1604958 (2016).

7 Sucker, A. *et al.* Acquired IFNgamma resistance impairs anti-tumor immunity and gives rise to T-cell-resistant melanoma lesions. *Nat Commun* **8**, 15440, doi:10.1038/ncomms15440 (2017).

8 Manguso, R. T. *et al.* In vivo CRISPR screening identifies Ptpn2 as a cancer immunotherapy target. *Nature* **547**, 413-418, doi:10.1038/nature23270 (2017).

9 Seliger, B. Novel insights into the molecular mechanisms of HLA class I abnormalities. *Cancer immunology, immunotherapy : CII* **61**, 249-254, doi:10.1007/s00262-011-1153-9 (2012).

10 Garrido, F., Cabrera, T. & Aptsiauri, N. "Hard" and "soft" lesions underlying the HLA class I alterations in cancer cells: implications for immunotherapy. *Int J Cancer* **127**, 249-256, doi:10.1002/ijc.25270 (2010).

11 van Hall, T. *et al.* Selective cytotoxic T-lymphocyte targeting of tumor immune escape variants. *Nature medicine* **12**, 417-424, doi:10.1038/nm1381 (2006).

12 Neefjes, J., Jongsma, M. L., Paul, P. & Bakke, O. Towards a systems understanding of MHC class I and MHC class II antigen presentation. *Nature reviews. Immunology* **11**, 823-836, doi:10.1038/nri3084 (2011).

13 Thomas, C. & Tampe, R. Proofreading of Peptide-MHC Complexes through Dynamic Multivalent Interactions. *Frontiers in immunology* **8**, 65, doi:10.3389/fimmu.2017.00065 (2017).

14 Melero, I. *et al.* Therapeutic vaccines for cancer: an overview of clinical trials. *Nature reviews. Clinical oncology* **11**, 509-524, doi:10.1038/nrclinonc.2014.111 (2014).

15 Morgan, R. A. *et al.* Cancer regression and neurological toxicity following anti-MAGE-A3 TCR gene therapy. *J Immunother* **36**, 133-151, doi:10.1097/CJI.0b013e3182829903 (2013).

16 Melief, C. J., van Hall, T., Arens, R., Ossendorp, F. & van der Burg, S. H. Therapeutic cancer vaccines. *The Journal of clinical investigation* **125**, 3401-3412, doi:10.1172/JCI80009 (2015).

17 Ott, P. A. *et al.* An immunogenic personal neoantigen vaccine for patients with melanoma. *Nature*, doi:10.1038/nature22991 (2017).

18 Sahin, U. *et al.* Personalized RNA mutanome vaccines mobilize poly-specific therapeutic immunity against cancer. *Nature* **547**, 222-226, doi:10.1038/nature23003 (2017).

19 Le, D. T. *et al.* Mismatch repair deficiency predicts response of solid tumors to PD-1 blockade. *Science* **357**, 409-413, doi:10.1126/science.aan6733 (2017).

20 McGranahan, N. *et al.* Clonal neoantigens elicit T cell immunoreactivity and sensitivity to immune checkpoint blockade. *Science* **351**, 1463-1469, doi:10.1126/science.aaf1490 (2016).

21 Snyder, A. *et al.* Genetic basis for clinical response to CTLA-4 blockade in melanoma. *The New England journal of medicine* **371**, 2189-2199, doi:10.1056/NEJMoa1406498 (2014).

22 Blum, J. S., Wearsch, P. A. & Cresswell, P. Pathways of antigen processing. *Annual review of immunology* **31**, 443-473, doi:10.1146/annurev-immunol-032712-095910 (2013).

23 Dunn, G. P., Bruce, A. T., Ikeda, H., Old, L. J. & Schreiber, R. D. Cancer immunoediting: from immunosurveillance to tumor escape. *Nat Immunol* **3**, 991-998, doi:10.1038/ni1102-991 (2002).

24 Sharma, P., Hu-Lieskovan, S., Wargo, J. A. & Ribas, A. Primary, Adaptive, and Acquired Resistance to Cancer Immunotherapy. *Cell* **168**, 707-723, doi:10.1016/j.cell.2017.01.017 (2017).

25 Mittal, D., Gubin, M. M., Schreiber, R. D. & Smyth, M. J. New insights into cancer immunoediting and its three component phases--elimination, equilibrium and escape. *Current opinion in immunology* **27**, 16-25, doi:10.1016/j.coi.2014.01.004 (2014).

26 Marincola, F. M., Jaffee, E. M., Hicklin, D. J. & Ferrone, S. Escape of human solid tumors from T-cell recognition: molecular mechanisms and functional significance. *Adv Immunol* **74**, 181-273 (2000).

27 Hicklin, D. J., Marincola, F. M. & Ferrone, S. HLA class I antigen downregulation in human cancers: T-cell immunotherapy revives an old story. *Mol Med Today* **5**, 178-186 (1999).

28 Restifo, N. P. *et al.* Identification of human cancers deficient in antigen processing. *J Exp Med* **177**, 265-272 (1993).

29 Robert, C. *et al.* Pembrolizumab versus Ipilimumab in Advanced Melanoma. *The New England journal of medicine* **372**, 2521-2532, doi:10.1056/NEJMoa1503093 (2015).

30 Patel, S. J. *et al.* Identification of essential genes for cancer immunotherapy. *Nature*, doi:10.1038/nature23477 (2017).

31 Tran, E. *et al.* T-Cell Transfer Therapy Targeting Mutant KRAS in Cancer. *The New England journal of medicine* **375**, 2255-2262, doi:10.1056/NEJMoa1609279 (2016).

32 Hammer, G. E., Gonzalez, F., Champsaur, M., Cado, D. & Shastri, N. The aminopeptidase ERAAP shapes the peptide repertoire displayed by major histocompatibility complex class I molecules. *Nat Immunol* **7**, 103-112, doi:10.1038/ni1286 (2006).

33 Doorduijn, E. M. *et al.* TAP-independent self-peptides enhance T cell recognition of immune-escaped tumors. *The Journal of clinical investigation* **126**, 784-794, doi:10.1172/JCI83671 (2016).

34 Doorduijn, E. M. *et al.* T cells specific for a TAP-independent self-peptide remain naïve in tumor-bearing mice and are fully exploitable for therapy. *OncoImmunology* (2017).

35 Oliveira, C. C. & van Hall, T. Importance of TAP-independent processing pathways. *Molecular immunology* **55**, 113-116, doi:10.1016/j.molimm.2012.10.005 (2013).

36 Voorhees, R. M. & Hegde, R. S. Structure of the Sec61 channel opened by a signal sequence. *Science* **351**, 88-91, doi:10.1126/science.aad4992 (2016).

37 Dalbey, R. E., Lively, M. O., Bron, S. & van Dijl, J. M. The chemistry and enzymology of the type I signal peptidases. *Protein Sci* **6**, 1129-1138, doi:10.1002/pro.5560060601 (1997).

38 Weihofen, A., Binns, K., Lemberg, M. K., Ashman, K. & Martoglio, B. Identification of signal peptide peptidase, a presenilin-type aspartic protease. *Science* **296**, 2215-2218, doi:10.1126/science.1070925 (2002).

39 Martoglio, B. & Dobberstein, B. Signal sequences: more than just greasy peptides. *Trends Cell Biol* **8**, 410-415 (1998).

40 Weinzierl, A. O. *et al.* Features of TAP-independent MHC class I ligands revealed by quantitative mass spectrometry. *European journal of immunology* **38**, 1503-1510, doi:10.1002/eji.200838136 (2008).

41 Wei, M. L. & Cresswell, P. HLA-A2 molecules in an antigen-processing mutant cell contain signal sequence-derived peptides. *Nature* **356**, 443-446, doi:10.1038/356443a0 (1992).

42 Henderson, R. A. *et al.* HLA-A2.1-associated peptides from a mutant cell line: a second pathway of antigen presentation. *Science* **255**, 1264-1266 (1992).

43 El Hage, F. *et al.* Preprocalcitonin signal peptide generates a cytotoxic T lymphocyte-defined tumor epitope processed by a proteasome-independent pathway. *Proc Natl Acad Sci U S A* **105**, 10119-10124, doi:10.1073/pnas.0802753105 (2008).

44 Oliveira, C. C. *et al.* New role of signal peptide peptidase to liberate C-terminal peptides for MHC class I presentation. *Journal of immunology* **191**, 4020-4028, doi:10.4049/jimmunol.1301496 (2013).

45 Gil-Torregrosa, B. C., Raul Castano, A. & Del Val, M. Major histocompatibility complex class I viral antigen processing in the secretory pathway defined by the trans-Golgi network protease furin. *J Exp Med* **188**, 1105-1116 (1998).

46 Leonhardt, R. M. *et al.* Post-endoplasmic reticulum rescue of unstable MHC class I requires proprotein convertase PC7. *Journal of immunology* **184**, 2985-2998, doi:10.4049/jimmunol.0900308 (2010).

47 Medina, F. *et al.* Furin-processed antigens targeted to the secretory route elicit functional TAP1-/-CD8+ T lymphocytes in vivo. *Journal of immunology* **183**, 4639-4647, doi:10.4049/jimmunol.0901356 (2009).

48 Oliveira, C. C. *et al.* Dominant contribution of the proteasome and metalloproteinases to TAP-independent MHC-I peptide repertoire. *Molecular immunology* **62**, 129-136, doi:10.1016/j.molimm.2014.06.006 (2014).

49 Lorente, E. *et al.* Role of metalloproteases in vaccinia virus epitope processing for transporter associated with antigen processing (TAP)-independent human leukocyte antigen (HLA)-B7 class I antigen presentation. *J Biol Chem* **287**, 9990-10000, doi:10.1074/jbc.M111.314856 (2012).

50 Oliveira, C. C. & van Hall, T. Alternative Antigen Processing for MHC Class I: Multiple Roads Lead to Rome. *Frontiers in immunology* **6**, 298, doi:10.3389/fimmu.2015.00298 (2015).

51 Oliveira, C. C. *et al.* Peptide transporter TAP mediates between competing antigen sources generating distinct surface MHC class I peptide repertoires. *European journal of immunology* **41**, 3114-3124, doi:10.1002/eji.201141836 (2011).

52 Durgeau, A. *et al.* Different expression levels of the TAP peptide transporter lead to recognition of different antigenic peptides by tumor-specific CTL. *Journal of immunology* **187**, 5532-5539, doi:10.4049/jimmunol.1102060 (2011).

53 Hafstrand, I. *et al.* The MHC Class I Cancer-Associated Neoepitope Trh4 Linked with Impaired Peptide Processing Induces a Unique Noncanonical TCR Conformer. *Journal of immunology* **196**, 2327-2334, doi:10.4049/jimmunol.1502249 (2016).

54 Falk, K., Rotzschke, O., Stevanovic, S., Jung, G. & Rammensee, H. G. Allele-specific motifs revealed by sequencing of self-peptides eluted from MHC molecules. *Nature* **351**, 290-296, doi:10.1038/351290a0 (1991).

55 Young, A. C., Zhang, W., Sacchettini, J. C. & Nathenson, S. G. The three-dimensional structure of H-2Db at 2.4 A resolution: implications for antigen-determinant selection. *Cell* **76**, 39-50 (1994).

56 Klein, L., Hinterberger, M., Wirnsberger, G. & Kyewski, B. Antigen presentation in the thymus for positive selection and central tolerance induction. *Nature reviews. Immunology* **9**, 833-844, doi:10.1038/nri2669 (2009).

57 Breed, E. R., Lee, S. T. & Hogquist, K. A. Directing T cell fate: How thymic antigen presenting cells coordinate thymocyte selection. *Semin Cell Dev Biol*, doi:10.1016/j.semcdb.2017.07.045 (2017).

58 Wolkers, M. C., Brouwenstijn, N., Bakker, A. H., Toebes, M. & Schumacher, T. N. Antigen bias in T cell cross-priming. *Science* **304**, 1314-1317, doi:10.1126/science.1096268 (2004).

59 Verweij, M. C. *et al.* Inhibition of mouse TAP by immune evasion molecules encoded by non-murine herpesviruses. *Molecular immunology* **48**, 835-845, doi:10.1016/j.molimm.2010.12.008 (2011).

60 Ressing, M. E., Luteijn, R. D., Horst, D. & Wiertz, E. J. Viral interference with antigen presentation: trapping TAP. *Molecular immunology* **55**, 139-142, doi:10.1016/j.molimm.2012.10.009 (2013).

61 Lampen, M. H. *et al.* CD8+ T cell responses against TAP-inhibited cells are readily detected in the human population. *Journal of immunology* **185**, 6508-6517, doi:10.4049/jimmunol.1001774 (2010).

62 Rodgers, J. R. & Cook, R. G. MHC class Ib molecules bridge innate and acquired immunity. *Nature reviews. Immunology* **5**, 459-471, doi:10.1038/nri1635 (2005).

63 Strong, R. K. *et al.* HLA-E allelic variants. Correlating differential expression, peptide affinities, crystal structures, and thermal stabilities. *J Biol Chem* **278**, 5082-5090, doi:10.1074/jbc.M208268200 (2003).

64 van Hall, T., Oliveira, C. C., Joosten, S. A. & Ottenhoff, T. H. The other Janus face of Qa-1 and HLA-E: diverse peptide repertoires in times of stress. *Microbes Infect* **12**, 910-918, doi:10.1016/j.micinf.2010.07.011 (2010).

65 Lampen, M. H. *et al.* Alternative peptide repertoire of HLA-E reveals a binding motif that is strikingly similar to HLA-A2. *Molecular immunology* **53**, 126-131, doi:10.1016/j.molimm.2012.07.009 (2013).

66 Oliveira, C. C. *et al.* The nonpolymorphic MHC Qa-1b mediates CD8+ T cell surveillance of antigen-processing defects. *J Exp Med* **207**, 207-221, doi:10.1084/jem.20091429 (2010).

67 van Hall, T. *et al.* The varicellovirus-encoded TAP inhibitor UL49.5 regulates the presentation of CTL epitopes by Qa-1b1. *Journal of immunology* **178**, 657-662 (2007).

68 Nagarajan, N. A., Gonzalez, F. & Shastri, N. Nonclassical MHC class Ib-restricted cytotoxic T cells monitor antigen processing in the endoplasmic reticulum. *Nat Immunol* **13**, 579-586, doi:10.1038/ni.2282 (2012).

69 Lampen, M. H. & van Hall, T. Strategies to counteract MHC-I defects in tumors. *Current opinion in immunology* **23**, 293-298, doi:10.1016/j.coi.2010.12.005 (2011).

70 Garrido, F., Aptsiauri, N., Doorduijn, E. M., Garcia Lora, A. M. & van Hall, T. The urgent need to recover MHC class I in cancers for effective immunotherapy. *Current opinion in immunology* **39**, 44-51, doi:10.1016/j.coi.2015.12.007 (2016).

71 Talebian Yazdi, M. *et al.* The positive prognostic effect of stromal CD8+ tumor-infiltrating T cells is restrained by the expression of HLA-E in non-small cell lung carcinoma. *Oncotarget* **7**, 3477-3488, doi:10.18632/oncotarget.6506 (2016).

72 van Esch, E. M. *et al.* Alterations in classical and nonclassical HLA expression in recurrent and progressive HPV-induced usual vulvar intraepithelial neoplasia and implications for immunotherapy. *Int J Cancer* **135**, 830-842, doi:10.1002/ijc.28713 (2014).

73 Gooden, M. *et al.* HLA-E expression by gynecological cancers restrains tumor-infiltrating CD8(+) T lymphocytes. *Proc Natl Acad Sci U S A* **108**, 10656-10661, doi:10.1073/pnas.1100354108 (2011).

74 van der Burg, S. H., Arens, R., Ossendorp, F., van Hall, T. & Melief, C. J. Vaccines for established cancer: overcoming the challenges posed by immune evasion. *Nature reviews. Cancer* **16**, 219-233, doi:10.1038/nrc.2016.16 (2016).

Chapter 5

Identification of non-mutated neoantigens presented by TAP-deficient tumors

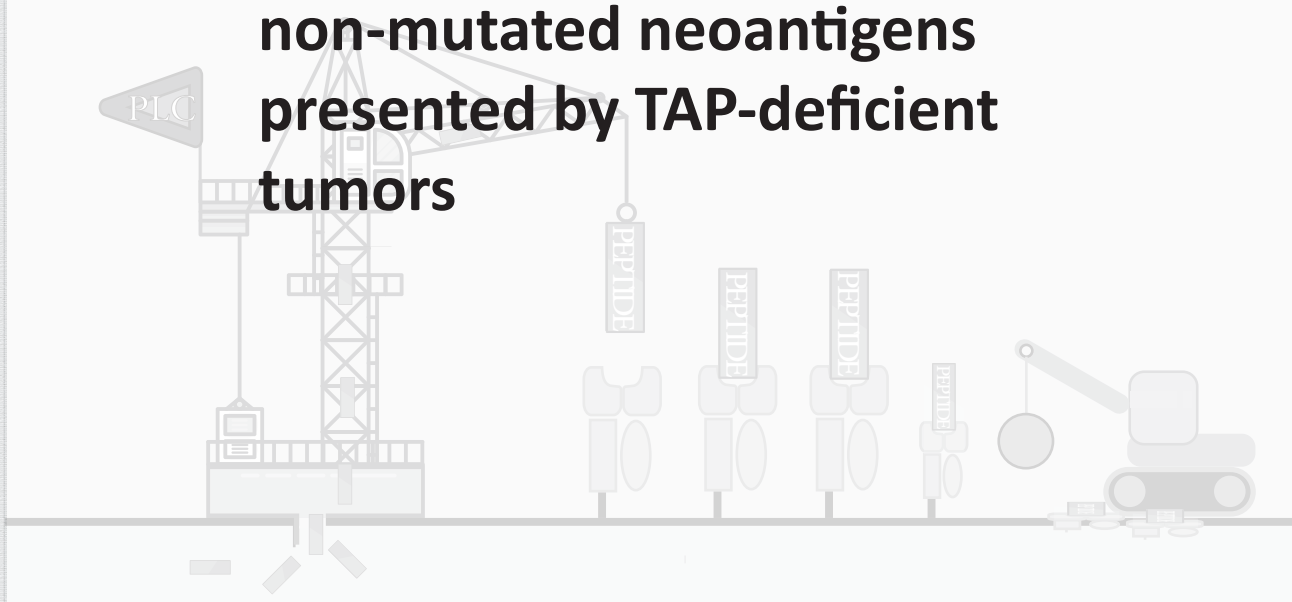

K. A. Marijt, *L. Blijleven, E. M. E. Verdegaal, M. G. Kester, D. J. Kowalewski, H. G. Rammensee, S. Stevanovic, M. H. M. Heemskerk, S. H. van der Burg and T. van Hall*

Journal of Experimental Medicine 215(9): 2325-2337 (2018)

Graphical abstract

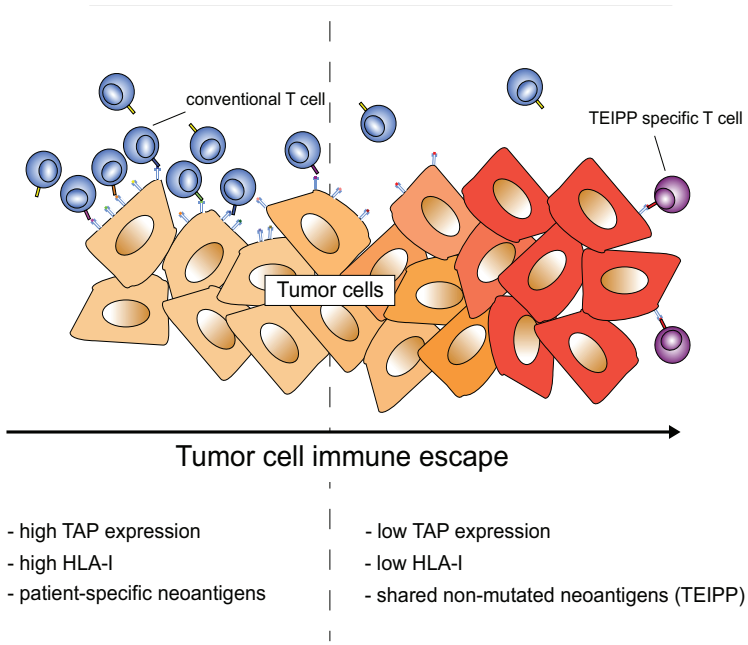

Most T-cell based immunotherapies of cancer depend on intact antigen presentation by HLA class I molecules (HLA-I). However, defects in the antigen processing machinery can cause down regulation of HLA-I, rendering tumor cells resistant to $CD8^+$ T cells. Previously, we demonstrated that a unique category of cancer antigens is selectively presented by tumor cells deficient for the peptide transporter TAP, enabling specific attack of such tumors without causing immunopathology in mouse models. With a novel combinatorial screening approach, we now identified 16 antigens of this category in humans. These HLA-A*02:01 presented peptides do not derive from the mutanome of cancers, but are of 'self' origin and therefore constitute universal neoantigens. Indeed, $CD8^+$ T cells specific for the leader-peptide of the ubiquitously expressed LRPAP1 protein recognized TAP-deficient, HLA-I^{low} lymphomas, melanomas, renal and colon carcinomas, but not healthy counterparts. In contrast to personalized mutanome-targeted therapies, these conserved neoantigens and their cognate receptors can be exploited for immune-escaped cancers across diverse histological origin.

Introduction

Many T-cell based immunotherapies for cancer are based on recognition of tumor antigens presented in human leukocyte antigen class I (HLA-I) molecules by tumor cells [1,2]. Success of immune checkpoint blockade therapy is strongly correlated with mutational load and mismatch repair deficient cancers, irrespective of tumor type [3,4]. Point mutated peptides indeed constitute formidable tumor antigens due to their non-self nature for which a non-curtailed T cell repertoire is available. An absolute requirement for such T cells to exert their action against cancer is the display of HLA-I at the surface of tumor cells. However, HLA-I down modulation on cancer cells is observed in many immune-escaped cancers, often caused by epigenetic silencing of antigen processing components, like the transporter associated with antigen processing (TAP) [5-7]. Recent studies implicated that acquired resistance to checkpoint therapy can occur through alterations in genes relevant for antigen processing and presentation [8,9]. For instance, mutations in the JAK1/JAK2 interferon signalling pathway represented acquired and primary resistance mechanisms in cancer patients who relapsed from or did not respond at all to checkpoint therapy, respectively. Notably, these mutations resulted in the inability to respond to interferon-**γ** (IFN-**γ**) and thus to upregulate antigen processing and presentation by HLA-I [10-12].

Our group previously discovered a novel category of tumor antigens, referred to as TEIPP (T cell epitopes associated with peptide processing), that are presented at the surface of tumor cells carrying defects in antigen processing [13]. In mouse tumor models in which MHC-I display is down modulated by defects in the peptide transporter TAP, we showed a selective presentation of TEIPP peptides, and successful targeting of immune-escaped tumor variants by TEIPP specific T cells [14,15]. Thus, targeting TEIPP neoantigens is a potent strategy to induce anti-tumor responses for tumors with low MHC-I expression. TEIPPs are derived from ubiquitously expressed non-mutated 'self' proteins, however, their processed peptides fail to be loaded into MHC-I in healthy cells. Their surface presentation is highly promoted by defects in the antigen processing machinery, especially in the absence of the peptide transporter TAP. Due to this virtue, TEIPP peptides constitute tumor-specific antigens. We have shown that the $CD8^+$ T cell repertoire against TEIPP neoantigens is positively selected in the thymus and that these cells remain naïve, even in tumor-bearing mice, making this subset fully exploitable for T-cell based therapies against immune-escaped cancers without any signs of autoimmune reactivity [15]. Yet, as to date only one human TEIPP neoantigen has been identified at the molecular level [16,17].

In order to identify multiple human TEIPP antigens, we developed a systematic hybrid forward-reversed immunology screen to identify human TEIPP antigens. This approach encompassed an *in silico* prediction of TEIPP neoantigen-candidates from the whole humane

proteome, matching of candidates to the cancer-specific peptidome, and an *ex vivo* screen to confirm the presence of a TEIPP T cell repertoire in healthy donors. Here, we present data on 16 identified HLA-A*02:01 binding TEIPP epitopes and a full characterization of the T cell reactivity against one of them.

Results

Strategy for target identification from the complete human proteome

To identify human TEIPP antigens that are presented by TAP-deficient cancer cells, we developed a hybrid forward-reversed immunology identification approach based on alternative antigen processing rules in combination with cancer-specific peptidome database matching (figure 1a). The whole human proteome was chosen as starting point, since TEIPP antigens are nonmutated 'self' antigens that are preferentially displayed on cells with deficiency in the peptide transporter TAP. This TAP-independent loading in HLA-I molecules can occur via two known alternative processing pathways: liberation of N-terminal 'signal peptides' and C-terminal 'tail peptides' [18-22] (figure 1a-b). A list of signal peptide-containing proteins was selected from the human proteome with the use of a web-based algorithm that predicts the signal peptidase (SP) cleavage site [23]. Most of these leader peptides need further processing by the proteolytic enzyme signal peptide peptidase (SPP) in order to release them from the endoplasmic reticulum (ER)-membrane and thereby generating peptides of different lengths suitable for loading in HLA-I [18,21]. This 'signal peptide' search yielded 111,525 different 9- and 10-mer TEIPP candidates. Additionally, C-terminal 'tail peptides' were selected using information on the topology of transmembrane proteins in the same web-based algorithm, knowing that liberation and TAP-independent processing of C-termini can be exerted by proteases like furin and SPP [20,24-27]. This search resulted in 6,674 'tail peptides' (figure 1a-b). Next, we filtered these combined peptides for a predicted high HLA-I binding-affinity (IC50<500 nM) to one of the so-called HLA 'supertypes', representing most alleles in the Caucasian population (HLA-A*01:01, HLA-A*02:01, HLA-A*03:01, HLA-B*07:02, HLA-B*40:01, HLA-A*24:02) [28-31]. This final list of 13,731 TEIPP candidates was then cross-matched with a large peptidome database, containing peptides eluted from over 200 tumor samples and 120 healthy tissue control samples (supplementary table I). Thereby, we focused on those TEIPP candidates that were endogenously processed and exclusively presented by tumor cells (figure 1c). This strategy yielded a short-list of 65 TEIPP neoantigen-candidates of which 40 had a predicted binding to the HLA-A*02:01 allele (supplementary figure 1a-d). These 40 HLA-A*02:01 binding peptides were chosen to explore the existence of cognate $CD8^+$ T cells (figure 1a).

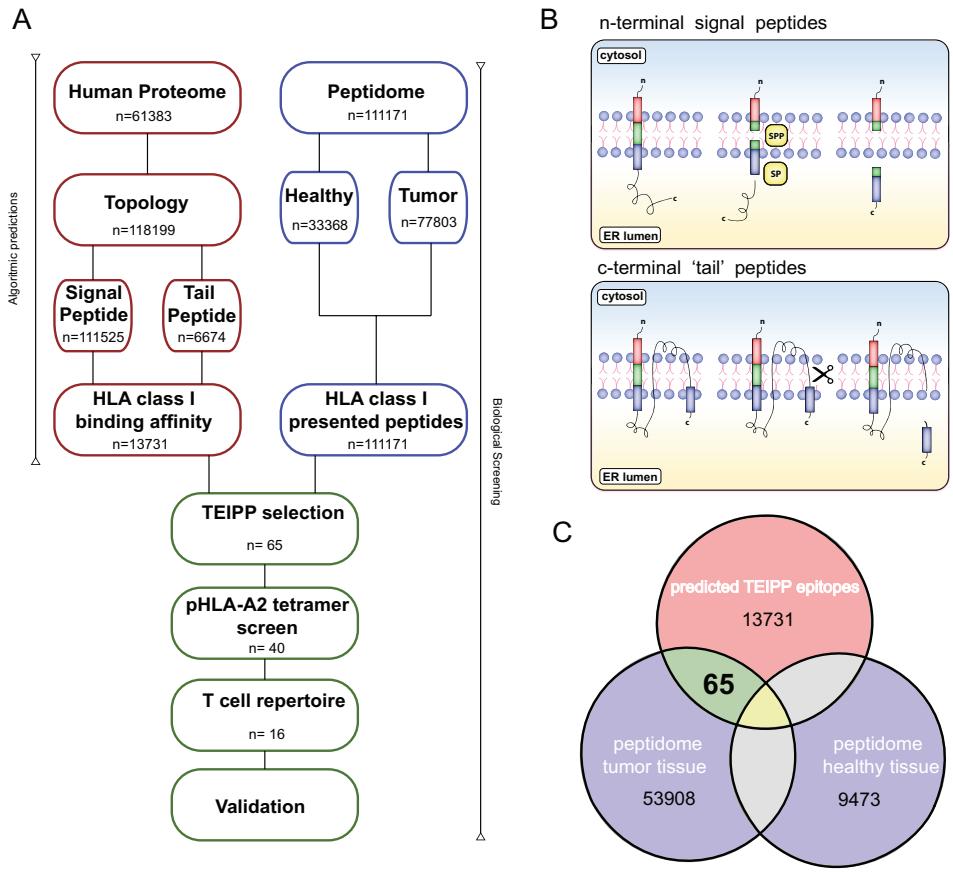

Figure 1: Identification approach of TEIPP neoantigens associated with immune-edited cancers

(**A**) A schematic overview of the applied screening approach. Human peptide sequences were selected via algorithms-based predictions on the whole human proteome for presentation by HLA-I molecules independent of the peptide transporter TAP. Two main unraveled pathways have been described for which algorithms are available: the processing of signal peptides and of C-terminal 'tail' peptides (*red*). The resulting peptide selection was matched with a large database of naturally presented peptides from human cancers and healthy tissue (*blue*). The subsequent shortlist of candidates with a predicted binding to HLA-A*02:01 was subjected to functional testing for T cell immunogenicity and recognition of tumor cells deficient for the peptide transporter (*green*). (**B**) Graphical display of the two molecularly described TAP-independent processing mechanisms. Top panel: Signal peptide containing proteins are processed in the ER membrane by the proteolytic enzymes signal peptidase (SP) and signal peptide peptidase (SPP), resulting in the liberation of small peptides in the lumen of the ER where they can bind to HLA class I molecules [18,53]. Bottom panel: Proteins with their C-terminal tail protruding in the ER can be cleaved by proteases like furins or SPP [20,26]. (**C**) Venn diagram of *in silico* predicted TEIPP neoantigens matched with databases comprising naturally presented peptides from tumor tissues or healthy tissues.

Detectable frequencies of CD8$^+$ T cells against 16 out of 40 HLA-A*02:01 binding TEIPP neoantigens

To validate that T cells against these TEIPP neoantigens were present in the repertoire of healthy donors, we grouped forty different HLA-A*02:01 tetramers containing the TEIPP neoantigens in eight pools of five peptides each, based on predicted binding affinity (high in 'peptide pool 1' to low in 'peptide pool 8'). Next, CD8$^+$ T cell cultures were started with tetramer-assisted 'pull-downs' from peripheral blood mononuclear cells (PBMC). These enriched CD8$^+$ T cell pools were stimulated with the five respective synthetic peptides of that particular pool for several rounds and analyzed for presence of peptide-specific T cells by flow cytometry (figure 2a). In an initial screen of three different HLA-A*02:01-positive healthy donors we observed T cell repertoires for 16 out of 40 TEIPP neoantigen candidates (figure 2a). Frequencies of tetramer-stained CD8$^+$ T cells varied from 0.1% up to 78% in these short-term expanded cultures. These percentages differed between the three tested donors, indicating that this protocol enabled the detection of TEIPP-specific CD8$^+$ T cells but that the observed frequencies reflected variation of the *in vitro* steps of enrichment and expansion. Additional donors were examined for the 16 positive peptides to evaluate the consistency of this finding and against most peptides CD8$^+$ T cells were detected, in the majority of the donors (figure 2b and Table 1). Collectively, these data indicated that our TEIPP identification strategy had a high success rate to identify human antigens to which a CD8$^+$ T cell repertoire existed in healthy individuals.

Most TEIPP-specific CD8$^+$ T cells reside in the naïve repertoire

Previous investigations in our mouse tumor model of TEIPP showed that TEIPP-specific T cells remain naïve, even in the presence of TAP-deficient tumor cells [15]. This was shown to be an advantage for their exploitability in therapeutic interventions [15]. To test this aspect for human TEIPP-specific T cells, we again enriched tetramer-positive CD8$^+$ T cells from PBMC for the five peptides p14, p29, p34, p35 and p55 that were frequently positive in our screen. Naïve CD8$^+$ T cells were directly separated from antigen-experienced CD8$^+$ T cells by flow cytometry sorting, based on differentiation markers CD62L and CD45RA at the cell surface (supplementary figure 2a). After this *ex vivo* sorting, the two populations were expanded by three rounds of *in vitro* stimulation and analyzed for the presence of tetramer-positive CD8$^+$ T cells (figure 3a-b). Importantly, T cells against p14, p34 and p35 were exclusively found in the sorted naïve population in all tested donors, indicating that these specificities had never encountered cognate antigen in these healthy individuals. In addition, T cells against p29 and p55 were found in the naïve subset of some donors while in other donors, these specificities were detected in the antigen-experienced repertoire (figure 3b). These data indicated that some TEIPP-specific CD8$^+$ T cells already had been

primed in a few healthy individuals, but that the majority of them reside in a naïve state. We speculated that this priming could have been triggered by bacterial species in the gut with antigens that show striking sequence similarity with peptide 29 and 55 (supplementary figure 2b). In summary, these data demonstrate a universal existence of naïve T cells with TEIPP specificity in healthy individuals.

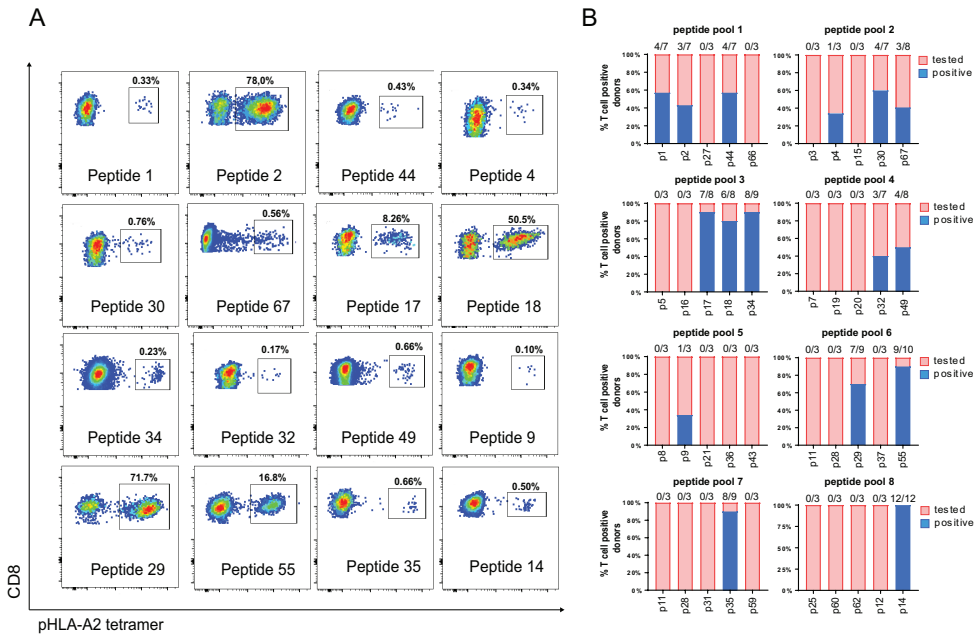

Figure 2: Detection of CD8⁺ T cells against TEIPP neoantigens in PBMC of healthy donors

PBMCs of healthy donors were screened with HLA-A*02:01 tetramers to identify whether a T cell repertoire is present for TEIPP neoantigens. HLA-A*02:01 tetramers folded with the selected 40 TEIPP neoantigen candidates were arranged in eight pools based on predicted peptide binding. (**A**) TEIPP enriched T cell pools were analyzed by flow cytometry (n=3). Representative dot plots of TEIPP neoantigen-specific CD8⁺ T cells are shown. (**B**) PBMCs of additional healthy donors were tested to validate the presence of a TEIPP T cell repertoire. All 40 TEIPP neoantigen-candidates were tested in at least three different donors. Shown are data of all tested donors. Each bar represents one TEIPP neoantigen-candidate. In blue the percentage of T cell positive donors based on flow cytometry analysis. Numbers above each bar indicate the fraction of positive donors out of total tested.

Functional avidity of clonal CD8⁺ T cell cultures

To functionally study TEIPP-specific CD8⁺ T cells, we generated clonal cultures against the five TEIPP peptides p14, p29, p34, p35, and p55. Four of these peptides were derived from N-terminal signal sequences of proteins and one was derived from a C-terminal 'tail peptide' (supplemental figure 2c). We evaluated the binding affinity and stability of these five peptides to HLA-A*02:01, since these determinants are critically involved in immunogenicity for T cells [32,33]. Four of the five peptides displayed an intermediate affinity and formed complexes with HLA-A*02:01 for at least four hours, however, p29 surprisingly failed to show binding in these cellular assays (supplementary figure 2d-e). Multiple T cell clones were generated using an antigen-independent expansion protocol of tetramer-positive CD8⁺ T cells after single cell sorting. Since the functional avidity correlates with high affinity TCRs and thus for *in vivo* efficacy [34-37], we assessed the peptide concentrations resulting in half maximum cytokine response (EC50) of the several TEIPP-specific T cell clones when exposed to antigen-presenting cells pulsed with titrated concentrations of cognate peptide (figure 3c). All isolated T cell clones exhibited a functional avidity between 0.4-66 nM, with the highest avidity for clones recognizing p34 and p55. The other clones, like those against p14, were considered to display moderate avidity. Of note, all clones with the same peptide specificity used different TCRβ V-segments, pointing at their independent origin and the availability of a broad repertoire (supplementary figure 2f). These results demonstrated that the broad repertoire of TEIPP-specific T cells in healthy individuals exhibits a usual functional avidity for their cognate peptide and is competent to respond upon antigen encounter.

CD8⁺ T cells against p14 recognize TAP-deficient tumors across diverse histological origin

In search for TEIPP antigens on immune-escaped cancers, we selected the p14 peptide-epitope with sequence FLGPWPAAS from the ubiquitously expressed LRPAP1 protein (from now on called $LRPAP1_{21-30}$) for in depth examination (Table I). First, we confirmed specificity for the $LRPAP1_{21-30}$ epitope for T cell clone 1A8 by testing different peptide length variants of the LRPAP1 signal peptide (supplementary figure 3a). Although unconventional, this examination confirmed the serine amino acid as C-terminus for this HLA-A*02:01 allele. Next, LRPAP1 gene expression data was collected from the TCGA database for different tumor types, revealing that its expression is ubiquitous with exceptionally high expression levels in skin melanomas (figure 4a). We therefore selected the HLA-A*02:01 positive skin melanoma cell line '518A2' and confirmed the expression of the LRPAP1 gene (figure 4b, supplementary figure 3b). For this cell line an TAP1 knock-out variant, a CRISPR/CAS9 control TAP1-WT variant, and an TAP1/antigen double knock-out variant were generated by CRISPR/CAS9 technology and these gene edited variants were tested for recognition by the

Table I. Overview TEIPP neoantigen candidates

#	Gene Name	Peptide[1] Sequence	Accession[2] Number	HLA-A2[3] Affinity (IC50)	Expression[4]			T cell Repertoire
					Tissue[5]	Normal	Cancer	
Ubiquitous TEIPP								
p1	ERGIC3	FLSELQYYL	Q9Y282	2	All	++	++	4/7
p4	TTYH3	ALFSFVTAL	Q9C0H2	10	All	+	+	1/3
p9	IGJ	VLAVFIKAV	P01591	52	All	++	++	1/3
p14	LRPAP1	FLGPWPAAS	D6REW6	353	All	++	++	14/14
p29	ARSA	LLALAAGLAV	P15289	79	All	++	++	9/10
p44	EMILIN2	FLYPFLSHL	Q9BXX0	4	All	+	++	4/7
p49	H2AFV	ILEYLTAEV	E5RJU1	30	All	++	++	6/9
p67	SEP15	LSEKLERI	O60613	15	All	+	+	4/8
Tissue Specific TEIPP								
p2	IL12A	VLLDHLSLA	P29459	7	Mixed	+	+	3/7
p17	HPR	LLWGRQLFA	P00739	24	Liver	+++	+	6/7
p18	FSTL4	TLLGASLPA	Q6MZW2	27	Mixed	+	+++	5/7
p30	IFI30	LLLDVPTAAV	M0QZG3	10	Mixed	++	++	5/8
p32	CD79B	LLLSAEPVPA	P40259	41	Lymphoid	+	++	3/7
p34	PCDHGA6	LTLLGTLWGA	Q9Y5G7	24	Mixed	+/-	+/-	8/8
p35	C20orf141	SVLWLGALGL	Q9NUB4	161	Testis	+	+	16/16
p55	APCS	VIIKPLVWV	P02743	113	Liver	+++	+++	9/10

[1.] Peptide sequence based on predicted signal peptide cleavage site
[2.] Accession number uniprot.org
[3.] Predicted peptide affinity binding in HLA-A2:01
[4.] Protein expression scores based on data proteinatlas.org
[5.] Protein expression based on TCGA database score

LRPAP1$_{21\text{-}30}$-specific CD8$^+$ T cell clone 1A8 (figure 4b, supplementary figure 3c-d). Surface display of HLA-A*02:01 decreased after knocking out the gene for the peptide transporter TAP1 (figure 4c). The LRPAP1$_{21\text{-}30}$-specific CD8$^+$ T cell clone selectively recognized the TAP1-deficient variant of 518A2. This suggested that the LRPAP1$_{21\text{-}30}$ signal peptide was only presented by the TAP-deficient tumor variant, despite equal expression of the *LRPAP1* gene and lower HLA-A*02:01 levels on these cells (figure 4d). Furthermore, selective knockout of the epitope ('LRPAP1$_{21\text{-}30}$ Ag-KO') resulted in complete abrogation of T cell recognition (figure 4d). To control for artificial CRISPR/CAS9-induced immunogenicity, we included a previously established T cell clone (HSS1 PRAME) that recognizes the TAP-dependent

PRAME (SLLQHLIGL) tumor antigen. This $PRAME_{425-433}$-specific $CD8^+$ T cells only recognized 518A2 WT cells whereas it completely failed to respond towards the TAP KO variant. In contrast, $LRPAP1_{21-30}$-specific T cells displayed clear preference for the TAP KO variant (figure 4e). Collectively, these data confirmed that the applied tetramer-based selection approach allows the isolation of functional $CD8^+$ T cells with a bona fide specificity for the antigen from which the TEIPP was derived. Moreover, these data excluded potential cross-reactivity of T cell clone 1A8 against other peptides presented by the 518A2 melanoma cells. Finally, antibodies against HLA-I molecules were able to block the tumor recognition by T cells, demonstrating dependency on peptide/HLA-I (figure 4f).

The ubiquitous expression of the *LRPAP1* gene in diverse tumor types prompted us to test T cell recognition of other HLA-A*02:01 positive melanomas and tumors of other histological origin, including renal cell carcinoma and lymphoma. The panel of T1 and T2 lymphoma cells are known for their characterized genomic TAP status (supplementary figure 3e) [38,39]. We confirmed equal *LRPAP1* gene expression by quantitative PCR (supplementary figure 3f) and examined recognition by multiple $LRPAP1_{21-30}$-specific T cell clones (figure 4g). All tested $CD8^+$ T cell clones selectively recognized the TAP-deficient T2 cells, again displaying a typical TEIPP specificity.

Next, a panel of HLA-A*02:01 positive TAP-deficient melanomas and renal cell carcinomas were generated by genetically disrupting the *TAP1* gene. Tumor cell mRNA levels of the *LRPAP1* gene were again comparable as quantified by PCR (supplementary figure 3g). Flow cytometry analysis revealed that HLA-A*02:01 levels varied between the lines, but that these decreased after *TAP1* gene knockout (figure 4h). As observed for the 518A2 melanoma and the T2 lymphoma, multiple $LRPAP1_{21-30}$-specific T cell clones exhibited a preferential recognition of the TAP1-deficient tumor lines (figure 4i). Interestingly, some parental tumors were already recognized even before silencing the *TAP1* gene (e.g. melanoma 93.04), implying that the endogenous *TAP1* levels were already lower expressed to allow presentation of the $LRPAP1_{21-30}$ antigen. Indeed, quantitative PCR confirmed low *TAP1* gene expression in the melanoma 93.04 (supplementary figure 3h). In line with this, complete abolishment of the *TAP1* gene in tumor line 93.04 did not result in much improved T cell recognition (figure 4i). To further corroborate the shared character across multiple tumor types, we also tested T cell recognition of our 1A8 clone against two colon carcinomas (supplementary figure 3i-j). Interestingly, we observed specific T cell responses towards the TAP KO variants of these two colon carcinoma cell lines (supplementary figure 3k). Overall, these data clearly demonstrated that the $LRPAP1_{21-30}$ TEIPP epitope is universally presented in HLA-A*02:01 by cancers of diverse histology when the peptide transporter TAP is not functional. TEIPP specific $CD8^+$ T cells specific for this TEIPP antigen enables targeting of this shared, nonmutated peptide on immune-escaped HLA-I^{low} cancers.

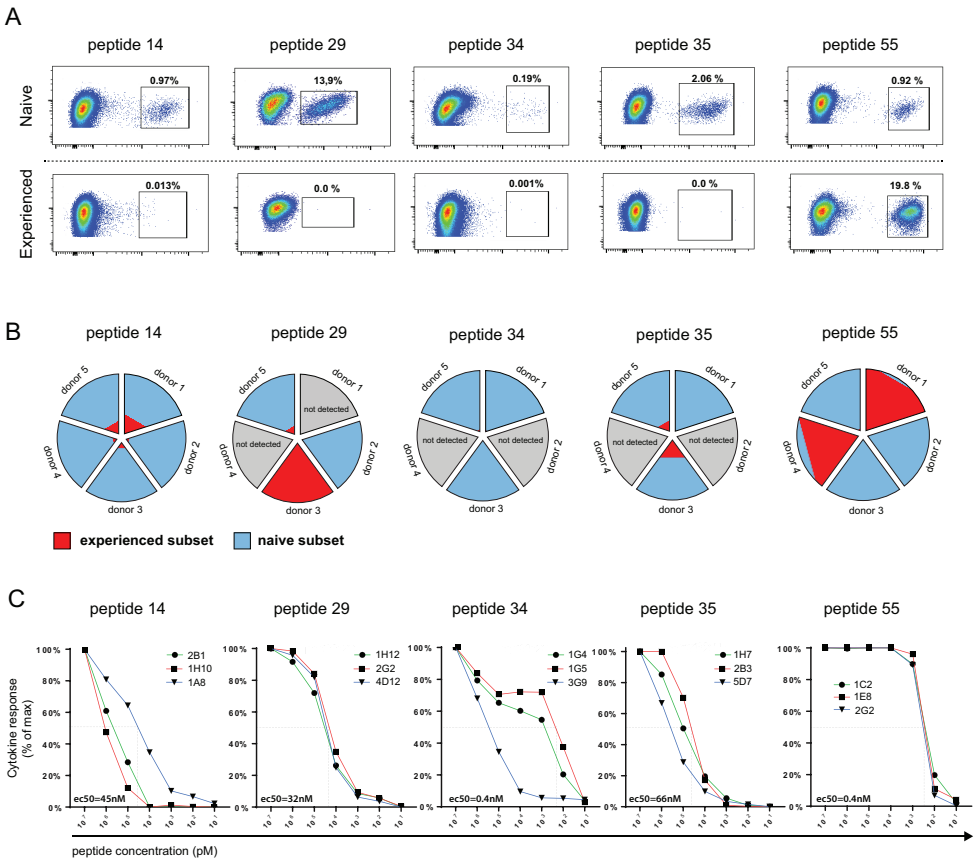

Figure 3: Most TEIPP-specific CD8⁺ T cells reside in the naïve repertoire

The status and functional avidity of TEIPP specific T cells peptide-candidates p14, p29, p34, p35, and p55 were examined. CD8⁺ T cells to these peptides were most abundantly detected in PBMCs of healthy donors. (**A**) Representative dot plots of pHLA-A*02:01 tetramer stained CD8+ T cells cultured from either the naïve subset or the experienced subset. Percentages represent pHLA-A*02:01 tetramer positive cells out of total CD8⁺ T cells. (**B**) Pie-charts for each of the TEIPP neoantigen-candidates. Five donors were tested and each slice represents one donor. Relative percentage of naïve cells (*blue)* and percentage of experienced cells (*red)* is calculated out of total pHLA-A*02:01 tetramer positive CD8⁺ cells. (**C**) T cell clones against these peptides were generated by single cell sorting on HLA-A*02:01 tetramer-positive cells and subsequent expansion. Functional T cell avidity was examined by measuring cytokine production of activated T cells recognizing TEIPP peptide pulsed HLA-A*02:01 positive T2 cells with different concentrations of peptide. EC50 was determined by calculating the peptide concentration (nM) corresponding to the 50% cytokine production of the maximum response (n=3). Individual clones were tested at least twice.

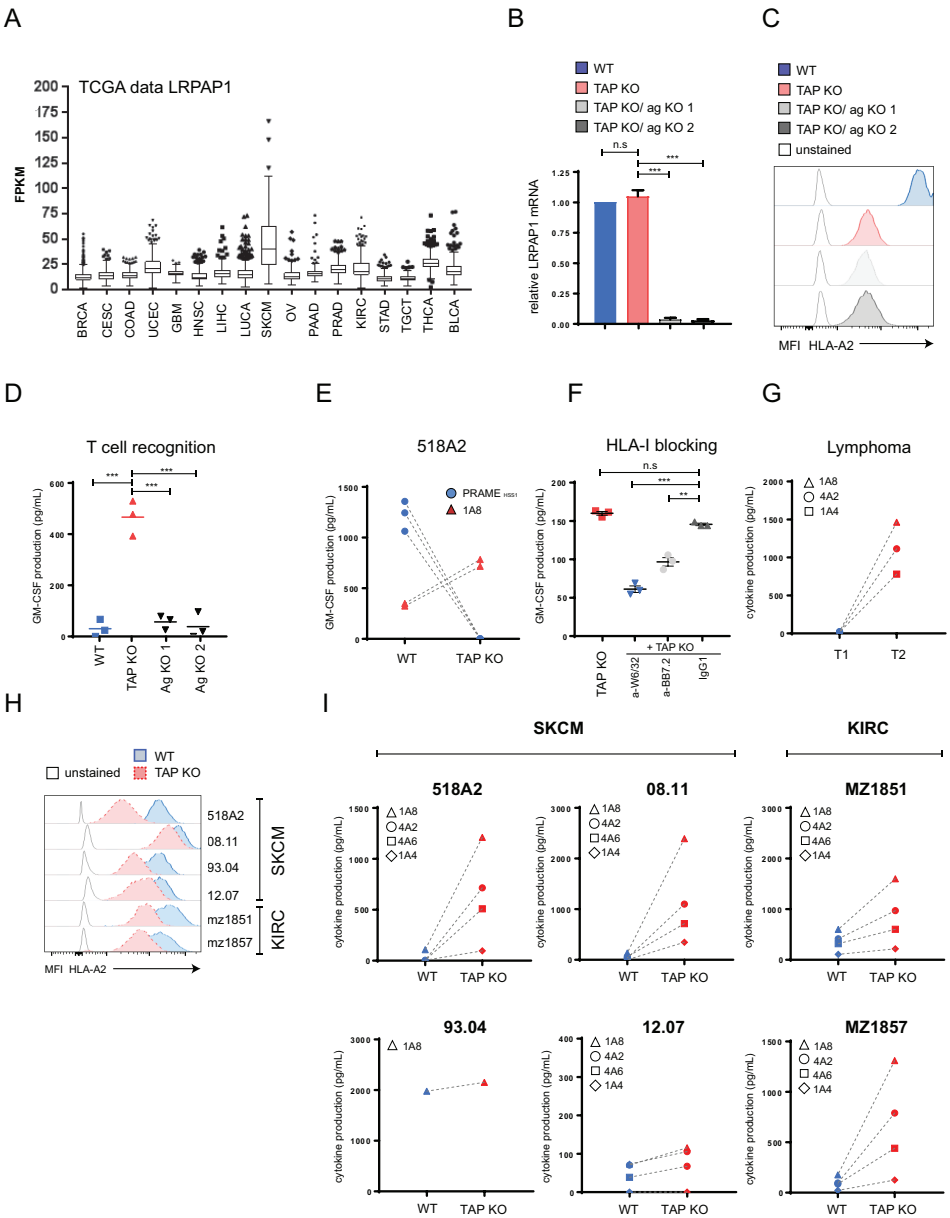
A
TCGA data LRPAP1
FPKM
BRCA
CESC
COAD
UCEC
GBM
HNSC
LIHC
LUCA
SKCM
OV
PAAD
PRAD
KIRC
STAD
TGCT
THCA
BLCA
B
WT
TAP KO
TAP KO/ ag KO 1
TAP KO/ ag KO 2
n.s
relative LRPAP1 mRNA
C
WT
TAP KO
TAP KO/ ag KO 1
TAP KO/ ag KO 2
unstained
MFI HLA-A2
D
T cell recognition
GM-CSF production (pg/mL)
WT
TAP KO
Ag KO 1
Ag KO 2
E
518A2
PRAME
1A8
GM-CSF production (pg/mL)
WT
TAP KO
F
HLA-I blocking
n.s
GM-CSF production (pg/mL)
TAP KO
+ TAP KO
a-W6/32
a-BB7.2
IgG1
G
Lymphoma
1A8
4A2
1A4
cytokine production (pg/mL)
T1
T2
H
WT
TAP KO
unstained
518A2
08.11
93.04
12.07
mz1851
mz1857
SKCM
KIRC
MFI HLA-A2
I
SKCM
KIRC
518A2
08.11
MZ1851
93.04
12.07
MZ1857
1A8
4A2
4A6
1A4
cytokine production (pg/mL)
WT
TAP KO

Figure 4: CD8⁺ T cells against p14 recognize TAP-deficient tumors of different histological origin

T cell clones were tested for their specificity to selectively recognize the $LRPAP1_{21-30}$ TEIPP epitope presented on TAP-impaired tumors. (**A**) Whisker plots of LRPAP1 gene expression in human cancers (data collected from TCGA database). (**B**) The TAP1 gene in the melanoma 518A2 was knocked out (TAP KO) using CRISPR/CAS9. In addition, the $LRPAP1_{21-30}$ epitope was knocked out in these cells (ag KO). mRNA expression of LRPAP1 was examined by qPCR. Data are shown as mean ± SD of triplicates. Significance testing: unpaired t test, n.s., not significant; ***, p<0.001 (n=3). (**C**) HLA-A*02:01 surface expression on 518A2 melanoma variants, measured by flow cytometry. Plots are representative of three independent experiments. (**D**) GM-CSF production of T cell clone 1A8 upon 518A2 TAP KO recognition. When $LRPAP1_{21-30}$ epitope was knocked out (ag-KO), recognition by the T cells were abolished. Representative data of three independent experiments is shown. Each dot represents a technical replicate. Significance testing: unpaired t test, ***, p<0.001. **(E)** To control for artificial CRISPR/CAS9 mediated immunogenicity, we co-cultured T cell clones specific for $LRPAP1_{21-30}$ (TAP-independent epitope) or $PRAME_{425-433}$ (TAP-dependent epitope) together with the 518A2 melanoma (WT vs TAP KO). GM-CSF cytokine response was measured. Each dot represents one independent experiment with technical triplicates. (**F**) HLA-dependency was tested using HLA-ABC or HLA-A*02:01 blocking antibodies. Representative data of two independent experiments is shown. Each dot represents a technical replicate. Significance testing: unpaired t test, n.s., not significant, **, p<0.01; ***, p<0.001. (**G**) TEIPP T cell specificity was determined by co-culturing three different T cell clones together with TAP-proficient T1 cells and TAP-deficient T2 lymphoma cells. Cytokine responses were measured to detect T cell recognition. Representative data of three independent experiments with technical triplicates is shown. (**H**) HLA-A*02:01 surface expression of the TAP-impaired tumor panels as measured by flow cytometry (SKCM: melanoma; KIRC: renal carcinoma). Representative data of three independent experiments is shown. (**I**) Cytokine production of indicated T cell clones upon antigen recognition of four melanomas and two renal carcinomas. Each dot represents one T cell clone specific for the $LRPAP1_{21-30}$ epitope. Representative data of three independent experiments with technical triplicates is shown.

Targeting TEIPP antigens appear safe despite ubiquitous expression of their proteins in healthy cells

The fact that human TEIPP antigens derive from ubiquitously expressed nonmutated proteins may raise concerns for autoimmune pathology. Indeed, the LRPAP1 protein is clearly expressed in several critical organs of our body, as revealed by tissue slide staining images available from proteinatlas.org (figure 5a, supplementary figure 4a)[40]. Therefore, two primary melanocyte cultures and two immortalized kidney cell lines were tested for $CD8^+$ T cell recognition. These non-transformed cells contained similar high levels of LRPAP1 transcripts as the 518A2 tumor (figure 5b) and displayed sufficient levels of HLA-A*02:01 at their cell surface (figure 5c). Despite these optimal conditions, $LRPAP1_{21-30}$-specific T cells did not respond to these healthy cells (figure 5d). Exogenous loading of synthetic LRPAP1 peptide to the cells, however, did lead to LRPAP1-specific T cell response, suggesting that healthy cells were capable of presenting peptides (figure 5e). These data confirmed a crucial role for low TAP function for the presentation of TEIPP antigens and suggested that TEIPP targeting might be considered a safe therapy, even though these proteins are present in healthy tissues as well.

In summary, our data reveals an array of novel nonmutated tumor antigens displayed by tumors with (partial) TAP deficiency (Table I). Some of these are tissue restricted, but others, like the LRPAP1 signal peptide, are ubiquitously expressed and represent universal HLA-presented tumor antigens on cancers with impaired antigen processing.

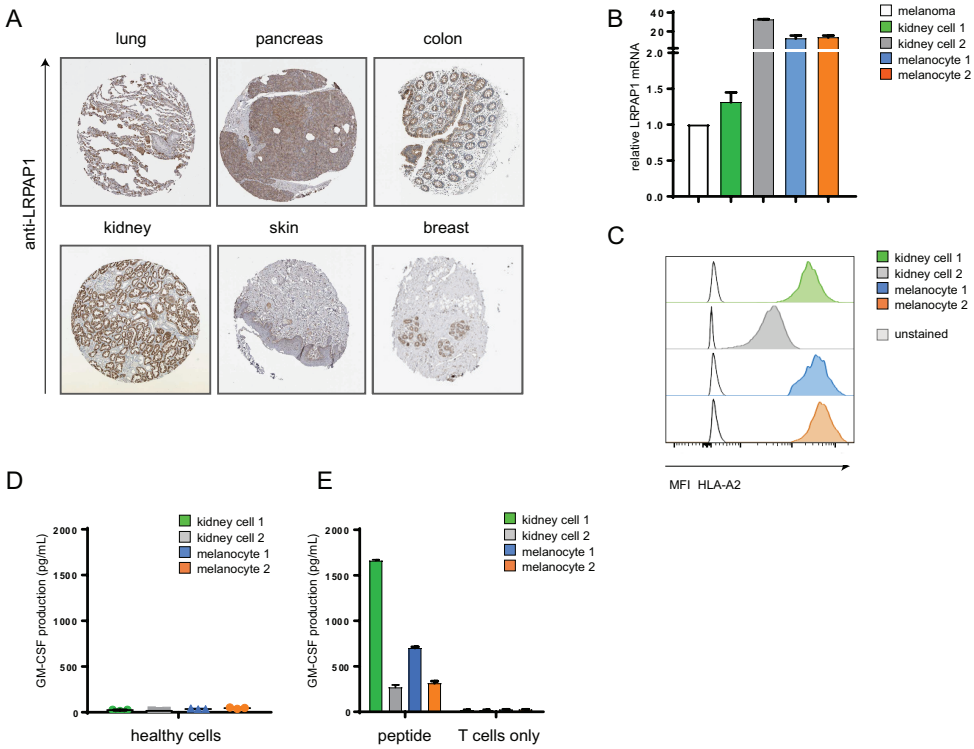

Figure 5: Targeting TEIPP antigens is safe despite ubiquitous expression of their proteins in healthy cells

To assess the safety of targeting nonmutated TEIPP neoantigens we examined the T cell recognition of healthy cells. (**A**) Histological tissue stainings for LRPAP1 were collected from an online accessible database (www.proteinatlas.org). Positive protein detection was observed in various healthy organs. (**B**) *LRPAP1* mRNA levels were determined of two primary melanocyte cultures and two non-transformed kidney epithelial cell lines by qPCR. Data are shown as mean ± SD from one out of two experiments. (**C**) Surface HLA-A*02:01 expression of the healthy cells was determined by flow cytometry. Representative data of three independent experiments is shown. (**D**) No cytokine responses were detected when T cells specific for $LRPAP1_{21-30}$ were co-cultured with these healthy cells. Representative triplicate data of two independent experiments are shown. (**E**) To assess the ability of the healthy cells to present the epitope in HLA-A*02:01, peptide was exogenously loaded. $LRPAP1_{21-30}$ specific T cell clone 1A8 was co-cultured with peptide pulsed healthy cells and GM-CSF cytokine production was measured. Representative triplicate data of two independent experiments are shown.

Discussion

We developed a screening approach to identify human antigens belonging to the novel category of non-mutated neoantigens of 'self' origin, called TEIPP. Our screen yielded 65 potential TEIPP candidates, which are exclusively present in the peptidome of cancer cells. Analysis of the 40 HLA-A*02:01 binding TEIPP candidates revealed a consistent $CD8^+$ T cell repertoire to 16 of these 40 peptides. Additional analyses demonstrated that these $CD8^+$ T cells were present in the naïve pool for five peptide-candidates and that they were not affected by central or peripheral tolerance. Monoclonal T cell cultures against the TEIPP epitope $LRPAP1_{21\text{-}30}$ selectively recognized TAP1-deficient cancers from different histological origins, including lymphoma, melanoma, colon carcinoma, and renal cell carcinoma, whereas TAP-proficient primary cells were spared from T cell recognition. This emphasizes the attractiveness of targeting TEIPP neoantigens on HLA-I^{low} cancers, namely for its shared character on those tumor cells. Thus far we focused on HLA-A*02:01 binding TEIPP peptides, but our screen also predicted a broad array of antigens presented by other HLA types. Furthermore, we realize that this proof-of-concept approach is far from complete. Most likely, many more undiscovered pathways enable the presentation of TAP-independently processed TEIPP neoantigens.

We observed that knocking out the *TAP1* gene rendered all tested cancer cell lines vulnerable for TEIPP-specific T cells. Importantly, TEIPP-specific T cells exhibited moderate to high recognition of some wild-type skin melanomas and renal cell carcinomas (e.g. 93.04, mz1257), and CRISPR/CAS9 mediated knockout of the *TAP1* gene led to only modest improvement of cancer cell recognition. In other cancer lines (e.g. melanoma 518A2, 08.11), minimal T cell responses were detected to wild-type cancer cells and knockdown of TAP1 was necessary to induce strong T cell recognition. These data suggested that some cancer cell lines already down modulated TAP1 gene expression in such degree that was already sufficient for the presentation of TEIPP neoantigens. Although only 1-2% of melanomas have deleterious mutations in TAP1 or TAP2, a high frequency of metastatic melanomas display low TAP1 expression due to epigenetic silencing [5,7]. At this moment, we have not determined how low TAP1 function needs to be for TEIPP neoantigens to be presented on the cell surface of cancer cells. The exact mechanisms of selective TEIPP neoantigen presentation on antigen processing defective cells are still not completely known. Our previous experiments in mouse models suggested a competition between peptide antigens in the endoplasmic reticulum[37,41]. The peptide loading complex (PLC) is a multisubunit membrane complex orchestrating the loading and editing of peptides in HLA-I molecules, facilitated by the TAP1/TAP2 channel, and thereby responsible for the translocation of peptides from the cytosol into the PLC complex[42]. The TAP peptide transporter is incorporated in this

efficient peptide loading complex, in close proximity to HLA-I molecules, which could explain why peptides processed through different mechanisms, independent of TAP, will not have the chance to bind in HLA-I molecules. Besides TAP levels, the amount of available antigenic protein also needs to be taken into account. Interestingly, massive overexpression of a TEIPP antigen makes it possible to present its TEIPP peptide in the cell surface even in TAP-proficient cells[41]. We theorize that these two factors govern the efficiency of TEIPP neoantigen presentation. Low TAP function allows for low antigen expression, whereas moderate TAP function needs higher amounts of antigen expression[17,41]. Of utmost importance is that TAP function in healthy cells of our organs is high enough to prevent recognition by TEIPP-specific T cells[14,15].

The presence of a TEIPP T cell repertoire in healthy donors indicates that no negative selection has occurred in the thymus, even though gene expression in the thymus was observed for most of the TEIPP neoantigen-candidates (supplementary figure 4b). During T cell education in the thymus TEIPP-specific T cells are positively selected for low affinity interaction with peptide/MHC in the cortex of the thymus. To prevent autoimmune responses, negative selection of T cells in the medulla of the thymus is essential to delete self-reactive T cells. This strengthens the hypothesis that TAP-proficient medullary thymic epithelial cells (mTECs) might express the target proteins but do not present TEIPP antigens by their HLA-I and thus TEIPP T cells will undergo normal thymic selection. Indeed, TEIPP-specific T cells are deleted from the repertoire of TAP-deficient mice [14]. Moreover, most of the evaluated TEIPP-specific T cells were only found in the naïve pool in the circulation and have not encountered antigen yet, signifying that TAP-proficient healthy cells did not trigger TEIPP-specific immunity. Also, we presume this observation hold true in cancer patients, since tumor cells are no real APCs in an immune suppressive environment. Ex-vivo T cell activation or synthetic long peptide vaccination strategies are needed for proper TEIPP directed anti-tumor responses. These data mirror earlier observations in our mouse model for TEIPP [15]. Some viruses are also known to down regulate TAP (e.g. EBV, CMV). Yet, we find most TEIPP-specific T cells in the naïve repertoire. An explanation for this could be that viruses also manipulate other pathways () leading to immuno suppressive effect and no T cell activation accordingly. Noteworthy, in some donors we observed that T cells against p29 and p55 were derived from the antigen-experienced pool. We speculate that these TEIPP specificities had been triggered by cross-reactivity to microbiota-derived epitopes leaked from the gut, which can occur after the use of antibiotics or other intestinal injury [43,44]. Since the tested healthy donors did not suffer from severe autoimmune reactivity, even antigen-experienced TEIPP-specific T cells apparently do not target healthy TAP-proficient tissues. The safety of TEIPP-targeting therapies was thoroughly evaluated in mouse tumor models [14,15,45-47]. Vaccine-induced TEIPP-specific T cells via synthetic peptides or dendritic

cells, or adoptive transfer of TEIPP-specific T cells all reduced outgrowth of TAP-deficient tumors without any sign of autoimmune reactivity.

TEIPP neoantigens are selectively presented in cancer cells with deficient function of MHC-I processing machinery. Therefore, we anticipate a complementary role for these antigens to those of other categories, like patient-specific mutanome peptides or cancer-testis antigens. A combination of those might prevent immune-escape via shutdown of HLA-I expression due to defects in the antigen processing machinery. A great asset of TEIPP antigens is their non-mutated status and the fact that the tumor antigens are broadly shared across many cancer types. A few validated TEIPP antigens or gene transfer of their cognate cloned T cell receptors might be sufficient for increased efficacy of immunotherapy through prevention of tumor escape. Future investigations need to reveal safety and applicability of vaccination-based strategies and TCR-based gene transfer approaches for TEIPP. Together, we propose that TEIPP neoantigens are an interesting way to re-establish anti-tumor responses in human immune-escaped cancers.

Material and methods

Study design

The aim of this study was to test a systematic hybrid forward-reversed immunology approach to identify TEIPP specific T cells and their cognate antigen (Table I). For this, we collected the whole human proteome dataset from uniprot.org (ID: 9606, Release: 2014_06). For predictions of the N-terminal "signal" cleavage location and the topology prediction for C-terminal "tail" peptides the web-based topology algorithm Phobius was used (*htpp://www.phobius.edu/)*. For N-terminal peptide candidates, proteins with a predicted signal peptide probability of >0.5 were included. For C-terminal peptide candidates, proteins with a predicted C-terminal "tail" located in the ER were included. Peptide binding affinity to HLA-I molecules were predicted using MHCnet4.0 (*http://www.cbs.dtu.dk/*). Peptides with a predicted binding affinity <500 nM were included. We used the peptidome elution library (release 2014_10) of the Tübingen group (Department of Immunology, Tübingen) to select for biologically processed peptides. Next, in vitro analysis was performed on forty HLA-A*02:01 TEIPP candidates using healthy donor PBMC. In depth analysis was performed on five TEIPP candidates. To guarantee statistical power, we performed all experiments on at least three different PBMC batches isolated from different donors.

Tumor cell lines

Human tumor cell lines were obtained through ATCC or derived from patient surgery material. The clinical protocol was approved by the Medical Ethics Committee of the LUMC and

conducted in accordance with the declaration of Helsinki. All tumor cell lines were cultured at 37°C, 5% CO_2, in DMEM medium (Invitrogen, Carlsbad, CA) containing 8% heat-inactivated FCS, 100 U/mL penicillin, 100 µg/mL streptomycin (Life Technologies, Rockville, MD) and supplemented with 2 mM glutamine (Invitrogen).

Generation of TEIPP specific T-cell clones

Buffy coats from healthy donors were obtained from Sanquin (Sanquin blood facility). Informed consent was given in writing by all participants. PBMC's were isolated using a ficoll gradient (density 1.077 g/mL). Approximately $500x10^6$ PBMC's were incubated with PE-pHLA-A*02:01 tetramers for 30 min at 4°C. Anti-PE magnetic beads (MACS) were used to pull out pHLA-A*02:01 tetramer positive cells over a MACS LS column as instructed by the manufacturer (Miltenyi Biotech). T cells were cultured in complete IMDM containing 8% human serum (Sanquin blood facility), and 100 U/mL IL-2 (Proleukine, Novartis). Bulk T cells were stimulated every two weeks with a mixture of T cells ($1x10^6$), 10 µM synthetic peptide, irradiated PBMCs ($1x10^6$ cells, 80Gy) and EBV-JY ($1x10^5$ cells, 100Gy) in complete T cell culture medium supplemented with 100 U/mL IL-2 in 24-well plates (Costar). Culture medium was replenished every 2 to 3 days with fresh complete T cell medium. After two rounds of specific stimulation, the polyclonal T cell bulk was incubated with PE labeled tetramers and single cell sorted using flow cytometry to obtain monoclonal T cells. After monoclonal cell sorting, T cell clones were stimulated with a phytohemagglutinin (PHA) mixture (complete T cell medium supplemented with 800 ng/mL PHA (Murex Biotech) and 100 U/mL IL-2) together with irradiated PBMCs ($50x10^5$ cells, 80Gy) and EBV-JY cells ($10x10^4$ cells, 100Gy) per 96-well.

Generation of pHLA-A*02:01 tetramers

Ultra-pure peptides were synthesized by JPT peptide technology. Recombinant HLA-A*02:01 and human β2m proteins were in-house synthesized in *Escherichia coli* [48,49]. Biotinylated HLA-A*02:01 molecules were produced containing an ultraviolet (UV)-sensitive peptide to enable easy transfer of specific peptide, as previously described [50]. In brief, HLA-A*02:01 complexes were purified by gel filtration using Fast protein liquid chromatography (FPLC). pHLA-A*02:01 complexes were exposed to UV light to facilitate peptide exchange resulting in peptide specific monomers. pHLA-A*02:01 tetramers were formed by coupling biotinylated pHLA-A*02:01 monomers with streptavidin-coupled R-phycoerythrin conjugate (PE, ThermoFisher). Tetramers were stored at -80°C for long-term storage or 4°C for short-term storage.

Co-culture T cell reactivity assay

Dependent on the T cell clone, GM-CSF (T cell clone 1A8 and PRAME), or IFN-γ (all other tested T cell clones) ELISA assays (GM-CSF, MabTech, IFN-γ, Pelikine) were used to measure the cytokine production of activated T cells. ELISA plates were coated with human IFN-γ or GM-CSF primary antibody overnight at 4°C. T cell conditioned medium was collected incubated in the pre-coated ELISA plates for two hours at room temperature. Next, ELISA plates were washed with PBS-T followed by incubation with the HRP conjugated secondary antibody for one hour. ELISA plates were developed with TMB (3,3,5,5-tetramethyl-benzidine liquid substrate supersensitive, for ELISA; Sigma-Aldrich) and measured at 450 nm using a plate reader (Spectramax id3, Molecular Devices). Lower cut-off values for cytokine production were calculated as medium values plus three times the standard deviation. Values below this threshold were considered negative. All plotted values were within the upper and lower detection limits of the ELISAs.

Affinity and stability assay

Peptide affinity and stability were determined as previously described [33,51]. In brief, HLA-A*02:01^{+} T2 cells were pulsed with increasing concentrations of peptide (1 uM-100 uM) in serum free RPMI culture medium for 24 hours at 37°C. For MHC:peptide affinity, the maximum HLA-A*02:01 expression was measured by flow cytometry to calculate the EC50 concentration. For MHC:peptide stability, HLA-A*02:01 positive T2 cells were pulsed with 100 uM peptide for 24 hours at 37°C. Maximum HLA-A*02:01 expression was determined and followed over time to calculate the $T_{1/2}$ value.

Generation of gene knockouts in tumor cells using CRISPR-CAS9

sgRNAs were designed to target exon 1 of the human TAP1 gene (sgTAP1: GCTGCTACTTCTCGCCGACT) or the $LRPAP1_{21-30}$ epitope located in exon 1 ($LRPAP1_{21-30}$:AGGGTCAGGTCGTTTCTGCG). The sgRNA target sequence was cloned into the lentiCRISPR v2 vector [52]. Virus particles were generated by co-transfecting sgRNA/CAS9 containing plasmid together with PAX2/pMD2.G packaging vectors into HEK293T cells using lipofectamine 2000 (ThermoFisher). Tumor cells were incubated with medium containing the virus particles for 24 hours and transduced tumor cells were selected with 1-5 ug/mL puromycin (Gibco). TAP1 knockout-efficiency was analyzed by measuring surface HLA-ABC (w6/32, Biolegend) expression using flow cytometry. Polyclonal TAP knockout cell lines were generated by FACS sorting the HLA-I^{low} cell population. CRISPR/CAS9 TAP-WT control cells were generated by FACS sorting the HLA-I^{high} cell population of the polyclonal bulk. TAP1 expression was verified by Western-Blot using anti-TAP1 antibodies (Cell Signaling).

Western Blot

Proteins from cell cultures were extracted in lysis buffer (RIPA, Cell Signaling), and protein concentrations were assessed using the Bradford Protein Assay Kit (Thermo Fisher). Protein samples were separated on a 4-12% SDS–polyacrylamide gel electrophoresis gel and transferred onto nitrocellulose membranes using semi-dry transfer (BioRad). To prevent a-specific binding, membranes were blocked with 5% milk in TBS-T for one hour at room temperature. Antibodies used: anti-TAP1 (dilution 1:1000, 4°C¸ Cell Signaling), anti- β-actin (dilution 1:1000, 4°C, Cell Signaling), HRP linked mouse anti-Rabbit IgG (dilution 1:5000, RT, Cell Signaling).

Flow cytometry analysis

CD3 (SK7), CD4 (SK3), CD8 (SK1), CD45RO (UCHL1), HLA-A*02:01 (bb7.2)(BD Biosciences), and HLA-ABC (MCA81A), CD45RA (HI100), CD62L (DREG-56) (Biolegend) anti-human mAbs were used for flow cytometry analysis. Cells were incubated with mAbs for 30min at 4°C and washed three times. Unstained cells were used as negative controls. The Vβ Repertoire analysis kit was used to determine the TCR Vβ of the different monoclonal T cells (Beckman Coulter). For T cell specificity analysis, we incubated T cells with pHLA-A*02:01 tetramers for 30min at RT and washed 3 times. T cells were considered tetramer positive when MFI was at least 10^2 times higher than unstained control. Cells were measured using a LSR-II flow cytometer (BD biosciences) and analyzed using Flowjo software version 10 (Tree Star).

mRNA isolation, cDNA synthesis, and qPCR analysis

Cell pellets were washed twice with PBS and snapfrozen in liquid nitrogen. RNA was isolated using the RNAeasy kit (Qiagen), according to manufactures protocol. cDNA was synthesized using the High capacity RNA-to-cDNA kit (Applied Biosystems). Quantitative PCR was done using SybrGreen supermix (Bio-Rad). For qPCR analysis we used the following primers. GAPDH_f: GTGCTGAGTATGTCGTGGAGTCTAC; GAPDH_r: GGCGGAGATGATGACCCTTTTGG; TAP1_f: CTTGCAGGGAGAGGTGTTTG; TAP1_r: GAGCATGATCCCCAAGAGAC; LRPAP1_f: GACCGAAGAAATCCACGAGA; LRPAP1_r: AGGTCCCACAGGTCAATCAC.

Statistical analysis

All data are presented as means and SD. Statistical analysis was done using a paired Student's t test (two-tailed) to determine the statistical significance of the differences. A minimum of three technical replicates were used in all experiments, and were repeated at least two times.

Online supplemental material:

Table SI. shows an overview of the number of histological tissue samples and cancer samples that are used to create the peptide elution database. In Fig. S1, we plotted the results of the predicted TEIPP candidate peptide binding in HLA-I. Fig. S2 shows the characterization of TEIPP T cells, sequence, binding affinity and stability of the TEIPP antigens, and homology with bacterial peptides. In Fig. S3, mRNA and protein expression analysis of LRPAP1 and TAP1 on the tumor panel, and functional T cell assays are shown to support the findings in figure 4 in the main text. Fig. S4 illustrates the protein expression analysis of TEIPP candidates in healthy and cancer tissue.

Author contributions:

T.H. and S.H.B. designed the project. K.A.M. and L.B. performed and designed all experiments. M.G.K., and K.A.M. synthesized the tetramers. E.V. provided all cancer cell lines. K.A.M. and T.H. wrote the manuscript. D.K. performed peptide matching analysis. HG.R. and S.S. shared their peptidome databases. K.A.M., T.H. and S.H.B. interpreted data. S.H.B., HG.R., S.S., and M.H.M.H. reviewed and edited the manuscript.

Acknowledgments:

We thank the peptide synthesis core facility and the flow cytometry core facility for their contribution to this project. Funding: This work was supported by the Dutch Cancer Foundation (2013-6142 for K.A.M.). Data and materials availability: Peptide elution database was made available by the Department of Immunology, Tübingen. The authors declare no competing financial interests.

References and Notes:

1 Robbins, P. F. *et al.* Mining exomic sequencing data to identify mutated antigens recognized by adoptively transferred tumor-reactive T cells. *Nat Med* **19**, 747-752, doi:10.1038/nm.3161 (2013).

2 Schumacher, T. N. & Schreiber, R. D. Neoantigens in cancer immunotherapy. *Science* **348**, 69-74, doi:10.1126/science.aaa4971 (2015).

3 Lauss, M. *et al.* Mutational and putative neoantigen load predict clinical benefit of adoptive T cell therapy in melanoma. *Nat Commun* **8**, 1738, doi:10.1038/s41467-017-01460-0 (2017).

4 Snyder, A. *et al.* Genetic basis for clinical response to CTLA-4 blockade in melanoma. *N Engl J Med* **371**, 2189-2199, doi:10.1056/NEJMoa1406498 (2014).

5 Ritter, C. *et al.* Epigenetic priming restores the HLA class-I antigen processing machinery expression in Merkel cell carcinoma. *Sci Rep* **7**, 2290, doi:10.1038/s41598-017-02608-0 (2017).

6 Setiadi, A. F. *et al.* Epigenetic control of the immune escape mechanisms in malignant carcinomas. *Mol Cell Biol* **27**, 7886-7894, doi:10.1128/MCB.01547-07 (2007).

7 Garrido, F., Aptsiauri, N., Doorduijn, E. M., Garcia Lora, A. M. & van Hall, T. The urgent need to recover MHC class I in cancers for effective immunotherapy. *Curr Opin Immunol* **39**, 44-51, doi:10.1016/j.coi.2015.12.007 (2016).

8 Patel, S. J. *et al.* Identification of essential genes for cancer immunotherapy. *Nature* **548**, 537-542, doi:10.1038/nature23477 (2017).

9 Sucker, A. *et al.* Acquired IFNgamma resistance impairs anti-tumor immunity and gives rise to T-cell-resistant melanoma lesions. *Nat Commun* **8**, 15440, doi:10.1038/ncomms15440 (2017).

10 Gao, J. *et al.* Loss of IFN-gamma Pathway Genes in Tumor Cells as a Mechanism of Resistance to Anti-CTLA-4 Therapy. *Cell* **167**, 397-404 e399, doi:10.1016/j.cell.2016.08.069 (2016).

11 Shin, D. S. *et al.* Primary Resistance to PD-1 Blockade Mediated by JAK1/2 Mutations. *Cancer Discov* **7**, 188-201, doi:10.1158/2159-8290.CD-16-1223 (2017).

12 Zaretsky, J. M. *et al.* Mutations Associated with Acquired Resistance to PD-1 Blockade in Melanoma. *N Engl J Med* **375**, 819-829, doi:10.1056/NEJMoa1604958 (2016).

13 Marijt, K. A., Doorduijn, E. M. & van Hall, T. TEIPP antigens for T-cell based immunotherapy of immune-edited HLA class I(low) cancers. *Mol Immunol*, doi:10.1016/j.molimm.2018.03.029 (2018).

14 Doorduijn, E. M. *et al.* TAP-independent self-peptides enhance T cell recognition of immune-escaped tumors. *J Clin Invest* **126**, 784-794, doi:10.1172/JCI83671 (2016).

15 Doorduijn, E. M. *et al.* T cells specific for a TAP-independent self-peptide remain naive in tumor-bearing mice and are fully exploitable for therapy. *Oncoimmunology* **7**, e1382793, doi:10.1080/2162402X.2017.1382793 (2018).

16 El Hage, F. *et al.* Preprocalcitonin signal peptide generates a cytotoxic T lymphocyte-defined tumor epitope processed by a proteasome-independent pathway. *Proc Natl Acad Sci U S A* **105**, 10119-10124, doi:10.1073/pnas.0802753105 (2008).

17 Durgeau, A. *et al.* Different expression levels of the TAP peptide transporter lead to recognition of different antigenic peptides by tumor-specific CTL. *J Immunol* **187**, 5532-5539, doi:10.4049/jimmunol.1102060 (2011).

18 Martoglio, B. & Dobberstein, B. Signal sequences: more than just greasy peptides. *Trends Cell Biol* **8**, 410-415 (1998).

19 Yewdell, J. W. *et al.* TAP-independent delivery of antigenic peptides to the endoplasmic reticulum: therapeutic potential and insights into TAP-dependent antigen processing. *J Immunother* **21**, 127-131 (1998).

20 Oliveira, C. C. *et al.* New role of signal peptide peptidase to liberate C-terminal peptides for MHC class I presentation. *J Immunol* **191**, 4020-4028, doi:10.4049/jimmunol.1301496 (2013).

21 Blum, J. S., Wearsch, P. A. & Cresswell, P. Pathways of antigen processing. *Annu Rev Immunol* **31**, 443-473, doi:10.1146/annurev-immunol-032712-095910 (2013).

22 Neefjes, J., Jongsma, M. L., Paul, P. & Bakke, O. Towards a systems understanding of MHC class I and MHC class II antigen presentation. *Nat Rev Immunol* **11**, 823-836, doi:10.1038/nri3084 (2011).

23 Kall, L., Krogh, A. & Sonnhammer, E. L. A combined transmembrane topology and signal peptide prediction method. *J Mol Biol* **338**, 1027-1036, doi:10.1016/j.jmb.2004.03.016 (2004).

24 Leonhardt, R. M. *et al.* Post-endoplasmic reticulum rescue of unstable MHC class I requires proprotein convertase PC7. *J Immunol* **184**, 2985-2998, doi:10.4049/jimmunol.0900308 (2010).

25 Leonhardt, R. M., Vigneron, N., Rahner, C. & Cresswell, P. Proprotein convertases process Pmel17 during secretion. *J Biol Chem* **286**, 9321-9337, doi:10.1074/jbc.M110.168088 (2011).

26 Medina, F. *et al.* Furin-processed antigens targeted to the secretory route elicit functional TAP1-/- CD8+ T lymphocytes in vivo. *J Immunol* **183**, 4639-4647, doi:10.4049/jimmunol.0901356 (2009).

27 Tiwari, N. *et al.* A transporter associated with antigen-processing independent vacuolar pathway for the MHC class I-mediated presentation of endogenous transmembrane proteins. *J Immunol* **178**, 7932-7942 (2007).

28 Sette, A. & Sidney, J. Nine major HLA class I supertypes account for the vast preponderance of HLA-A and -B polymorphism. *Immunogenetics* **50**, 201-212 (1999).

29 Sidney, J., Peters, B., Frahm, N., Brander, C. & Sette, A. HLA class I supertypes: a revised and updated classification. *BMC Immunol* **9**, 1, doi:10.1186/1471-2172-9-1 (2008).

30 Andreatta, M. & Nielsen, M. Gapped sequence alignment using artificial neural networks: application to the MHC class I system. *Bioinformatics* **32**, 511-517, doi:10.1093/bioinformatics/btv639 (2016).

31 Nielsen, M. *et al.* Reliable prediction of T-cell epitopes using neural networks with novel sequence representations. *Protein Sci* **12**, 1007-1017, doi:10.1110/ps.0239403 (2003).

32 Mullbacher, A. *et al.* High peptide affinity for MHC class I does not correlate with immunodominance. *Scand J Immunol* **50**, 420-426 (1999).

33 van der Burg, S. H., Visseren, M. J., Brandt, R. M., Kast, W. M. & Melief, C. J. Immunogenicity of peptides bound to MHC class I molecules depends on the MHC-peptide complex stability. *J Immunol* **156**, 3308-3314 (1996).

34 McKee, M. D., Roszkowski, J. J. & Nishimura, M. I. T cell avidity and tumor recognition: implications and therapeutic strategies. *J Transl Med* **3**, 35, doi:10.1186/1479-5876-3-35 (2005).

35 Snyder, J. T., Alexander-Miller, M. A., Berzofskyl, J. A. & Belyakov, I. M. Molecular mechanisms and biological significance of CTL avidity. *Curr HIV Res* **1**, 287-294 (2003).

36 Dutoit, V. *et al.* Heterogeneous T-cell response to MAGE-A10(254-262): high avidity-specific cytolytic T lymphocytes show superior antitumor activity. *Cancer Res* **61**, 5850-5856 (2001).

37 Vigano, S. *et al.* Functional avidity: a measure to predict the efficacy of effector T cells? *Clin Dev Immunol* **2012**, 153863, doi:10.1155/2012/153863 (2012).

38 Anderson, K. S., Alexander, J., Wei, M. & Cresswell, P. Intracellular transport of class I MHC molecules in antigen processing mutant cell lines. *J Immunol* **151**, 3407-3419 (1993).

39 Wei, M. L. & Cresswell, P. HLA-A2 molecules in an antigen-processing mutant cell contain signal sequence-derived peptides. *Nature* **356**, 443-446, doi:10.1038/356443a0 (1992).

40 Uhlen, M. *et al.* Proteomics. Tissue-based map of the human proteome. *Science* **347**, 1260419, doi:10.1126/science.1260419 (2015).

41 Oliveira, C. C. *et al.* Peptide transporter TAP mediates between competing antigen sources generating distinct surface MHC class I peptide repertoires. *Eur J Immunol* **41**, 3114-3124, doi:10.1002/eji.201141836 (2011).

42 Blees, A. *et al.* Structure of the human MHC-I peptide-loading complex. *Nature* **551**, 525-528, doi:10.1038/nature24627 (2017).

43 Lee, Y. K., Menezes, J. S., Umesaki, Y. & Mazmanian, S. K. Proinflammatory T-cell responses to gut microbiota promote experimental autoimmune encephalomyelitis. *Proc Natl Acad Sci U S A* **108 Suppl 1**, 4615-4622, doi:10.1073/pnas.1000082107 (2011).

44 Zitvogel, L., Ayyoub, M., Routy, B. & Kroemer, G. Microbiome and Anticancer Immunosurveillance. *Cell* **165**, 276-287, doi:10.1016/j.cell.2016.03.001 (2016).

45 van Hall, T. *et al.* Selective cytotoxic T-lymphocyte targeting of tumor immune escape variants. *Nat Med* **12**, 417-424, doi:10.1038/nm1381 (2006).

46 Chambers, B. *et al.* Induction of protective CTL immunity against peptide transporter TAP-deficient tumors through dendritic cell vaccination. *Cancer Res* **67**, 8450-8455, doi:10.1158/0008-5472.CAN-07-1092 (2007).

47 Doorduijn, E. M. *et al.* T Cells Engaging the Conserved MHC Class Ib Molecule Qa-1(b) with TAP-Independent Peptides Are Semi-Invariant Lymphocytes. *Front Immunol* **9**, 60, doi:10.3389/fimmu.2018.00060 (2018).

48 Garboczi, D. N., Hung, D. T. & Wiley, D. C. HLA-A2-peptide complexes: refolding and crystallization of molecules expressed in Escherichia coli and complexed with single antigenic peptides. *Proc Natl Acad Sci U S A* **89**, 3429-3433 (1992).

49 Burrows, S. R. *et al.* Peptide-MHC class I tetrameric complexes display exquisite ligand specificity. *J Immunol* **165**, 6229-6234 (2000).

50 Bakker, A. H. *et al.* Conditional MHC class I ligands and peptide exchange technology for the human MHC gene products HLA-A1, -A3, -A11, and -B7. *Proc Natl Acad Sci U S A* **105**, 3825-3830, doi:10.1073/pnas.0709717105 (2008).

51 Harndahl, M. *et al.* Peptide-MHC class I stability is a better predictor than peptide affinity of CTL immunogenicity. *Eur J Immunol* **42**, 1405-1416, doi:10.1002/eji.201141774 (2012).

52 Sanjana, N. E., Shalem, O. & Zhang, F. Improved vectors and genome-wide libraries for CRISPR screening. *Nat Methods* **11**, 783-784, doi:10.1038/nmeth.3047 (2014).

53 Oliveira, C. C. & van Hall, T. Alternative Antigen Processing for MHC Class I: Multiple Roads Lead to Rome. *Front Immunol* **6**, 298, doi:10.3389/fimmu.2015.00298 (2015).

Supplementary figures

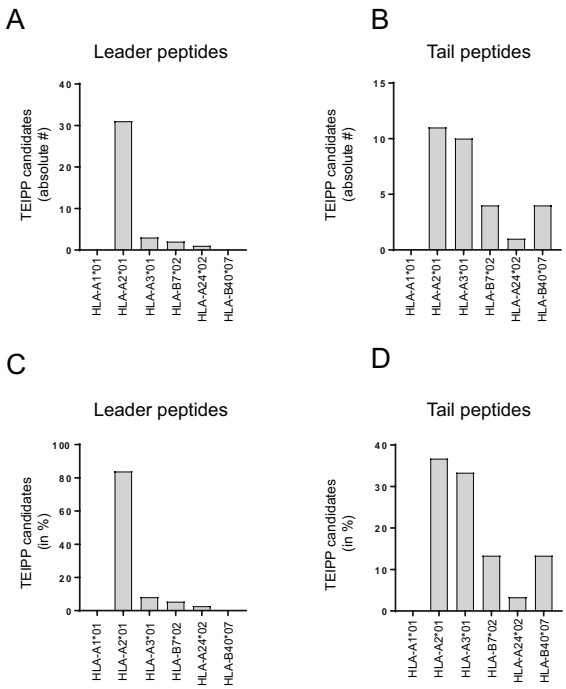

Figure S1. Prediction results of HLA-I binding of TEIPP neoantigen candidates.

TEIPP neoantigen candidate peptides (n=65) were aligned according to HLA binding specificity using a web-based algorithm. (A and B) Absolute number of TEIPP candidates with predicted binding in HLA superclasses for leader peptides and tail peptides. (C and D) Percentage of total TEIPP candidates with predicted binding in HLA superclasses for leader peptides and tail peptides.

A

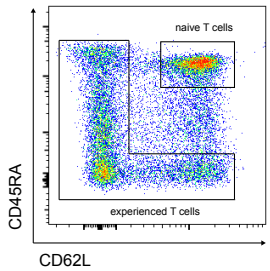

B

Bacteria family name:	peptide sequence
Ruminococcaceae:	TIIKPLIWV
p55:	VIIKPLVWV
Mycobacteriaceae:	LLALAAGLAV
p29:	LLALAAGLAV

C

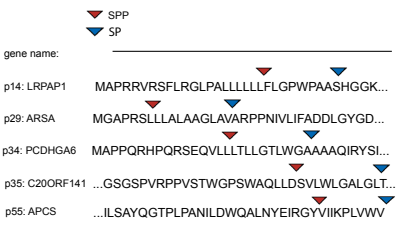

D

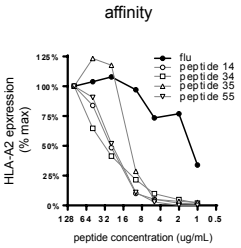

E

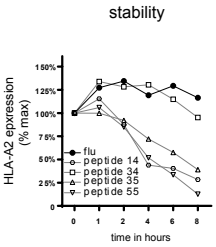

F

p14 TCRs	Vb	p29 TCRs	Vb
1H10	TRBV9	1H12	*
2B1	TRBV28	2G2	*
1A8	TRVB20-1	4D12	*

p34 TCRs	Vb	p35 TCRs	Vb
1G4	TRBV28	1H7	*
1G5	TRBV28	2B3	TRBV28
3G9	TRBV27	5D7	TRBV4

p55 TCRs	Vb
1C2	TRBV17
1E8	TRBV19
2G2	N.D

* unknown Vβ
N.D not determined

Figure S2. Characterization of TEIPP T cells and cognate antigen.

(A) Flow cytometry gating strategy for flow sorting PBMCs into experienced T cells and naive T cells. (B) Overview of bacterial peptide sequences with TEIPP peptide homology. (C) Gene name, peptide sequence, and predicted peptidase cleavage sites (SP [signal peptidase; blue triangle] and SPP [signal peptide peptidase; red triangle]) of p14, p29, p34, p35, and p55. (D) pHLA peptide affinity was measured by a cellular-based assay. Percentage of maximum HLA-I expression was determined by flow cytometry to calculate EC50 values. (E) pHLA peptide stability was measured by calculating EC50 values of maximum HLA-I expression over time. (D and E) Representative data of four independent experiments are shown. (F) Multiple T cell clones with different Vβs for the different specificities were isolated. Shown are the T cell clone name and corresponding T cell receptor β variable gene name, determined by using a TCR Vβ Screening Kit analyzed by flow cytometry

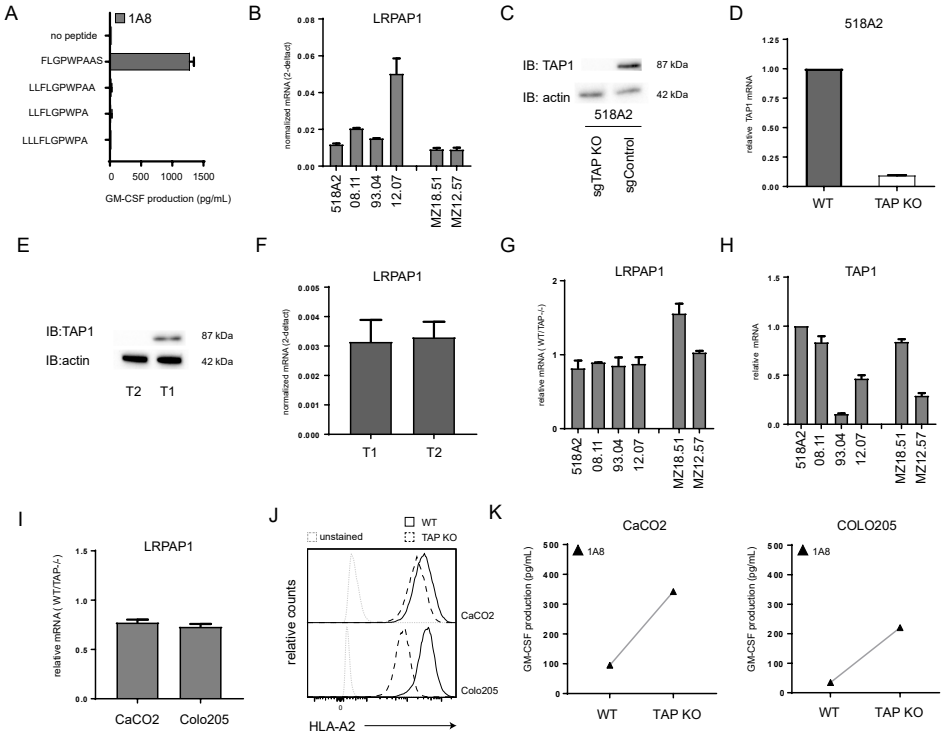

Figure S3. mRNA and protein expression analysis on tumor panel.

(A) Peptide specificity of the LRPAP121-30-specific T cell clone 1A8 was assessed by testing different length variants of the p14 peptide at different locations of the signal peptide. Peptides with a predicted HLA-A*02:01 binding (IC50 < 500 nM) were tested. GM-CSF cytokine production was measured by ELISA. (B) LRPAP1 mRNA levels of the tumor panel were determined by qPCR. (A and B) Data are shown as mean ± SD; n = 3. (C) TAP1 protein levels of the 518A2 skin melanoma cell line variants were measured using Western blot. No TAP1 expression was observed in the 518A2 TAP KO variant. (D) mRNA expression of TAP1 gene of the 518A2 skin melanoma cell line variants was determined by qPCR. Data are shown as mean ± SD; n = 2. (E) TAP1 protein levels of the T1 and T2 lymphoma were measured using Western blot. No TAP1 expression was observed in the T2 lymphoma. (F) LRPAP1 mRNA expression levels of the T1 and T2 lymphoma were determined by qPCR. Both cell lines had equal LRPAP1 mRNA expression. Data are shown as mean ± SD; n = 2. (G) LRPAP1 mRNA expression levels of the tumor panel were examined by qPCR. Relative mRNA gene expression of the TAP KO variant compared with WT variant was calculated. (H) Relative TAP1 mRNA levels of the tumor panel were determined by qPCR. (G and H) Data are shown as mean ± SD; n = 3. (I) LRPAP1 mRNA expression levels of two colon carcinoma cell lines were determined by qPCR. Equal levels of LRPAP1 mRNA expression were observed. Data are shown as mean ± SD; n = 2. (J) HLA-A*02:01 surface expression of the antigen-processing machinery–impaired colon carcinoma lines were measured by flow cytometry. (K) GM-CSF production of T cell clone 1A8 upon antigen recognition of two colon carcinomas (WT versus TAP KO). (J and K) Representative data of two independent experiments are shown.

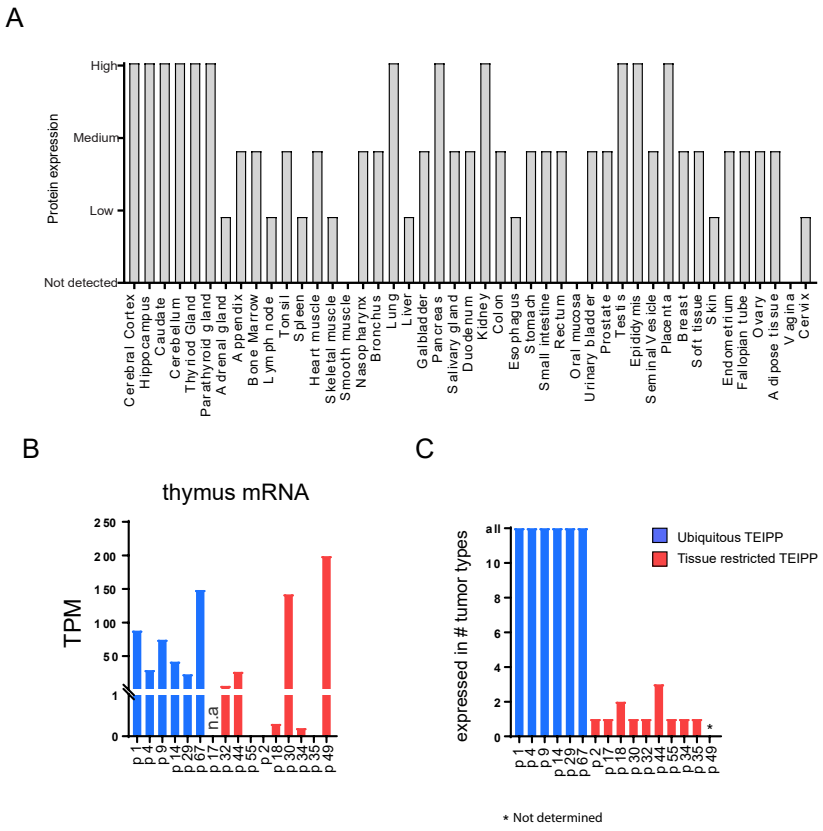

Figure S4. Database analysis of TEIPP candidates.

(A) LRPAP1 protein expression in 44 different healthy tissues. Data collected from the Human Protein Atlas. (B) mRNA expression of 16 identified TEIPP antigens in the thymus, expressed in tags per million (TPM). Data collected from FANTOM5 datasets. n.a., not applicable. (C) mRNA expression data of the TEIPP antigens were of different tumor types and were extracted from the Cancer Genome Atlas database. Our list with 16 TEIPP antigens is categorized in two groups: ubiquitous TEIPP, all examined tumor types have mRNA expression of the respective TEIPP antigen (TPM > 5); and tissue-restricted TEIPP, mRNA expression was only detected in some tumor types (TPM > 5).

Table S1. Overview of peptidome analyses from human tumor samples

Tissue Type	Malignant / Benign	n
Bone Marrow Mononuclear Cells	Benign	10
Granulocytes	Benign	2
PBMC	Benign	30
Liver	Benign (adjacent to tumor)	12
Colon	Benign (adjacent to tumor)	35
Ovary	Benign (adjacent to tumor)	4
Kidney	Benign (adjacent to tumor)	27
AML	Malignant	19
Breast Cancer	Malignant	2
CLL	Malignant	32
CML	Malignant	16
Glioblastoma	Malignant	6
HCC	Malignant	12
CRC	Malignant	35
Leiomyosarcoma	Malignant	1
Merkel Cell Carcinoma	Malignant	1
Meningioma	Malignant	1
Multiple Myeloma	Malignant	9
NSCLC	Malignant	1
Ovarian Cancer	Malignant	35
Peritoneal Carcinomatosis	Malignant	1
Polycythemia vera	Malignant (pre-)	10
RCC	Malignant	31
T-ALL	Malignant	2
Cell lines	Malignant / Immortalized	17
Total	Malignant	231
	Benign	120

Chapter 6

Dendritic cell vaccination therapy for immune escaped cancers

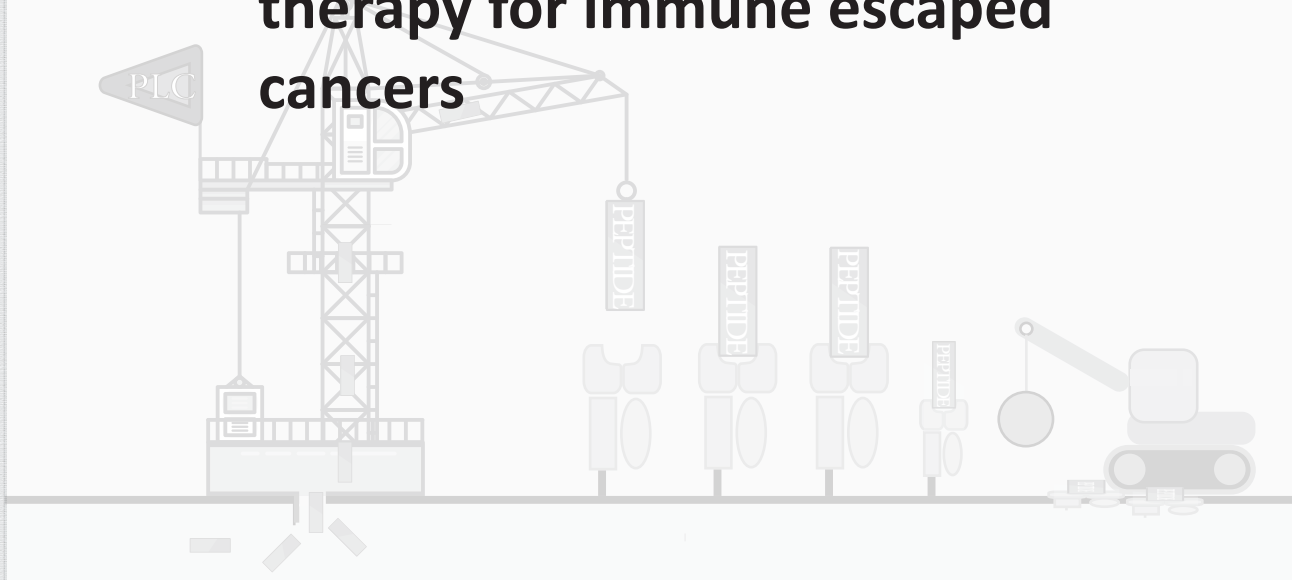

K.A. Marijt*, L. Griffioen, L. Blijleven, S.H. van der Burg, T. van Hall*

Manuscript in preparation (2020)

Abstract

TEIPP antigens are presented on cancer cells with defects in the antigen-processing pathway, in particular the peptide pump TAP. Therefore, CD8 T cell immunity to TEIPP peptides might constitute a salvage therapy for immune-escaped cancers. However, clinical application for TEIPPs have yet to be developed. Here, we describe the pre-clinical development of synthetic long peptide (SLP) vaccine for the most immunogenic TEIPP antigen identified thus far, derived from the LRPAP1 signal peptide. We show that dendritic cells were unable to cross-present a long version of the HLA-A*0201 presented $LRPAP_{21-30}$ epitope when elongated with its natural flanking sequence. Remarkably, amino acid exchange of the C-terminal anchor residue from a serine (S) to a valine (V) resulted in an enhanced T cell stimulation. $LRPAP_{21-30}$-specific CD8+ T cells isolated with multimers presenting either the S- or V-variant could be co-stained with the other multimer to the same extent, recognized the other peptide as well as recognized TAP-deficient tumor cells. Similar findings were obtained when CD8+ T cells were transfected with an isolated $LRPAP_{21-30}$-specific T cell receptor. Importantly, *in vitro* vaccination with the V-variant SLP resulted in cross-presentation of the peptide vaccine and in polyclonal LRPAP1-specific CD8 T cell cultures isolated from the normal T cell repertoire. Expanded CD8 T cell clones from these cultures not only recognized the natural S-containing peptide but also displayed a highly selective capacity to recognize TAP-deficient melanoma cells. We are currently developing TEIPP epitope vaccines for clinical testing in patients with immune escaped, TAP-impaired cancers.

Introduction

The success of T cell targeted immunotherapy relies on the presentation of tumor antigens on the cell surface of cancer cells. However, cancer cells often downregulate components of the antigen processing machinery to prevent the presentation of tumor-associated and tumor-specific antigens by HLA class I molecules[1-3]. One critical step in this intracellular process is the transport of liberated peptides over the ER membrane by the dedicated pump TAP, which functions as a bottleneck and delivers peptides for all HLA class I molecules[2-4]. Such processing defects allow the tumor to escape from CD8 T cell immunity and are frequently observed in human cancers. We have previously described a novel subset of tumor antigens that are selectively presented by cancers with down modulated TAP expression and called these TEIPP (Tumor Epitopes associated with Impaired Peptide Processing)[5-7]. In a recent study, we reported on the molecular identification of 16 HLA-A*0201 presented human TEIPP antigens by means of a novel hybrid forward-reverse approach[7]. The identified antigen from the signal sequence of the LRPAP1 protein was presented on multiple HLA-A*0201 positive TAP-deficient cancers, including renal cell carcinoma, lymphoma, melanoma, and colon carcinoma. Additionally, LRPAP1-specific T cells were detectable in all tested healthy donors and this repertoire could be activated *in vitro* to target these immune escaped cancers.

We now aim to exploit these findings for the benefit of cancer patients and develop therapeutic formats for immunotherapy. Although interest in cancer vaccines waned long ago due to a sheer lack of objective clinical responses in hundreds of trials, they recently regained attention since novel platforms demonstrated efficacy to induce broad CD4 and CD8 anti-tumor T cell immunity, increase immune infiltration of human cancers and eradicate pre-malignant lesions[8-10]. Moreover, vaccination therapy seems to combine very well with immune checkpoint blockade in that relapsed vaccinated patients responded extremely well to PD-1 therapy and, importantly, the addition of a long peptide vaccine to a standardized PD-1 treatment schedule improved the overall response rate and median overall survival [11,12].

All T cell-geared vaccination platforms depend on delivery of tumor antigens to the host and on the exceptional capability of dendritic cells to cross-present these tumor antigens in HLA class I and II molecules for subsequent T cell activation. Many parameters are important for successful development a therapeutic cancer vaccine, including delivery systems, route of administration and adjuvants, which are supposed to activate the innate immune system and induce T cell co-stimulatory molecules. Our group developed the synthetic long peptide (SLP) vaccination platform and showed that long peptides (20-35 amino acids) possess the capacity to trigger CD4 and CD8 T cell responses, and results in eradication

of premalignant lesions[9,13,14] as well as improves overall survival of patients with cancer when vaccinated during chemotherapy. Cross-presentation of long peptides by host dendritic cells depends on uptake and processing the proteasome, the dominant proteolytic enzyme, and TAP-mediated transport resulting in HLA class I loading[14-17]. However, most identified TEIPP tumor antigens derive from signal peptides at the N-terminus of nascent proteins and are thus processed in a proteasome- and TAP-independent way[7,18,19]. Thus, TEIPP antigens might need modifications in order to be exploited as SLP.

Here, we describe the pre-clinical development of the most prominent human TEIPP antigen derived from the LRPAP1 protein[7]. In short, we demonstrate that a single amino acid exchange in the sequence of this signal peptide allows application in the SLP platform. The alteration at position 9 resulted in a higher binding affinity to HLA-A*0201 and more efficient cross-presentation by monocyte-derived dendritic cells. *In vitro* vaccination with the altered peptide, led to the generation of CD8 T cells that exhibit an indistinguishable reactivity to the altered peptide sequence as well as the natural peptide, and were highly selective in recogning TAP-negative tumor cells. These data indicate that small alterations to signal peptide-epitopes retains immunogenicity of TEIPP antigens and render them suitable candidates for the SLP format.

Results

The signal peptide of LRPAP1 is not cross-presented by dendritic cells when provided as long peptide

We previously showed that the TEIPP antigen derived from the signal peptide of the ubiquitously expressed LRPAP1 protein is presented in HLA-A*0201 on a wide variety of TAP-deficient cancer types[7]. Here, we set out to exploit the TEIPP concept for vaccination strategies, in particular the synthetic long peptide (SLP) platform that we developed for viral-induced cancers. We assessed the efficiency of cross-presentation of a long version of this signal peptide $LRPAP_{21-30}$ in dendritic cells. Three different SLP variants were synthesized with natural flanking amino acids extending the amino-terminus, the carboxy-terminus or at both ends (figure 1a). We incubated these SLPs together with monocyte-derived dendritic cells (moDC), and used a LRPAP1-specific CD8 T cell clone to assess correct processing and presentation of the minimal TEIPP epitope. Cytokine release was measured and showed that none of the three SLPs were cross-presented to T cells, whereas exogenous pulsing of the short $LRPAP_{21-30}$ peptide did stimulate the T cells (figure 1a). These results suggested that cross-presentation of the $LRPAP_{21-30}$ epitope from its longer peptide stretch is not efficient and had to be optimized for vaccine applications.

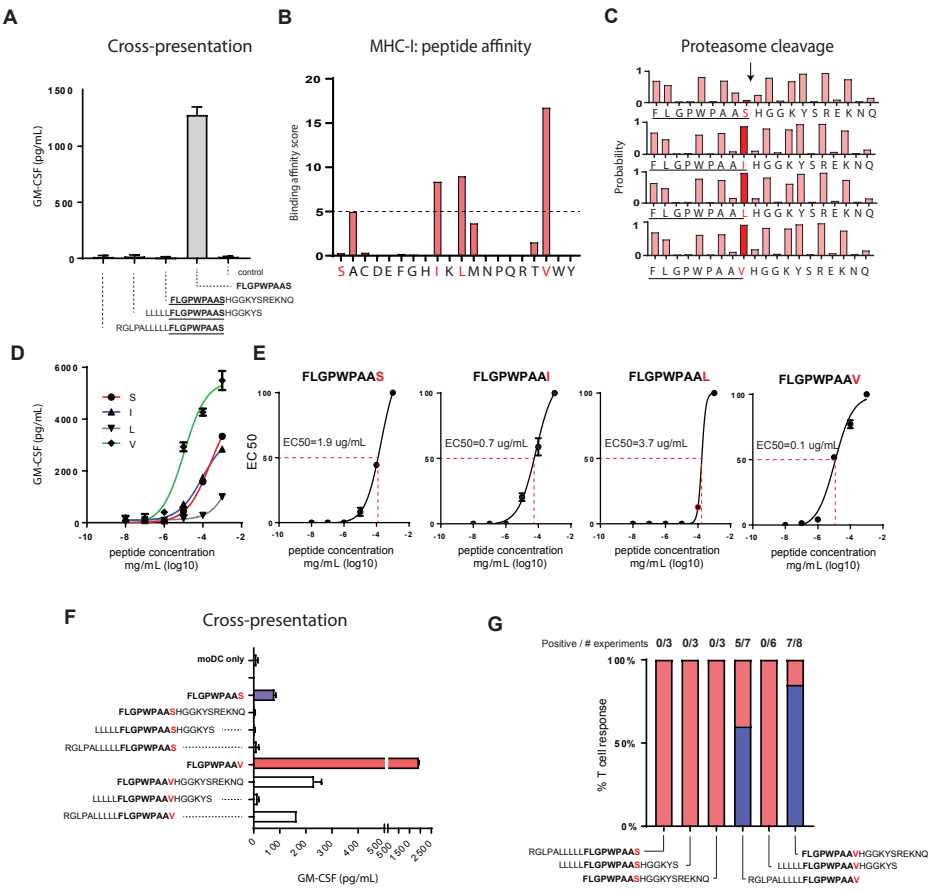

Figure 1: Substitution of the C-terminal amino acid of the signal peptide of LRPAP1 allows for cross-presentation by dendritic cells.

(A) Monocyte-derived dendritic cells were incubated with long peptides of the LRPAP1 epitope and co-cultured with a TEIPP-specific CD8 T cell clone. Natural flanking amino acids were used to elongate the minimal epitope. GM-CSF secretion by the TEIPP-specific T cell clone was used to determine cross-presentation efficiency and pulsing with short peptide was used as positive control. (B) Predicted HLA-A2*01 binding affinity scores of LRPAP1 peptides with substituted amino acids at the C-terminal p9 (MHCnet 4.1 algorithm). Binding affinity score was calculated on basis of the IC50 values and ranking percentage (see Table 1 for exact values). (C) Predicted proteasome cleavage activity for four different LRPAP1 peptides using NetCHop 3.1 algorithm. A score of 1 is maximal and predicts cleavage by the proteasome after the indicated amino acid. Arrow indicates the C-terminus of the LRPAP1 epitope. (D) Functional T cell avidity was measured as GM-CSF secretion by TEIPP-specific T cell clone stimulated with short peptide–pulsed EBV-JY cells in serial dilutions of the peptides. Mean and SD are plotted from one out of three experiments with similar outcome. (E) EC50 values were calculated from values obtained in D. (F) Monocyte-derived dendritic cells were cultured with different long S- and V-peptides of the LRPAP1 sequence. Cross-presentation of the long peptides was determined by T cell clone. Pulsed short peptide served as positive controls. (G) Overview of cross-presentation experiments using dendritic cells from eight different donors.

Serine to Valine substitution of the C-terminal anchor allows efficient binding and cross-presentation

Cross-presentation of long peptides by dendritic cells involves multiple sequential steps, including uptake via endocytosis, cytosolic cleavage of the SLP into short peptides by the proteasome, transport over the ER membrane by TAP and loading onto MHC-I molecules[15]. Previous studies have shown that the $LRPAP_{21-30}$ epitope has a moderate binding affinity onto HLA-A*0201[7], since the C-terminal serine is not a preferred anchor residue for binding into this allele[7]. This anchor residue is important for binding to MHC-I molecules and can be replaced because T cell receptors (TCR) do not interact with these residues. We investigated if serine exchange into another amino acid would result in a more efficiently processed epitope. First, the binding affinity to HLA-A*0201 of all possible peptide sequences with varying amino acids at position 9 was estimated using an *in silico* algorithm (table 1, figure 1b). The C-terminal serine had indeed a low predicted binding score and ranking (affinity=364nM, %rank=2.50, respectively). However, substitution of serine (S) into, isoleucine (I), leucine (L), or valine (V) resulted in strongly enhanced predicted binding affinities. Replacement with a valine resulted in an affinity of 6nM and rank percentage of 0.05%. Additionally, proteasome cleavage probability analysis using netCHOP, revealed a probability score close to the maximum of 1, for isoleucine (I), leucine (L), and valine (V), whereas the natural serine (S) at the C-terminus had a cleavage probability score of almost 0 (figure 1c). These *in silico* analyses indicated that these two important parameters might be strongly improved by substitution of the serine (S) by an isoleucine (I), leucine (L), or valine (V) at the C-terminus.

To examine whether these substitutions would interfere with LRPAP1-specific T cell recognition, we exogenously pulsed short peptide variants of the exact epitope in titrated concentrations on HLA-A*0201 positive T2 cells and measured T cell activation (figure 1d). Unexpectedly, the I- and L-variant peptides induced similar or worse cytokine responses when compared to the S-peptide, while the V-peptide induced a more potent IFNy response (figure 1d). Calculation of the EC50 values confirmed that the V-peptide variant elicited the strongest T cells response at limiting peptide concentrations (EC50 in ug/mL= V: 0.1, S: 1.9, I: 0.7, L: 3.7) (figure 1e). We concluded that substitution of serine (S) to valine (V) at the C-terminus of the $LRPAP_{21-30}$ peptide resulted in better MHC-I binding affinity and a 19-fold better T cell activation. We then evaluated cross-presentation of the V-peptide variant as SLP. moDCs were incubated with SLPs containing the S (S-SLP) or the V (V-SLP) variant of the TEIPP epitope. After uptake and processing of the SLPs, the moDCs were co-cultured with a LRPAP1-specific T cell clone and cytokine production was measured (figure 1f). While the three S-SLP variants again failed to activate T cells, the C- and the N-terminal extended peptide of V-SLP, but not the variant with elongations at both ends, were efficiently processed

Peptide sequence	NetMHC		
	Affinity (nM)	%Rank	[1]
FLGPWPAAS	364.80	2.50	WB
FLGPWPAAA	20.23	0.30	SB
FLGPWPAAC	303.14	2.50	WB
FLGPWPAAD	6719.97	12.00	NB
FLGPWPAAE	4516.70	9.00	NB
FLGPWPAAF	521.16	3.00	NB
FLGPWPAAG	984.43	4.00	NB
FLGPWPAAH	7052.81	12.00	NB
FLGPWPAAI	11.98	0.15	SB
FLGPWPAAK	4183.99	8.50	NB
FLGPWPAAL	11.14	0.15	SB
FLGPWPAAM	27.46	0.40	WB
FLGPWPAAN	4995.00	9.50	NB
FLGPWPAAP	1762.34	5.50	NB
FLGPWPAAQ	3029.38	7.50	NB
FLGPWPAAR	3690.59	8.00	NB
FLGPWPAAT	66.98	0.80	WB
FLGPWPAAV	5.98	0.05	SB
FLGPWPAAW	2198.56	6.00	NB
FLGPWPAAY	3105.78	7.50	NB

[1] SB, strong binder; WB, weak binder; ND, non-binder

Table 1: HLA-A*02:01 peptide binding scores of the LRPAP1 epitope

Overview of predicted binding affinity of p14 peptide variants where the anchor residue at position 9 is substituted with all other known amino acids using NetMHC 4.1. Peptide variants highlighted in green are predicted as strong binders in HLA-A*02:01.

and presented by the moDCs (figure 1f). These results were reproducible in nearly all of the independent experiments with different moDC donors and revealed that the C-terminal extension was most efficiently processed (7/8 donors) (figure 1g). To summarize, these data showed that the substitution of serine (S) to valine (V) at the C-terminus of the LRPAP1-derived TEIPP antigens allows for application in the SLP vaccination platform.

Characterization of CD8 T cell repertoire isolated with the optimized TEIPP peptide

Next, we evaluated the cross-reactivity of the CD8 T cell repertoire, isolated and expanded with the V-peptide, to the wild type $LRPAP_{21-30}$ peptide, as an SLP vaccine should ultimately generate T cell reactivity towards the natural peptide sequence as presented by TAP-deficient tumors. Therefore, we generated CD8 T cell cultures using our previously described approach with HLA-A*0201 tetramer pull-down and subsequent expansion by peptide stimulations[7]. This protocol resulted in the generation of polyclonal, LRPAP1-specific CD8 T cell cultures induced by the V-variant or the natural S-variant (figure 2a). Combined tetramer staining revealed that both T cell cultures bound tetramers with the S-variant as well as the V-variant, indicating that these T cell repertoires were indistinguishable in specificity (figure 2b). The CD8 T cell repertoire isolated and stimulated with V-peptide variant seemed to bind the tetramers with somewhat lower affinity, as mean fluorescence intensities were lower (figure 2b, c). This might reflect the weaker binding capacity of the S-peptide whereby only high-affinity TCRs are recruited from the total repertoire, whereas the strongly binding V-peptide was able to also recruit lower-affinity TCRs.

Figure 2: Isolation of LRPAP1-specific T cells with HLA-A2*01 tetramers containing the short V-substituted peptide.

(A) Schematic overview of the tetramer pull-down approach and subsequent stimulation with short peptides. (B) Specificity of polyclonal T cells measured by double tetramer staining of FLGPWPAAS peptide isolated T cells (upper panel) or FLGPWPAAV peptide isolated T cells (bottom panel) by flow cytometry. (C) Geomeans for double tetramer positive cells on FLGPWPAAS or FLGPWPAAV peptide isolated T cells. (D) Reactivity of polyclonal T cell bulks by measurement of IFNγ and GM-CSF production upon peptide pulsed EBV-JY cells. Means and SD are plotted of one out of three independent experiments. (E) Reactivity of these polyclonal T cell bulks to 518A2 melanoma panel.

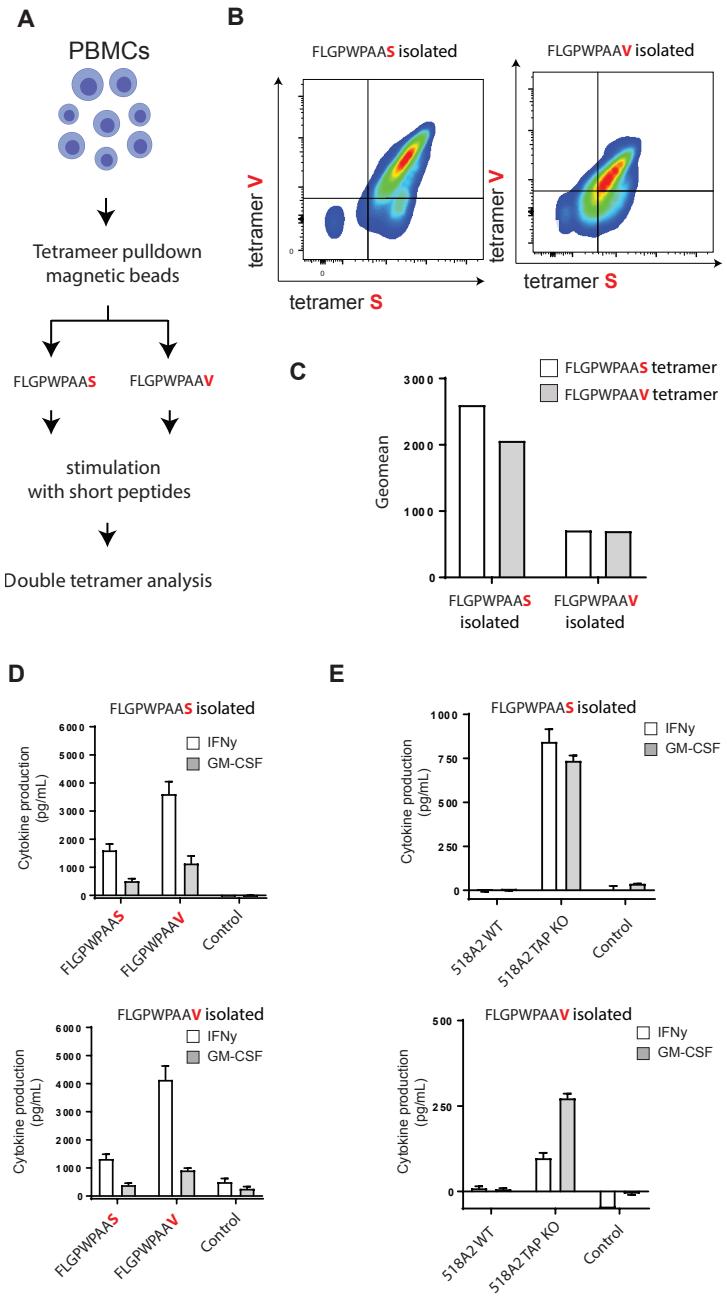
A
PBMCs
Tetrameer pulldown
magnetic beads
FLGPWPAAS
FLGPWPAAV
stimulation
with short peptides
Double tetramer analysis
B
FLGPWPAAS isolated
FLGPWPAAV isolated
tetramer V
tetramer S
C
FLGPWPAAS tetramer
FLGPWPAAV tetramer
Geomean
FLGPWPAAS isolated
FLGPWPAAV isolated
D
FLGPWPAAS isolated
IFNy
GM-CSF
Cytokine production (pg/mL)
FLGPWPAAS
FLGPWPAAV
Control
FLGPWPAAV isolated
E
FLGPWPAAS isolated
518A2 WT
518A2 TAP KO
Control
FLGPWPAAV isolated

To test the functionality of these T cell bulks, we measured cytokine responses towards both short peptides pulsed on immortalized HLA-A*0201 positive B cells (figure 2d). Both T cell bulks responded to both peptides by secretion of IFNy and GM-CSF, indicating that the T cell repertoire selected via the high affinity binding V-peptide is cross-reactive to the natural S-peptide. Finally, we tested the recognition of naturally presented S-peptides on the surface of the TAP-negative melanoma 518A2 cell line (figure 2e). Importantly, V-peptide induced polyclonal T cell cultures exhibited preferred recognition of the TAP-negative tumor line as compared to the TAP-proficient counterpart. These data are in line with previous findings that the C-terminal amino acid is an anchor position for binding to HLA-A2*01 molecules and is not directly involved in the TCR interface. We concluded that the exchange of C-terminus into a valine of the LRPAP1-derived TEIPP antigen results in the isolation of a comparable peptide-specific CD8 T cell repertoire from the total pool of CD8 T cells.

TCR gene transfer confers LRPAP1-specificity

Vaccination with synthetic long peptides aims to elicit T cell reactivity from the natural T cell repertoire. TCR gene transfer from TEIPP-specific CD8 T cells constitutes an alternative immunotherapeutic approach to introduce T cell immunity to TAP-deficient cancers. We examined this with the rearranged TCR from the previously described CD8 T cell clone 1A8 (figure 3). DNA sequencing of both TCR-alpha and TCR-beta chains revealed the rearranged sequences and the TCR-Vβ2 usage was confirmed by flow cytometry (table 2 and figure 3a). Retroviral constructs of this TCR with mouse C-domains to improve correct pairing of the transduces genes resulted in successful generation of TCR-transduced CD8 T cells as measured by an antibody to mouse TCR-Cβ domain (figure 3b). Tetramer staining confirmed that both TCR chains were expressed and recognized both S-variant and V-variant peptides, indicating that the specificity T cell clone 1A8 was preserved (figure 3c). Moreover, T cell reactivity was conferred by TCR gene transfer in that stronger cytokine responses were observed against the V-variant peptide than to the S-variant (figure 3d). Finally, TCR transduced T cells selectively recognized TAP-deficient melanomas in a comparable way as the original T cell clone (figure 3e)[7]. Together, these proof-of-concept data demonstrated the feasibility of TCR gene transfer as a mode of immunotherapy for TEIPP antigens and suggests that vaccination with the V-SLP may provide *in vivo* help to prevent T cell contraction.

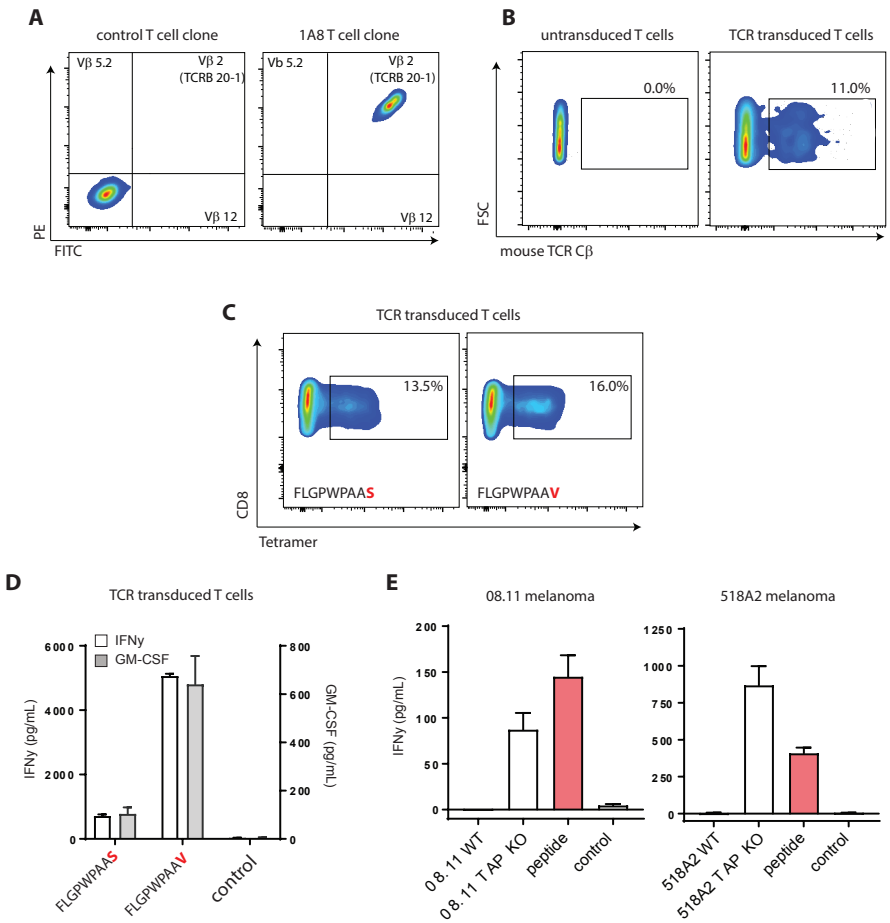

Figure 3: T cell receptor gene transfer of LRPAP1-specific CD8 T cells.

(A) Flow cytometry staining of LRPAP1-specific T cell clone 1A8 using three different Vβ antibodies revealing expression of TCR Vβ2 usage. (B) TCRαβ gene transduction into T cells from a healthy donor. The introduced genes contain the murine TCR-Cβ domain which enhances correct pairing of transgenic alpha and beta chains. (C) Tetramer staining of TCRαβ transduced CD8 T cells. (D) Functional reactivity to peptide pulsed EBV-JY cells of tetramer-enriched TCR-transduced T cells. T cell activation was measured by IFNγ or GM-CSF production. Means and SD are depicted from one out of three experiments with similar outcome. (D) TCR transduced T cells were co-cultured with two melanoma cell lines, which were rendered TAP-deficient by CRISPR/CAS9 technology.

In vitro vaccination with V-SLP promotes the expansion of LRPAP$_{21-30}$-specific TEIPP T cells.

The validate the concept of V-exchanged SLP vaccination for the induction of LRPAP1-directed TEIPP T cell responses a so-called *in vitro* vaccination protocol was used[20,21]. SLP-loaded moDC were co-cultured for two sequential stimulations with tetramer-enriched autologous T cells (figure 4a). Already after one round of stimulation a great expansion of LRPAP1-specific T cells was observed compared to control cultures, as measured by tetramer analysis (16.6% versus 1.5%, respectively) (figure 4b). This specific expansion was even more pronounced after the second stimulation (38.5% versus 0.2%, respectively) (figure 4b), indicating that professional antigen-presenting cells are capable to cross-present the V-SLP and activate TEIPP-specific T cells. These results were remarkable in the light of our previous finding that all LRPAP1-specific CD8 T cells were still in the naïve state of healthy donors[7] and suggest that we observed real *in vitro* priming in our co-cultures.

Next, we generated CD8 T cell clones in order to determine their reactivity towards TAP-deficient cancers. Tetramer-positive T cells were sorted by flow cytometry as single cells and expanded in an antigen-unrelated way using the mitogen phytohaemagglutinin (PHA). T cell clones were analyzed for their specificity by tetramer analysis (figure 4c). Five new T cell clones showed equal staining for both V-peptide and S-peptide tetramers, comparable to the previously isolated clone 1A8[7]. Importantly, two TAP-deficient melanomas were efficiently recognized by three (2H11, 2B9, and 1A10) of these five SLP-induced CD8 T cell clones, in a manner very similar to the previously established clone 1A8 (figure 4d). Collectively, these observations demonstrated that the V-SLP constitutes a functional TEIPP vaccine ready to be exploited for the induction of LRPAP1-specific T cell immunity.

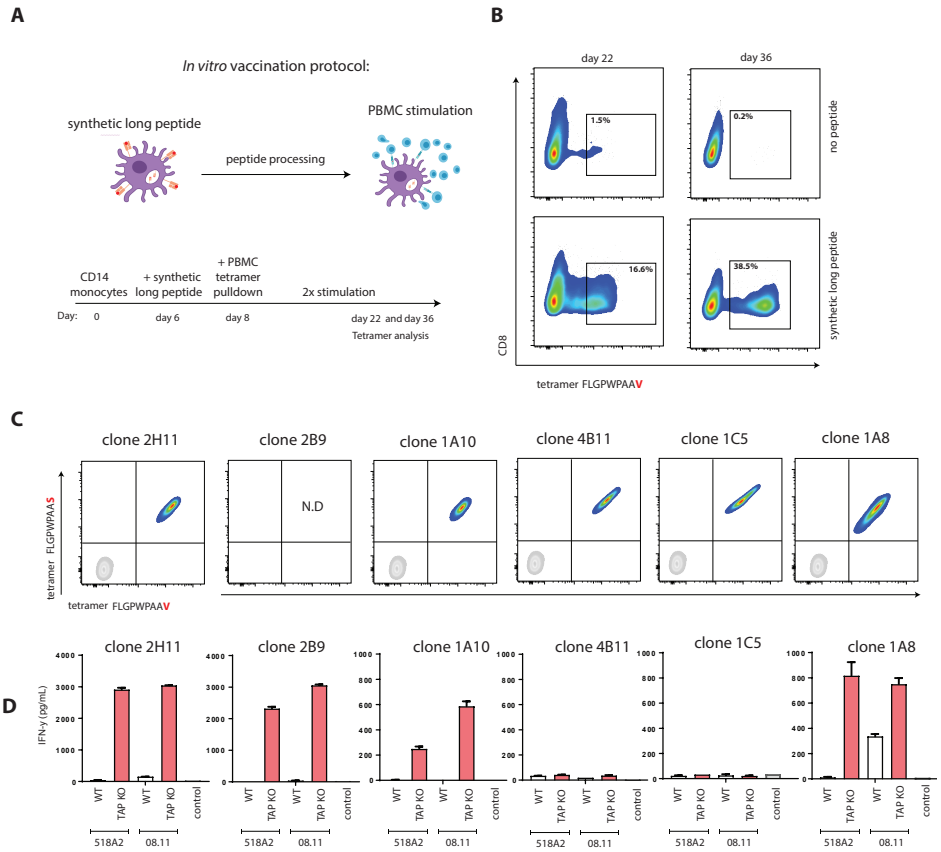

Figure 4: In vitro vaccination with V-SLP results in stimulation of LRPAP1-specific T cell repertoires.

(A) Schematic overview of the *in vitro* vaccination protocol using two V-variant peptides (C-terminal and N-terminal extended) as synthetic long peptides that require cross-presentation by monocyte-derived dendritic cells for priming of CD8 T cells. (B) *In vitro* vaccination protocol resulted in T cell bulk cultures containing LRPAP1-specific CD8 T cells as determined with tetramer staining. Control co-cultures were incubated without any long peptide. (C) LRPAP1-specific T cell clones were generated from single cell FACS sort and tested for reactivity to the natural S-variant peptide. Clone 1A8 was isolated from a previous study[7], and used as a reference clone. (D) LRPAP1-specific T cells clones were examined for recognition of TAP-deficient melanoma cell lines and their wild-type counterparts. Means and SD are shown from one out of two experiments with similar outcome.

Discussion

The aim of this study was to design a synthetic long peptide (SLP) vaccine for the TEIPP antigen derived from the LRPAP1 protein. The HLA-A*0201 presented peptide-epitope $LRPAP_{21-30}$ (FLGPWPAAS) is encoded by the signal peptide (also referred to as 'leader sequence') which functions to dock protein translational products to the sec61 translocation channel in the ER membrane[22]. These signal peptides are usually cleaved from nascent proteins by the protease Signal Peptidase (SPase), resulting in a small protein transmembrane remnant. These signal peptide stubs are liberated from the ER membrane by the protease Signal Peptide Peptidase (SPPase) and cleaves within the lipid bilayer[19]. A part of the signal peptide thus enters the ER in a TAP-independent fashion and this is the reason why signal peptides are overrepresented in the HLA class I binding repertoires of TAP-deficient cells[23-25]. Although not formally demonstrated, the liberation of the $LRPAP_{21-30}$ peptide is most likely not mediated by the proteasome, which is involved in proteolytic cleavage of the majority of HLA class I presented peptides[4]. Indeed, the *in silico* probability algorithm NetCHop predicted that cleavage after the natural serine at p9 of the $LRPAP_{21-30}$ sequence is not likely (figure 1c). We therefore conclude that this signal peptide is processed in a proteasome- and TAP-independent way. Application of synthetic long peptide vaccines, however, depends on uptake by host dendritic cells and processing via the classical route, involving proteasomes and the peptide transporter TAP[26]. We demonstrated that the long peptide of LRPAP1 encompassing the minimal peptide-epitope fails to be cross-presented in dendritic cells (figure 1). The single amino acid substitution from serine to a valine at p9 of the epitope rendered the long peptide sensitive for proteasomal cleavage and, in addition, improved binding affinity to HLA-A*0201. We hypothesize that this single amino acid exchange may alter the processing pathway of this signal sequence peptide, from SPase- and SPPase-mediated to proteasome-mediated.

Table 2: Specification of TCR the LRPAP1-specific T cell clone 1A8

	TCRa chain	TCRb chain
V-GENE and allele	TRAV12-1*01F	TRBV20-1*01F
J-GENE and allele	TRAJ26*01F	TRBJ2-3*01F
(D)-GENE and allele	-	TRBD1*01F
CDR3 region		
Nucleotide sequence	tgt gtg gtg atg ggc tat ggt cag aat ttt gtc ttt	tgc agt gct atg ggg aga cag agc aca gat acg cag tat ttt
Amino acid sequence	CVVMGYGQNFVF	CSAMGRQSTDTQYF
V(D)J region sequence	cggaaggaggtggagcaggatcctggacccttcaatgttccaga gggagccactgtcgctttcaactgtacttacagcaacagtgcttct cagtctttcttctggtacagacaggattgcaggaaagaacctaag ttgctgatgtccgtatactccagtggtaatgaagatggaaggttt acagcacagctcaatagagccagccagtatatttccctgctcatc agagactccaagctcagtgattcagccacctacctctgtgtggtg atgggctatggtcagaattttgtctttggtcccggaaccagattgt ccgtgctgccct	cggaagatgctgctgcttctgctgcttctggggccaggctccggg cttggtgctgtcgtctctcaacatccgagctgggttatctgtaaga gtggaacctctgtgaagatcgagtgccgttccctggactttcagg ccacaactatgttttggtatcgtcagttcccgaaacagagtctcat gctgatggcaacttccaatgagggctccaaggccacatacgagc aaggcgtcgagaaggacaagtttctcatcaaccatgcaagcctg accttgtccactctgacagtgaccagtgcccatcctgaagacagc agcttctacatctgcagtgctatggggagacagagcacagatac gcagtattttggcccaggcacccggctgacagtgctcgaggacct gaaaaacgtgttccca

Side-by-side comparison of S- and V-peptide induced T cell responses with the use of an *in vitro* vaccination protocol revealed that both repertoires were comparable concerning cross-reactivity and functionality (figure 4). Stimulation with the short V-peptide seemed to recruit a CD8 T cell repertoire with lower affinity as witnessed by less intense staining with tetramers (figure 2b). However, stimulation with dendritic cells loaded with long peptides, which require intracellular cross-presentation, resulted in polyclonal CD8 T cell bulks and clones with high affinity and strong capacity to recognize the natural S-variant on TAP-deficient melanomas (figure 4). These findings imply that vaccination with the optimized V-SLP would result in the generation of LRPAP1-specific T cells with high affinity TCRs. This advantage of SLP over vaccination with short minimal epitopes is in line with our previous investigations in pre-clinical mouse models and suggest that the SLP platform is well suited to recruit a high affinity TCR repertoire[14,17].

Interestingly, we previously showed that LRPAP1-specific T cells all reside in the naïve repertoire of healthy blood donors, indicating that our *in vitro* vaccination protocol actually primed CD8 T cells and not merely reactivated memory T cells[7]. The differentiation status of LRPAP-1-specific T cells in cancer patients and in particular those harboring TAP-deficient tumor cells needs further analysis, however, data from our mouse tumor model revealed that TEIPP-directed CD8 T cells are still naïve in these situations[6,27]. We found that TAP-deficient tumors failed to prime TEIPP T cells and also host dendritic cells were unable to pick up TEIPP antigens and cross-prime them. Consequently, TEIPP immunity might need to be installed by active immunizations, like we suggested here via SLP vaccines, or by TCR gene transfer into host T cells. Thus, the optimized long peptide of the signal peptide of LRPAP1 containing one amino acid exchange constitute an ideal vaccine candidate to induce TEIPP immunity in cancer patients. Although cancer vaccines lack potential to induce cancer remission as standalone therapy[8], combinations with checkpoint blockade or other immunomodulatory compounds might lead to successful immune attack to immune-escaped TAP-deficient cancers, as has been shown for the combination of cancer-virus vaccination with PD-1 blockade[11].

Material and methods

Cell culture

Tumor cells were cultured in DMEM medium (Gibco) supplemented with 100ug/mL streptomycin, 100 U/mL penicillin, 2mM L-glutamine (Invitrogen) and 10% FCS (Gibco). Genetic disruption of the TAP1 gene in human tumor cell lines was performed with CRISPR/CAS9 and described before[7]. T cells were cultured in IMDM medium (Gibco) supplemented with 2mM L-glutamine, 10% human serum (Sanquin), and 50U/mL IL-2 (proleukine, Novartis). T cells were stimulated every 10-14 days using synthetic short peptide (in house synthesis) or 800 ng/ml PHA (Phytohaemagglutinin) (Murex Biotech), supplemented with 100 U/ml IL-2 and IL-7 (5ng/mL), and a feeder mix containing irradiated PBMCs (1×10^6 cells, 80 Gy), and EBV-JY cells (1×10^5 cells, 100 Gy). All cell types were maintained in humidified air incubator at 37°C and 5% CO_2.

In vitro vaccination protocol

HLA-A*02:01 positive PBMCs were isolated from buffy-coats from consented donors (Sanquin bloodbank, Amsterdam), using a gradient ficoll layer. PBMCs were incubated with anti-CD14 magnetic beads for 20 min at 4 °C and the CD14 positive monocytes were isolated using magnetic separation columns (miltenyi). CD14+ monocyte were cultured in RPMI medium supplemented with 10% FCS, GM-CSF (800 units/ml), and IL-4 (500 units/ml) for 6 days to generate immature monocyte-derived dendritic cells. On day 6, the immature moDCs were incubated with synthetic long peptide (20 µg/ml, in house synthesized) for 24h, and matured with LPS (20 ng/ml) stimulation on day 7. Differentiation of monocytes to matured moDCs was verified by flow cytometry analysis. Matured moDCs were co-cultured with tetramer enriched T cell bulks in complete T cell medium. T cell bulks were stimulated a second time after 14 days. T cell specificity and reactivity were analyzed by flow cytometry.

T cell clone isolation from expanded T cell bulks

Expanded CD8 T cells were single cell sorted on tetramer positive cells in 96-well plates, using an Aria III machine (BD). Following FACS sorting, single T cells were non-specifically stimulated using PHA (800ng/mL), a feeder mix containing irradiated PBMCs (1×10^6 cells, 80 Gy), and EBV-JY cells (1×10^5 cells, 100 Gy), supplemented with IL-2 (100 units/mL) and IL-7 (5ng/mL) every 10-14 days. Expanded T cell clones were analyzed on tetramer specificity and further expanded in T25 culture flasks using the non-specific (PHA) T cell expansion protocol.

T cell receptor sequencing

Monoclonal T cells ($2x10^6$) were washed in cold PBS/BSA and pelleted by centrifugation. mRNA from T cell clones were isolated using the Dynabeads mRNA purification kit (Thermofisher). Full-length cDNA from the TCRα and TCRβ was generated using SMARTscribe reverse transcriptase with oligo's binding the constant domain of the TCRs[28]. Amplification of the cDNA transcript was done by standard PCR reaction using nested primers and high fidelity Taq polymerase. The PCR reaction mix was purified over a DNA purification column and nucleotide sequence analysis was done using Sanger sequencing (in house sequence facility). TCR sequencing results were analyzed using the T cell receptor sequence alignment software (V-quest) from IMGT (http://www.imgt.org/). Full-length codon optimized cDNA transcripts for murinized TCRs for both TCR-alpha and TCR-beta chains were cloned into a retroviral pMP71 flex expression vector[28].

Retrovirus production and T cell transductions

Platinum-Amphotropic retrovirus production (Plat-A) retroviral packing cells (Cell Biolabs) were used for retrovirus production. Plat-A cells were seeded in 6-well plates and incubated overnight until fully attached. Next, the cells were transfected with 2 µg pMP71_1A8 TCR vector using lipofectamine 2000. Retrovirus supernatant was collected on 24h and

48h after transfection, spun down to remove cells, and stored in -80 ^{0}C. CD8 T cells were purified from PBMC using magnetic bead isolation (Miltenyi), and a-specifically activated by aCD3/aCD28 beads (Thermofisher). After 48h, 1x10^{6} activated CD8 T cells were plated in a retronectin (Takara) coated 24-well together with 0.5mL retrovirus supernatant. Subsequently, CD8 T cells and retrovirus containing supernatant was spun down for 120min at 1300g to increase the efficiency of transduction. 48h after transduction, the T cells were placed in a cell culture incubator for another 48h.

Flow cytometry analysis

Tetramer staining on CD8 T cells was performed by 15min incubation at 4°C and washed three times with cold PBS/BSA prior to cell surface staining. T cells were stained with anti-CD3 (clone SK-7, BD), anti-CD4 (clone SK-3, BD), anti-CD8 (clone SK-1, BD) antibodies for 30min at 4°C and washed three times with cold PBS/BSA. T cell activation was measured by intracellular IFNγ staining (XMF1.2, Biolegend) using an ICS kit (BioLegend) according to manufactures protocol. moDCs were stained with anti-CD1a (clone HI149, BD), anti-CD14 (clone M5E2, BD), anti-CD80 (clone L307.4, BD), anti-CD83 (clone HB15e, BD), anti-CD86 (clone IT2.2, biolegend), and anti HLA-DR (clone G46-6, BD) antibodies for 30min at 4°C and washed three times with cold PBS/BSA. Samples were acquired using a BD LSRFortessa™ flow cytometry system and analyzed using FlowJo software (Tree Star). Single cell sorting was done using a BD Aria III™ FACS.

Statistics

Statistical analysis was calculated using the T-test (paired, two-tailed) with welch correction to determine the statistical significance of the differences. A minimum of two technical replicates was used in all experiments. All experiments were at least performed two times. Differences were considered statistically significant at $p < 0.05$. (* $p<0.05$, ** $p<0.01$, *** $p<0.001$).

Acknowledgements

We thank the flow cytometry facility for their support with the FACS based work. Also, we thank G. Moray for his creative insights. This work was financially supported by the Dutch Cancer Society (grant KWF 2013-6142).

References

1 Seliger, B., Maeurer, M. J. & Ferrone, S. Antigen-processing machinery breakdown and tumor growth. *Immunol Today* **21**, 455-464 (2000).

2 Korkolopoulou, P., Kaklamanis, L., Pezzella, F., Harris, A. L. & Gatter, K. C. Loss of antigen-presenting molecules (MHC class I and TAP-1) in lung cancer. *Br J Cancer* **73**, 148-153 (1996).

3 Pandha, H., Rigg, A., John, J. & Lemoine, N. Loss of expression of antigen-presenting molecules in human pancreatic cancer and pancreatic cancer cell lines. *Clin Exp Immunol* **148**, 127-135, doi:10.1111/j.1365-2249.2006.03289.x (2007).

4 Cresswell, P., Ackerman, A. L., Giodini, A., Peaper, D. R. & Wearsch, P. A. Mechanisms of MHC class I-restricted antigen processing and cross-presentation. *Immunol Rev* **207**, 145-157, doi:10.1111/j.0105-2896.2005.00316.x (2005).

5 van Hall, T. *et al.* Selective cytotoxic T-lymphocyte targeting of tumor immune escape variants. *Nat Med* **12**, 417-424, doi:10.1038/nm1381 (2006).

6 Doorduijn, E. M. *et al.* TAP-independent self-peptides enhance T cell recognition of immune-escaped tumors. *J Clin Invest* **126**, 784-794, doi:10.1172/JCI83671 (2016).

7 Marijt, K. A. *et al.* Identification of non-mutated neoantigens presented by TAP-deficient tumors. *J Exp Med* **215**, 2325-2337, doi:10.1084/jem.20180577 (2018).

8 van der Burg, S. H., Arens, R., Ossendorp, F., van Hall, T. & Melief, C. J. Vaccines for established cancer: overcoming the challenges posed by immune evasion. *Nat Rev Cancer* **16**, 219-233, doi:10.1038/nrc.2016.16 (2016).

9 Kenter, G. G. *et al.* Vaccination against HPV-16 oncoproteins for vulvar intraepithelial neoplasia. *N Engl J Med* **361**, 1838-1847, doi:10.1056/NEJMoa0810097 (2009).

10 Hilf, N. *et al.* Actively personalized vaccination trial for newly diagnosed glioblastoma. *Nature* **565**, 240-245, doi:10.1038/s41586-018-0810-y (2019).

11 Massarelli, E. *et al.* Combining Immune Checkpoint Blockade and Tumor-Specific Vaccine for Patients With Incurable Human Papillomavirus 16-Related Cancer: A Phase 2 Clinical Trial. *JAMA Oncol* **5**, 67-73, doi:10.1001/jamaoncol.2018.4051 (2019).

12 Ott, P. A. *et al.* An immunogenic personal neoantigen vaccine for patients with melanoma. *Nature* **547**, 217-221, doi:10.1038/nature22991 (2017).

13 Toes, R. E., Offringa, R., Blom, R. J., Melief, C. J. & Kast, W. M. Peptide vaccination can lead to enhanced tumor growth through specific T-cell tolerance induction. *Proc Natl Acad Sci U S A* **93**, 7855-7860 (1996).

14 Bijker, M. S. *et al.* CD8+ CTL priming by exact peptide epitopes in incomplete Freund's adjuvant induces a vanishing CTL response, whereas long peptides induce sustained CTL reactivity. *J Immunol* **179**, 5033-5040 (2007).

15 Rosalia, R. A. *et al.* Dendritic cells process synthetic long peptides better than whole protein, improving antigen presentation and T-cell activation. *Eur J Immunol* **43**, 2554-2565, doi:10.1002/eji.201343324 (2013).

16 Khan, S. *et al.* Distinct uptake mechanisms but similar intracellular processing of two different toll-like receptor ligand-peptide conjugates in dendritic cells. *J Biol Chem* **282**, 21145-21159, doi:10.1074/jbc.M701705200 (2007).

17 Bijker, M. S. *et al.* Superior induction of anti-tumor CTL immunity by extended peptide vaccines involves prolonged, DC-focused antigen presentation. *Eur J Immunol* **38**, 1033-1042, doi:10.1002/eji.200737995 (2008).

18 El Hage, F. *et al.* Preprocalcitonin signal peptide generates a cytotoxic T lymphocyte-defined tumor epitope processed by a proteasome-independent pathway. *Proc Natl Acad Sci U S A* **105**, 10119-10124, doi:10.1073/pnas.0802753105 (2008).

19 Martoglio, B. & Dobberstein, B. Signal sequences: more than just greasy peptides. *Trends Cell Biol* **8**, 410-415 (1998).

20 Vandebriel, R. & Hoefnagel, M. M. Dendritic cell-based in vitro assays for vaccine immunogenicity. *Hum Vaccin Immunother* **8**, 1323-1325, doi:10.4161/hv.21350 (2012).

21 Wullner, D. *et al.* Considerations for optimization and validation of an in vitro PBMC derived T cell assay for immunogenicity prediction of biotherapeutics. *Clin Immunol* **137**, 5-14, doi:10.1016/j.clim.2010.06.018 (2010).

22 Park, E. & Rapoport, T. A. Mechanisms of Sec61/SecY-mediated protein translocation across membranes. *Annu Rev Biophys* **41**, 21-40, doi:10.1146/annurev-biophys-050511-102312 (2012).

23 Weinzierl, A. O. *et al.* Features of TAP-independent MHC class I ligands revealed by quantitative mass spectrometry. *Eur J Immunol* **38**, 1503-1510, doi:10.1002/eji.200838136 (2008).

24 Anderson, K. S., Alexander, J., Wei, M. & Cresswell, P. Intracellular transport of class I MHC molecules in antigen processing mutant cell lines. *J Immunol* **151**, 3407-3419 (1993).

25 Wei, M. L. & Cresswell, P. HLA-A2 molecules in an antigen-processing mutant cell contain signal sequence-derived peptides. *Nature* **356**, 443-446, doi:10.1038/356443a0 (1992).

26 Guermonprez, P., Valladeau, J., Zitvogel, L., Thery, C. & Amigorena, S. Antigen presentation and T cell stimulation by dendritic cells. *Annu Rev Immunol* **20**, 621-667, doi:10.1146/annurev.immunol.20.100301.064828 (2002).

27 Doorduijn, E. M. *et al.* T cells specific for a TAP-independent self-peptide remain naive in tumor-bearing mice and are fully exploitable for therapy. *Oncoimmunology* **7**, e1382793, doi:10.1080/2162402X.2017.1382793 (2018).

28 Linnemann, C. *et al.* High-throughput identification of antigen-specific TCRs by TCR gene capture. *Nat Med* **19**, 1534-1541, doi:10.1038/nm.3359 (2013).

Chapter 7

TEIPP peptides: exploration of unTAPped cancer antigens

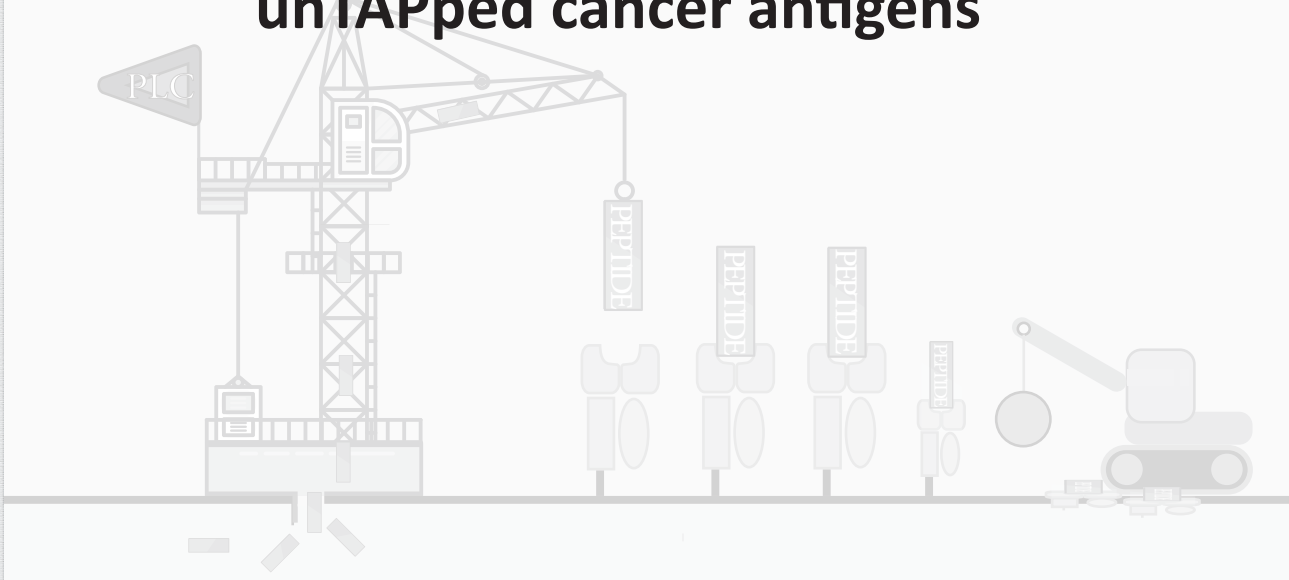

***K.A. Marijt**, S.H. van der Burg, T. van Hall*

Oncoimmunology 8:8, DOI:10.1080/2162402X.2019.1599639 (2019)

Abstract

The intracellular peptide pump TAP feeds antigenic peptides for loading onto HLA class I molecules and its down-modulation is a frequent immune evasion mechanism in human cancers. Two recent papers describe which 'hidden' antigens we might exploit to target these escaped cancer variants by CD8 T cells. These unTAPped peptides are now ready for clinical testing.

Introduction

Loss of essential components in the antigen-processing machinery is frequently observed in human cancers, including the peptide pump TAP. This results in low HLA class I antigen surface expression and facilitates immune escape from CD8 T cells. Interestingly, a novel category of non-mutated neoantigens (called 'TEIPP'- *T cell epitopes associated with impaired peptide processing*) is presented by these cancers and might function as salvage antigens. Two recent papers shed new light on clinical translation of TEIPP antigens. Marijt et al. described a hybrid forward-reverse immunological screen, which led to the identification of 16 novel human TEIPP peptides[1] and Durgeau et al. demonstrated that a pooled peptide vaccination strategy, which included a TEIPP peptide, was able to control the outgrowth of a TAP-deficient lung carcinoma in a humanized mouse model[2]. Together, these papers show the way for clinical exploration of these unTAPped cancer antigens.

Background of TEIPP research

The last years much effort has been put in the identification of many point-mutated neoantigens in human cancer, aiming at personalized immunotherapeutic strategies like T cell receptor gene transfer and peptide or mRNA vaccination therapies[3]. However, cancers can acquire resistance to CD8 T cell attack by immuno-editing, especially in cases of high immune pressure due to successful immunotherapy[4]. Acquired resistance in checkpoint therapy-refractory cancers has been ascribed to loss-of-function mutations in the IFNγ signaling pathway, as well as to lost expression of antigen processing genes, including the peptide pump TAP and other chaparones[5]. Consequently, this results in low HLA class I (HLA-I) antigen presentation, immune evasion, and cancer progression. The prevalence of cancers that down modulate gene expression *TAP1* and *TAP2* in a cohort non-small-cell lung carcinomas (NSCLCs) reached up to 71% when compared to levels in adjacent normal tissue[2]. Down modulation of TAP and other components of the antigen processing machinery is observed in many other cancer types, including melanoma, colon carcinoma, and cervical carcinoma, especially in progressed cancers[6]. Although these tumor cell variants might fail to present conventional tumor-specific cancer antigens, we reported back in 2006 that the residual presenting molecules accommodate antigenic peptides that selectively emerge on such immune-escaped cancers. We named these TEIPP (T cell Epitopes associated with Impaired Peptide Processing)[7]. TEIPPs are non-mutated "self" antigens derived from housekeeping proteins, but exclusively presented by HLA-I on TAP-deficient cancer cells (figure 1). Fundamental questions on the characteristics of TEIPP antigen processing, the thymus education of their cognate T cell repertoire and therapeutic potential, were all studied in mouse tumor models. These studies have led to a great understanding of TEIPPs and TEIPP-specific CD8 T cells, and were recently summarized in a review paper[8].

The hunt for human TEIPPs was rewarded when the group of Fathia Mami-Chouaib in Paris discovered the identity of the peptide-epitope of CD8 T cells recognizing TAP-deficient lung carcinomas[9]. The leader peptide of the preprocalcitonin protein was liberated by the proteolytic enzyme SPP (signal peptide peptidase) and loaded unto HLA-A2 in a TAP-independent way. Actually, restoration of the peptide pump TAP decreased recognition by the CD8 T cell clone, exactly as predicted by results obtained from the mouse tumor models[10]. Subsequently, we reported in 2010 that TEIPP-specific T cells are not rare, but can rather be readily isolated from blood of healthy donors, although their identity remained unknown[8].

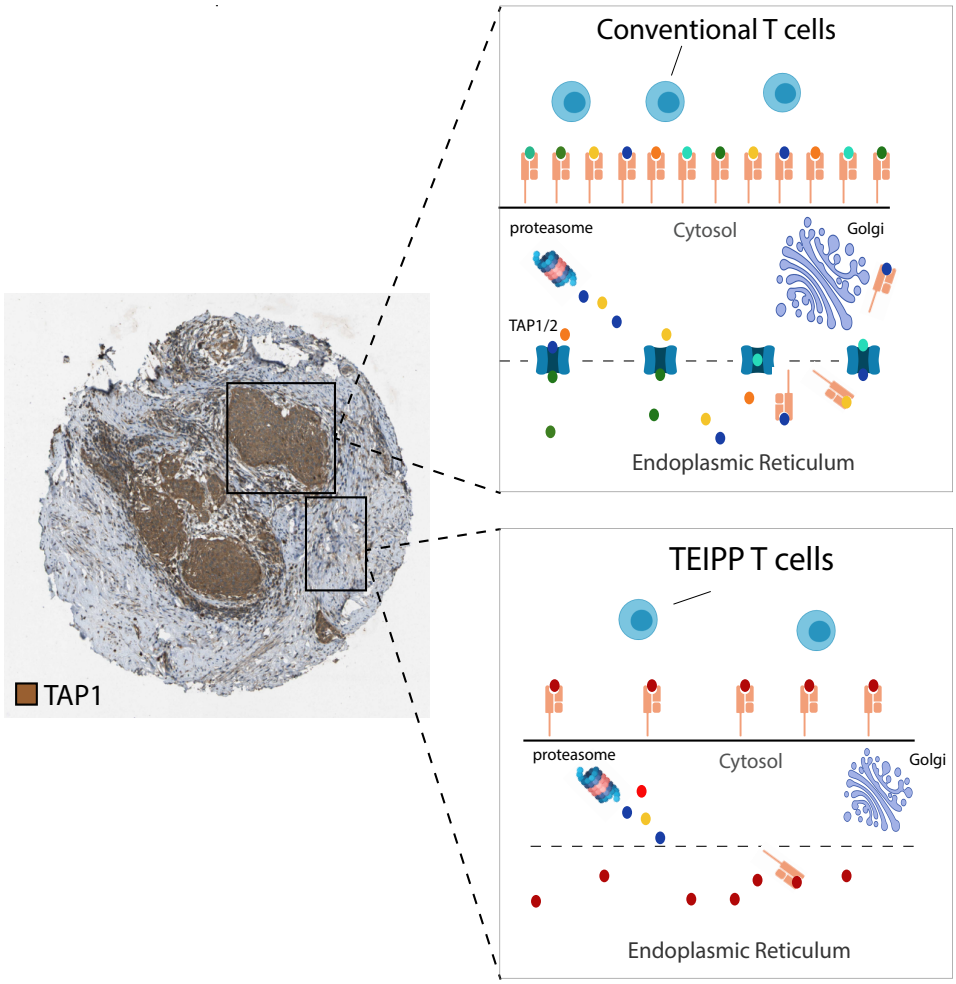

Recent characterization of 16 human TEIPP antigens and their efficacy *in vivo*

Since immune escape often limits the success of T cell mediated therapies, we wanted to investigate the broadness of TEIPPs in humans, and identify more TEIPP antigens for therapeutic purposes against immune-escaped cancers. Therefore, we developed a unique proteome-wide hybrid forward-reverse immunological screen[1]. Based on antigen processing rules learned from our mouse TEIPP models, protein topology, algorithms for HLA-I binding affinity and large databases of peptides purified from HLA-I molecules of cancers, we created a shortlist of 40 potential HLA-A2 restricted TEIPP candidates for further investigation. First, we examined the existence of a specific CD8 T cell repertoire in blood of healthy donors by performed HLA-I tetramer pull-down assays succeeded with *in vitro* peptide stimulations. T cells were detected against 16 out of 40 TEIPP peptide candidates in multiple donors. Second, we observed that T cell receptors of several clones behaved as intermediate-to-high affinity against titrated concentrations of peptide. Interestingly, CD8 T cells against some TEIPP peptides could only be detected in the naïve repertoire of these healthy donors, indicating they were never recruited during an immune response in these persons and ready for exploitation. In depth analysis of one TEIPP antigen (p14) revealed that TEIPP specific T cell clones were able to target a broad range of TAP-deficient cancer types, including lymphoma, renal cell carcinoma, melanoma, and colon carcinoma, without affecting their TAP-positive counterparts or healthy tissue. All these data involved *in vitro* culture systems. To assess therapeutic efficacy of human TEIPP antigens, Durgeau et al. developed an combinatorial peptide vaccination strategy, in which the TEIPP antigen from preprocalcitonin was included. Immunodeficient NSG mice were engrafted with a TAP-deficient human lung carcinoma and treated with blood cells and the peptide vaccine. Excitingly, this approach resulted in increased T cell infiltration of the tumor and improved survival duration of the animals, indicating that TEIPP antigens are capable of targeting immune-escaped tumor variants which are otherwise resistant to conventional antitumor T cells.

Figure 1.

TAP1 protein expression on cervical carcinoma tissue visualized by immunohistochemistry (http://proteinatlas.org). High expression of TAP1 facilitates the transport of cytosolic peptides into the endoplasmic reticulum (ER) and loading of those antigenic peptides onto HLA class I (HLA-I) molecules. When cancer cells down modulate the peptide pump TAP, it gives rise to the presentation of TEIPP antigens.

Future prospects of TEIPPs

These two recent studies strongly warrant the step forward. The molecular identification of TEIPP antigens enable vaccine applications in different formats, whether it be synthetic peptides, mRNA or DNA. In addition, cloned TEIPP-specific T cell receptors are formidable tools for 'of-the-shelf' therapeutics. TEIPPs are non-mutated and expressed by a large diversity of cancer types, so broadly applicable. We argue that targeting of TEIPP antigens might be combined with other immunotherapy modalities that target more conventional cancer antigens in order to prevent immune escape.

References

1 Marijt, K. A. *et al.* Identification of non-mutated neoantigens presented by TAP-deficient tumors. *J Exp Med* **215**, 2325-2337, doi:10.1084/jem.20180577 (2018).

2 Durgeau, A. *et al.* Human preprocalcitonin self-antigen generates TAP-dependent and -independent epitopes triggering optimised T-cell responses toward immune-escaped tumours. *Nat Commun* **9**, 5097, doi:10.1038/s41467-018-07603-1 (2018).

3 Vormehr, M., Tureci, O. & Sahin, U. Harnessing Tumor Mutations for Truly Individualized Cancer Vaccines. *Annu Rev Med* **70**, 395-407, doi:10.1146/annurev-med-042617-101816 (2019).

4 Verdegaal, E. M. *et al.* Neoantigen landscape dynamics during human melanoma-T cell interactions. *Nature* **536**, 91-95, doi:10.1038/nature18945 (2016).

5 Sharma, P., Hu-Lieskovan, S., Wargo, J. A. & Ribas, A. Primary, Adaptive, and Acquired Resistance to Cancer Immunotherapy. *Cell* **168**, 707-723, doi:10.1016/j.cell.2017.01.017 (2017).

6 Leone, P. *et al.* MHC class I antigen processing and presenting machinery: organization, function, and defects in tumor cells. *J Natl Cancer Inst* **105**, 1172-1187, doi:10.1093/jnci/djt184 (2013).

7 van Hall, T. *et al.* Selective cytotoxic T-lymphocyte targeting of tumor immune escape variants. *Nat Med* **12**, 417-424, doi:10.1038/nm1381 (2006).

8 Marijt, K. A., Doorduijn, E. M. & van Hall, T. TEIPP antigens for T-cell based immunotherapy of immune-edited HLA class I(low) cancers. *Mol Immunol*, doi:10.1016/j.molimm.2018.03.029 (2018).

9 El Hage, F. *et al.* Preprocalcitonin signal peptide generates a cytotoxic T lymphocyte-defined tumor epitope processed by a proteasome-independent pathway. *Proc Natl Acad Sci U S A* **105**, 10119-10124, doi:10.1073/pnas.0802753105 (2008).

10 Oliveira, C. C. *et al.* Peptide transporter TAP mediates between competing antigen sources generating distinct surface MHC class I peptide repertoires. *Eur J Immunol* **41**, 3114-3124, doi:10.1002/eji.201141836 (2011).

Chapter 8

General discussion

General discussion

MHC class I (MHC-I) antigen presentation plays a pivotal role in anti-tumor immunity. High surface expression of MHC-I molecules is generally correlated with high CD8 T cell infiltrate and improved overall survival in many cancers, including melanoma, lung carcinoma, and ovarium carcinoma[1-4]. In contrast, partial (>50% of cells) or complete loss of MHC-I surface expression is associated with lower overall survival and primary resistance to multiple types of immunotherapy in many cancer patients[5-8], underscoring the importance of MHC-I presentation for spontaneous and therapy-induced anti-tumor immunity. Expression of additional molecules in the tumor microenvironment (TME), such as PD-L1 and HLA-E inhibitory checkpoints, further shape immune responses. The presence of immune cells and the expression of immune-related genes together determine the 'immune landscape' or 'immune contexture' of cancers, while the local production of interferons (IFN) strongly impacts this environment[9]. Notably, immune contexture also includes infiltrating myeloid cells, such as tumor associated macrophages which also highly express PD-L1 immune suppressive molecules (**chapter 2**). Although MHC-I and PD-L1 are both regulated by the IFN pathway, an in-depth study on immune escape of NSCLC showed that the expression of co-inhibitory markers and the loss of MHC-I expression are two independent mechanisms of immune evasion[10]. This classifies tumors into different "types" depending on their surface expression of MHC-I and PD-L1[10,11]. The differential expression of MHC-I and PD-L1 suggests that immune escape of cancer cells occurs through a multitude of distinct "hard-wired" and "soft-wired" modifications[12-14] and knowing which of the mechanisms underlie immune escape determines which immunotherapeutic strategy has the most potential for clinical success. Here, we discuss several acquired immune resistance mechanisms and possible therapeutic strategies to overcome the resistance for immunotherapies.

Importance of IFN-signaling for T cell immunity

The IFNγ signaling pathway is essential for regulating innate and adaptive immune responses[15]. The absence of IFNγ production or cellular responsiveness sensitizes the host for microbial infection, supporting the importance of the cytokine IFNγ. Of note, IFNγ also plays important roles in inhibiting tumor angiogenesis[16], and directly has cytotoxic and cytostatic effects delaying tumor progression[17]. IFNγ is mainly secreted by activated type-I T cells and NK cells upon recognition of their target cells. IFNγ binds to the IFNγ-receptor, activating the IFNγ signaling pathway by phosphorylation of the JAKs and STATs, nuclear translocation, and binding of STAT1 homodimers onto interferon-gamma activation sequences. This triggers the transcription of many immunoregulatory genes, including the expression of antigen presentation molecules like MHC-I, but also immune -inhibiting receptors such as

PD-L1. Therefore, the exact downstream effects of IFNγ is context dependent and essential for regulating the efficacy of an anti-tumor immune response.

Cancers with high PD-L1/MHC-I expression are likely IFNγ-sensitive tumors. These tumors usually have a preexisting intratumoral T cell population, but are limited in exerting their effector function as a result of high inhibitory checkpoint expression. Patients with such tumors are most likely responders to PD-1/PD-L1 blockade mono-therapy, since alleviation the PD-1 inhibitory signals will reinvigorate preexisting anti-tumor T cell immunity.

However, cancers with defects in the IFNγ signaling pathway or downstream effector genes will not increase surface expression of MHC-I upon IFNγ stimulation, and will theoretically display weaker T cell reactivity to their tumors. As a consequence, reduced clinical response rates to checkpoint blockade therapies are indeed observed in this category of patients[6]. Moreover, two studies implicated the crucial role of proficient IFNγ signaling in melanoma patients who acquired resistance to PD-1 or CTLA-4 blockade therapies[18,19], and in patients who never responded to therapy[20]. Loss-of-function mutations in the IFNγ-receptor, and Jak1/ Jak2 caused the lack of response in these patients. Alternatively to these hard-wired defects, *in vivo* CRISPR-Cas9 studies have identified APLN2, PTPN2, and LNK as negative modulators of the IFNγ signaling, also limiting the efficacy of immune responses[21-23]. For patients with IFNγ-insensitive tumors, restoring the IFNγ signaling would be essential in order to fully benefit from immunotherapy, including checkpoint blockade therapies. Recently, using MEK inhibitors to increase IFNγ-sensitivity of cancer cells received considerable attention for immune combination therapies[24-26]. Inhibition of MEK signaling results in downregulation of LNK expression, increases the IFNγ signaling, and restores MHC-I presentation[23,25,26]. Similarly, inhibition of EGFR, upstream of MEK, also results in increased sensitivity to IFNγ and higher levels of MHC-I after IFNγ stimulation[27,28]. However, by enhancing the IFNγ signaling, it concurrently increases the expression of the inhibitory immune checkpoint receptor PD-L1, still limiting an effective immune response[24]. Therefore, IFNγ amplifying therapeutics, like EGFR and MEK inhibitors, need to be combined with immune checkpoint blockade therapy to become optimally effective as treatment for IFNγ-insensitive cancers, as suggested by several pre-clinical[24,26,29] and clinical studies[30].

PI3K inhibitors for combination immunotherapy

Cancer cells deprived from oxygen and glucose similarly lose their ability to perceive an active IFNγ response, resulting in low MHC-I and PD-L1 expression. These metabolically stressed cancers can therefore also be classified as IFNγ-insensitive, MHC-I^{low} tumors (**chapter 3**) and are also likely to benefit from therapies that aim to increase MHC-I presentation in combination with checkpoint blockade therapy. We experimentally showed that inhibi-

tion of PI3K signaling restored IFNγ signaling, increased MHC-I presentation, and improved T cell recognition *in vitro* of cancer cells in nutrient-deficient as well as nutrient-proficient conditions. Of note, although PI3K and MEK are downstream of EGFR signaling, they are part of two different pathways and execute distinct effector functions[31]. Therapeutic inhibition of PI3K signaling in combination with immunotherapy could therefore be an interesting new strategy to improve anti-tumor responses where IFNγ sensitivity is abrogated.

PI3K signaling is important for cancer cells, but is also essential for homeostasis of immune cells. The PI3K family can be divided into three classes, namely class I, II and III[32]. In our studies we used LY294002 and wortmannin (**chapter 3**), which are pan-PI3K inhibitors, inhibiting all classes of the PI3K family. It is important to determine which PI3K family is responsible for the observed MHC-I effects, since inhibition of different PI3K classes has differential effects on immune cells and therefore also may affect the therapeutic strategy. Several studies suggested that class I PI3K isoforms directly affect innate and adaptive immune cells. Selective inhibition of the gamma isoform of PI3K (PI3Kγ), highly expressed in infiltrating tumor associated myeloid cells, restored sensitivity to immune checkpoint blockade as a result of reduced immune suppression by M2-like macrophages in tumors[33,34]. Moreover, inhibition of the PI3K isoform delta (PI3Kδ) has been linked to break regulatory T cell mediated immune tolerance[35]. Interestingly, *ex vivo* inhibition of PI3K and its downstream effector AKT were shown to increase the formation of memory-like CD8 T cells and prolonged anti-tumor responses[36,37]. However, class I PI3K signaling also plays critical roles during development and differentiation of CD4 and CD8 T cells[38]. Inhibiting PI3K isoform gamma or delta during thymopoiesis stops T cell development at the CD4/CD8 double negative stage[39], while PI3Kγ is critical for exerting T cell function in matured T cells[40]. Interestingly, inhibition of AKT or mTOR, which are the main effector molecules of class I PI3K, did not restore MHC-I surface expression on tumor cells under oxygen and glucose deprived conditions (**chapter 3**, data not shown) and perhaps other PI3K classes or other non-canonical PI3K-signaling pathways[41] play important roles at the intersection of the PI3K and STAT1 axis. Class II PI3K was shown to be essential in TCR mediated activation of T cells by modulating the activation of potassium ion channels[42,43]. In cancers, increased expression of class II PI3K (PI3K-C2β) was suggested to be implicated in MEK1/2 activation, which implies that class II PI3K might has a role in MEK1 mediated suppression of MHC-I presentation[23,44,45]. Class III PI3K, or Vps34, plays a critical role in autophagy and endocytosis and is important for in the intracellular trafficking of the IL7-receptor in tumor cells[46]. Mice lacking Vps34 in T cells displayed a decreased number of T cells, suggesting that Vsp34 is an important regulator of naive T cell homeostasis, modulating IL-7Rα trafficking, signaling, and recycling.

Collectively, understanding the distinctive roles of the several isoforms of PI3K is critical for development of effective combination therapies, since modulation of the activity of these PI3K isoforms has differential effects on either tumor cells and host T cells. A delicate balance of single or combinatory specific PI3K inhibitors might be required to ensure improved IFNγ signaling and MHC-I presentation without compromising the effector function of immune cells. Therefore, the use of PI3K-signaling blocking compounds in combination therapies should be carefully evaluated with respect to their effects on T cells.

Immunotherapy using TEIPP antigens

Tumors with minimal MHC-I expression, irrespective of PD-L1 expression, might be a witness of previous ongoing immune response that resulted in acquired immune escape by downmodulation of MHC-I antigen presentation, making the tumor "invisible". Soft-wired loss of TAP function is often observed in cancers that lost their antigen presenting capabilities, especially in lung carcinomas, and melanomas[47,48]. Single agent checkpoint blockade therapy will most likely not result in an effective anti-tumor response, given the fact that the tumor (neo)antigens, that were initially recognized by tumor-reactive TILs, are not presented anymore by the immune escaped MHC-I^{low} cancer cells. Other T-cell based immunotherapeutic strategies, including dendritic cell vaccination, adoptive T cell therapy, and TCR-tg T cell transfers which target conventional tumor antigens are probably also not effective, because in all cases the presentation of their targeted (neo)antigens depends on TAP function[22]. Therefore, identification of alternative tumor antigens specifically presented on MHC-I^{low}, antigen processing-deficient cancer cells is an important objective. We designed a novel strategy to successfully identify those tumor antigens have resulted in the identification of so-called TEIPPs (**chapter 4**). TEIPPs are a subset of non-mutated antigens solely presented on MHC-I^{low} cancers as a result of downregulated TAP1/2 function[49]. TEIPP-presenting cancer cells typically have no TEIPP specific T cell infiltrate given the lack of sufficient MHC-I presentation which limits T cell activation through direct tumor recognition[50]. However, vaccination strategies were capable of igniting strong TEIPP-directed T cell immunity, and a multitude of studies in TEIPP animal models[50,51] motivated the search for human TEIPP antigens (**chapter 5**). After identification of 16 novel HLA-A*0201 binding TEIPP epitopes, we now look forward to therapeutic exploitation of these novel tumor antigens.

Vaccinating strategies with TAP-independent TEIPP peptides could initiate a CD8 T cell response of MHC-I^{low} cancers. Indeed therapeutic intervention via dendritic cell vaccination or therapeutic peptide vaccination resulted in priming of TEIPP-specific T cells and induced efficient homing to TAP-deficient MHC-I^{low} tumors in mouse models[51]. It can be envisioned that this results in increased local IFNγ levels in the tumor microenvironment. As most

TAP-deficient cancers typically have "soft-wired" epigenetic alterations[47,48], the epigenetic inhibition of TAP could be unleashed by this IFNγ and re-activate the antigen processing machinery. This would theoretically result in reduced presentation of TEIPP antigens and re-presentation of conventional tumor antigens, which may restore the efficacy of TILs responding to the conventional antigens. Alternatively, one could also add conventional tumor antigens to such TEIPP vaccines as this would also stimulate the generation of TAP-dependent peptide specific CD8 T cells and could boost the efficacy of the vaccine. This concept has been attractively shown by the group of Dr. Mami-Chouaib, where they combined long peptides of conventional tumor antigens together with a TEIPP peptide. With this combination vaccine they were able to strongly inhibit outgrowth of an immune escaped TAP-deficient lung carcinoma in a mouse model (**chapter 7**)[52]. Combinatorial vaccination therapy with checkpoint blockade therapy, or TCR gene transfers should be explored to fully take advantage of the re-activation of anti-tumor responses toward immune escaped cancers. In **chapter 6** we showed an approach for the development of a TEIPP vaccine as synthetic long peptide (SLP) and also demonstrated that gene transfer of a TEIPP TCR confers their unique specificity.

The exact threshold for decreased TAP function in cancer cells that is required to optimally present TEIPPs remains to be determined. This makes it difficult to predict how many cancer patients are susceptible to TEIPP targeted therapy. Analyses of *in vitro* cultured human cancer cell lines for TEIPP presentation, revealed that two out of six cancers were spontaneously recognized by TEIPP specific T cells. In four other cancer lines, further inactivation of TAP was necessary for proper TEIPP recognition (**chapter 5**). One cancer line, strongly recognized by TEIPP T cells, had relatively low levels of TAP, underscoring the importance of TAP downmodulation for efficient presentation of TEIPP. In a cohort of 135 lung cancer samples, approximately 53% and 32% displayed low to intermediate expression levels of TAP2, respectively[52]. For melanoma, TAP downregulation is observed in 50% of the primary lesions and a remarkable 83% in metastatic lesions[53], suggesting that a significant proportion of cancer patients might be eligible for TEIPP therapy. However, TEIPP antigen expression, proficiency of other components of the MHC-I antigen presentation pathway, and presence of IFNγ in the TME influencing TAP expression are additional factors expected to strongly influence efficient TEIPP presentation. Notably, when both antigen processing and MHC-I expression are reduced, for example in the case of nutrient deprived IFNγ-insensitive B16F10 cancer cells, no increased recognition was observed by TEIPP specific T cells, although the cancer cells were not expressing TAP proteins (data not shown). Interestingly, the nutrient deprived cancer cells were equally well recognized by TEIPP T cells as their proficient counterparts, suggesting that TEIPP peptides were not hampered in their presentation, in contrast to conventional cancer antigens (data not shown). In addition, IFNγ stimulation of cancer cells with hard-wired loss-of-function TAP mutations were bet-

ter recognized by TEIPP specific T cells, probably due to increased MHC-I gene transcription. Therefore, it seems that the ratio of TAP-mediated influx of peptides and availability of empty MHC-I molecules in the ER are important parameters for presentation of TEIPP antigens. Further studies should provide answers on the percentage of cancer patients that are sensitive for TEIPP therapy.

Alternatively, exploration how to induce TEIPP antigen presentation on cancers cells might be an interesting approach for combination immunotherapies. Interesting progress has been made in generating tools to deliver therapeutics specifically to cancer cells. This way, we could specifically target cancer cells with "tools" to temporarily abrogate TAP function in order induce susceptibility to TEIPP-specific T cells. Oncolytic viruses, which particularly replicate in cancer cells, can be armed with genetic products, like TAP-downmodulating proteins or siRNAs[54]. Engineering oncolytic viruses to express siRNA's towards TAP1/2 might induce TAP-deficiency specifically in cancers cells, making those infected cancer cells vulnerable for TEIPP therapy. Alternatively, aptamers conjugated with siRNAs are also used in the clinic to specifically target cancer cells to confer cancer specificity[55]. Currently, together with the group of Dr. Gilboa (Miller school of Medicine, Miami, USA) we are exploring the possibility of temporarily downregulating TAP function via siRNA in tumor cells by tumor directed targeting by nucleolin-binding aptamer conjugates. Our data show that treatment of TAP siRNA-aptamers specifically targets cancers cells, leaving healthy cells untouched. In preclinical mouse tumor models, treatment with TAP siRNA-aptamers results in strong inhibition of outgrowth of tumors and increased survival in mice[56]. The temporal decrease of TAP and thus MHC-I molecules ignited a broad immune response, including TEIPP-specific T cells. Follow up studies in which aptamer-targeted vaccines are included even show more dramatic anti-tumor responses[56]. These studies highlight the benefits of inducing alternative tumor antigens for effective immunotherapies of immune-escaped cancers.

Hard-wired loss of MHC class I presentation

Loss-of-function mutations in the β2m or HLA-A,B,C locus completely abrogates the presentation of MHC-I molecules. Especially in mismatch repair deficient (MMR-d) colon carcinomas as well as lung carcinomas, total loss of MHC-I expression is often observed[14,57]. Several studies illustrated that cancers acquired immune resistance after combination therapies with adoptive T cell transfer and checkpoint blockade, due to loss of HLA-I and/or β2m[7,58,59]. IFNγ stimulation or therapeutics amplifying the IFNγ signaling will not restore MHC-I antigen presentation in these type of cancers, making all previously discussed therapeutic approaches ineffective. However, NK-cells are innate immune cells specialized in targeting HLA-I negative cancers cells[60]. Unlike T cells, NK-cells do not have TCRs to recognize antigens, but are activated when inhibitory receptors are overruled by activating

receptors. The inhibitory receptors of NK cells bind to MHC-I molecules, which explains why NK cells mainly target MHC-I negative cells. One dominant inhibitory checkpoint molecule is NKG2A which is expressed on a majority of NK cells and limits the effector function of NK cells upon binding with non-classical MHC-I molecule HLA-E, overexpressed on most tumor cells[61,62]. Monalizumab, an anti-NKG2A blocking antibody, enhances NK cell activity against multiple tumor cells and is currently tested in several phase II clinical trials in combination with anti-EGFR (cetuximab) or anti-PD-L1 (Durvalumab) for solid cancer patients[62]. Of note, monalizumab not only antagonized the inhibitory signal on NK cells, but also on immunotherapy activated CD8 T cells, improving immune responses through distinct mechanisms[63].

Another exciting development is the manufacturing of TCR gene transfers in NK cells[64]. NK cells that obtained expression of a TCR, exerted the function of T cells phenotypically, metabolically and functionally, while maintaining their NK cell effector function. This way, when these tailored anti-tumor effector cells are used in (TEIPP) neoantigen mediated therapies, it might prevent cancer cells to immune escape by MHC-I loss, due to direct targeting of the NK cell effector function of these TCR-NK-cells.

References

1 Chowell, D. *et al.* Patient HLA class I genotype influences cancer response to checkpoint blockade immunotherapy. *Science* **359**, 582-587, doi:10.1126/science.aao4572 (2018).

2 Shehata, M. *et al.* Human leukocyte antigen class I expression is an independent prognostic factor in advanced ovarian cancer resistant to first-line platinum chemotherapy. *Br J Cancer* **101**, 1321-1328, doi:10.1038/sj.bjc.6605315 (2009).

3 Katz, S. C. *et al.* T cell infiltrate predicts long-term survival following resection of colorectal cancer liver metastases. *Ann Surg Oncol* **16**, 2524-2530, doi:10.1245/s10434-009-0585-3 (2009).

4 Stanton, S. E. & Disis, M. L. Clinical significance of tumor-infiltrating lymphocytes in breast cancer. *J Immunother Cancer* **4**, 59, doi:10.1186/s40425-016-0165-6 (2016).

5 Middha, S. *et al.* Majority of B2M-Mutant and -Deficient Colorectal Carcinomas Achieve Clinical Benefit From Immune Checkpoint Inhibitor Therapy and Are Microsatellite Instability-High. *JCO Precis Oncol* **3**, doi:10.1200/PO.18.00321 (2019).

6 Rodig, S. J. *et al.* MHC proteins confer differential sensitivity to CTLA-4 and PD-1 blockade in untreated metastatic melanoma. *Sci Transl Med* **10**, doi:10.1126/scitranslmed.aar3342 (2018).

7 Sade-Feldman, M. *et al.* Resistance to checkpoint blockade therapy through inactivation of antigen presentation. *Nat Commun* **8**, 1136, doi:10.1038/s41467-017-01062-w (2017).

8 Havel, J. J., Chowell, D. & Chan, T. A. The evolving landscape of biomarkers for checkpoint inhibitor immunotherapy. *Nat Rev Cancer* **19**, 133-150, doi:10.1038/s41568-019-0116-x (2019).

9 Castro, F., Cardoso, A. P., Goncalves, R. M., Serre, K. & Oliveira, M. J. Interferon-Gamma at the Crossroads of Tumor Immune Surveillance or Evasion. *Front Immunol* **9**, 847, doi:10.3389/fimmu.2018.00847 (2018).

10 Perea, F. *et al.* HLA class I loss and PD-L1 expression in lung cancer: impact on T-cell infiltration and immune escape. *Oncotarget* **9**, 4120-4133, doi:10.18632/oncotarget.23469 (2018).

11 Teng, M. W., Ngiow, S. F., Ribas, A. & Smyth, M. J. Classifying Cancers Based on T-cell Infiltration and PD-L1. *Cancer Res* **75**, 2139-2145, doi:10.1158/0008-5472.CAN-15-0255 (2015).

12 Chatterjee, A. *et al.* Marked Global DNA Hypomethylation Is Associated with Constitutive PD-L1 Expression in Melanoma. *iScience* **4**, 312-325, doi:10.1016/j.isci.2018.05.021 (2018).

13 Shi, Y. Regulatory mechanisms of PD-L1 expression in cancer cells. *Cancer Immunol Immunother* **67**, 1481-1489, doi:10.1007/s00262-018-2226-9 (2018).

14 McGranahan, N. *et al.* Allele-Specific HLA Loss and Immune Escape in Lung Cancer Evolution. *Cell* **171**, 1259-1271 e1211, doi:10.1016/j.cell.2017.10.001 (2017).

15 Ikeda, H., Old, L. J. & Schreiber, R. D. The roles of IFN gamma in protection against tumor development and cancer immunoediting. *Cytokine Growth Factor Rev* **13**, 95-109 (2002).

16 Hayakawa, Y. *et al.* IFN-gamma-mediated inhibition of tumor angiogenesis by natural killer T-cell ligand, alpha-galactosylceramide. *Blood* **100**, 1728-1733 (2002).

17 Schroder, K., Hertzog, P. J., Ravasi, T. & Hume, D. A. Interferon-gamma: an overview of signals, mechanisms and functions. *J Leukoc Biol* **75**, 163-189, doi:10.1189/jlb.0603252 (2004).

18 Zaretsky, J. M. *et al.* Mutations Associated with Acquired Resistance to PD-1 Blockade in Melanoma. *N Engl J Med* **375**, 819-829, doi:10.1056/NEJMoa1604958 (2016).

19 Gao, J. *et al.* Loss of IFN-gamma Pathway Genes in Tumor Cells as a Mechanism of Resistance to Anti-CTLA-4 Therapy. *Cell* **167**, 397-404 e399, doi:10.1016/j.cell.2016.08.069 (2016).

20 Shin, D. S. *et al.* Primary Resistance to PD-1 Blockade Mediated by JAK1/2 Mutations. *Cancer Discov* **7**, 188-201, doi:10.1158/2159-8290.CD-16-1223 (2017).

21 Manguso, R. T. *et al.* In vivo CRISPR screening identifies Ptpn2 as a cancer immunotherapy target. *Nature* **547**, 413-418, doi:10.1038/nature23270 (2017).

22 Patel, S. J. *et al.* Identification of essential genes for cancer immunotherapy. *Nature* **548**, 537-542, doi:10.1038/nature23477 (2017).

23 Ding, L. W. *et al.* LNK suppresses interferon signaling in melanoma. *Nat Commun* **10**, 2230, doi:10.1038/s41467-019-09711-y (2019).

24 Kang, S. H. *et al.* Inhibition of MEK with trametinib enhances the efficacy of anti-PD-L1 inhibitor by regulating anti-tumor immunity in head and neck squamous cell carcinoma. *Oncoimmunology* **8**, e1515057, doi:10.1080/2162402X.2018.1515057 (2019).

25 Brea, E. J. *et al.* Kinase Regulation of Human MHC Class I Molecule Expression on Cancer Cells. *Cancer Immunol Res* **4**, 936-947, doi:10.1158/2326-6066.CIR-16-0177 (2016).

26 Choi, H. *et al.* Pulsatile MEK Inhibition Improves Anti-tumor Immunity and T Cell Function in Murine Kras Mutant Lung Cancer. *Cell Rep* **27**, 806-819 e805, doi:10.1016/j.celrep.2019.03.066 (2019).

27 Garrido, G. *et al.* Upregulation of HLA Class I Expression on Tumor Cells by the Anti-EGFR Antibody Nimotuzumab. *Front Pharmacol* **8**, 595, doi:10.3389/fphar.2017.00595 (2017).

28 Watanabe, S. *et al.* Mutational activation of the epidermal growth factor receptor down-regulates major histocompatibility complex class I expression via the extracellular signal-regulated kinase in non-small cell lung cancer. *Cancer Sci* **110**, 52-60, doi:10.1111/cas.13860 (2019).

29 Dushyanthen, S. *et al.* Agonist immunotherapy restores T cell function following MEK inhibition improving efficacy in breast cancer. *Nat Commun* **8**, 606, doi:10.1038/s41467-017-00728-9 (2017).

30 Ribas, A. *et al.* Combined BRAF and MEK inhibition with PD-1 blockade immunotherapy in BRAF-mutant melanoma. *Nat Med* **25**, 936-940, doi:10.1038/s41591-019-0476-5 (2019).

31 Janku, F. Phosphoinositide 3-kinase (PI3K) pathway inhibitors in solid tumors: From laboratory to patients. *Cancer Treat Rev* **59**, 93-101, doi:10.1016/j.ctrv.2017.07.005 (2017).

32 Thorpe, L. M., Yuzugullu, H. & Zhao, J. J. PI3K in cancer: divergent roles of isoforms, modes of activation and therapeutic targeting. *Nat Rev Cancer* **15**, 7-24, doi:10.1038/nrc3860 (2015).

33 De Henau, O. *et al.* Overcoming resistance to checkpoint blockade therapy by targeting PI3Kgamma in myeloid cells. *Nature* **539**, 443-447, doi:10.1038/nature20554 (2016).

34 Kaneda, M. M. *et al.* PI3Kgamma is a molecular switch that controls immune suppression. *Nature* **539**, 437-442, doi:10.1038/nature19834 (2016).

35 Ali, K. *et al.* Inactivation of PI(3)K p110delta breaks regulatory T-cell-mediated immune tolerance to cancer. *Nature* **510**, 407-411, doi:10.1038/nature13444 (2014).

36 van der Waart, A. B. *et al.* Inhibition of Akt signaling promotes the generation of superior tumor-reactive T cells for adoptive immunotherapy. *Blood* **124**, 3490-3500, doi:10.1182/blood-2014-05-578583 (2014).

37 Bowers, J. S. *et al.* PI3Kdelta Inhibition Enhances the Antitumor Fitness of Adoptively Transferred CD8(+) T Cells. *Front Immunol* **8**, 1221, doi:10.3389/fimmu.2017.01221 (2017).

38 Qin, H. *et al.* The impact of PI3K inhibitors on breast cancer cell and its tumor microenvironment. *PeerJ* **6**, e5092, doi:10.7717/peerj.5092 (2018).

39 Okkenhaug, K. & Vanhaesebroeck, B. PI3K in lymphocyte development, differentiation and activation. *Nat Rev Immunol* **3**, 317-330, doi:10.1038/nri1056 (2003).

40 Finlay, D. K. Regulation of glucose metabolism in T cells: new insight into the role of Phosphoinositide 3-kinases. *Front Immunol* **3**, 247, doi:10.3389/fimmu.2012.00247 (2012).

41 Cao, H. *et al.* Functional role of SGK3 in PI3K/Pten driven liver tumor development. *BMC Cancer* **19**, 343, doi:10.1186/s12885-019-5551-2 (2019).

42 Srivastava, S. *et al.* The class II phosphatidylinositol 3 kinase C2beta is required for the activation of the K+ channel KCa3.1 and CD4 T-cells. *Mol Biol Cell* **20**, 3783-3791, doi:10.1091/mbc.E09-05-0390 (2009).

43 Feske, S., Skolnik, E. Y. & Prakriya, M. Ion channels and transporters in lymphocyte function and immunity. *Nat Rev Immunol* **12**, 532-547, doi:10.1038/nri3233 (2012).

44 Boller, D. *et al.* Targeting PI3KC2beta impairs proliferation and survival in acute leukemia, brain tumours and neuroendocrine tumours. *Anticancer Res* **32**, 3015-3027 (2012).

45 Russo, A. & O'Bryan, J. P. Intersectin 1 is required for neuroblastoma tumorigenesis. *Oncogene* **31**, 4828-4834, doi:10.1038/onc.2011.643 (2012).

46 McLeod, I. X., Zhou, X., Li, Q. J., Wang, F. & He, Y. W. The class III kinase Vps34 promotes T lymphocyte survival through regulating IL-7Ralpha surface expression. *J Immunol* **187**, 5051-5061, doi:10.4049/jimmunol.1100710 (2011).

47 Seliger, B. Novel insights into the molecular mechanisms of HLA class I abnormalities. *Cancer Immunol Immunother* **61**, 249-254, doi:10.1007/s00262-011-1153-9 (2012).

48 Garrido, F., Cabrera, T. & Aptsiauri, N. "Hard" and "soft" lesions underlying the HLA class I alterations in cancer cells: implications for immunotherapy. *Int J Cancer* **127**, 249-256, doi:10.1002/ijc.25270 (2010).

49 Marijt, K. A. *et al.* Identification of non-mutated neoantigens presented by TAP-deficient tumors. *J Exp Med* **215**, 2325-2337, doi:10.1084/jem.20180577 (2018).

50 Doorduijn, E. M. *et al.* T cells specific for a TAP-independent self-peptide remain naive in tumor-bearing mice and are fully exploitable for therapy. *Oncoimmunology* **7**, e1382793, doi:10.1080/2162402X.2017.1382793 (2018).

51 Doorduijn, E. M. *et al.* TAP-independent self-peptides enhance T cell recognition of immune-escaped tumors. *J Clin Invest* **126**, 784-794, doi:10.1172/JCI83671 (2016).

52 Durgeau, A. *et al.* Human preprocalcitonin self-antigen generates TAP-dependent and -independent epitopes triggering optimised T-cell responses toward immune-escaped tumours. *Nat Commun* **9**, 5097, doi:10.1038/s41467-018-07603-1 (2018).

53 Marincola, F. M., Jaffee, E. M., Hicklin, D. J. & Ferrone, S. Escape of human solid tumors from T-cell recognition: molecular mechanisms and functional significance. *Adv Immunol* **74**, 181-273 (2000).

54 Anesti, A. M., Simpson, G. R., Price, T., Pandha, H. S. & Coffin, R. S. Expression of RNA interference triggers from an oncolytic herpes simplex virus results in specific silencing in tumour cells in vitro and tumours in vivo. *BMC Cancer* **10**, 486, doi:10.1186/1471-2407-10-486 (2010).

55 Yoon, S. & Rossi, J. J. Emerging cancer-specific therapeutic aptamers. *Curr Opin Oncol* **29**, 366-374, doi:10.1097/CCO.0000000000000389 (2017).

56 Greta Garrido, B. S., Ailem Rabasa, Agata Levay, Francesca D'Eramo, Alexey Berezhnoy, Shrey Modi, Tal Gefen, Koen Marijt, Elien Doorduijn, Vikas Dudeja, Thorbald van Hall, Eli Gilboa Tumor-targeted silencing of the peptide transporter TAP induces potent antitumor immunity. *Nat Commun* (2019).

57 Ijsselsteijn, M. E. *et al.* Revisiting immune escape in colorectal cancer in the era of immunotherapy. *Br J Cancer* **120**, 815-818, doi:10.1038/s41416-019-0421-x (2019).

58 Paulson, K. G. *et al.* Acquired cancer resistance to combination immunotherapy from transcriptional loss of class I HLA. *Nat Commun* **9**, 3868, doi:10.1038/s41467-018-06300-3 (2018).

59 Gettinger, S. *et al.* Impaired HLA Class I Antigen Processing and Presentation as a Mechanism of Acquired Resistance to Immune Checkpoint Inhibitors in Lung Cancer. *Cancer Discov* **7**, 1420-1435, doi:10.1158/2159-8290.CD-17-0593 (2017).

60 Caligiuri, M. A. Human natural killer cells. *Blood* **112**, 461-469, doi:10.1182/blood-2007-09-077438 (2008).

61 Kaiser, B. K., Pizarro, J. C., Kerns, J. & Strong, R. K. Structural basis for NKG2A/CD94 recognition of HLA-E. *Proc Natl Acad Sci U S A* **105**, 6696-6701, doi:10.1073/pnas.0802736105 (2008).

62 Andre, P. *et al.* Anti-NKG2A mAb Is a Checkpoint Inhibitor that Promotes Anti-tumor Immunity by Unleashing Both T and NK Cells. *Cell* **175**, 1731-1743 e1713, doi:10.1016/j.cell.2018.10.014 (2018).

63 van Montfoort, N. *et al.* NKG2A Blockade Potentiates CD8 T Cell Immunity Induced by Cancer Vaccines. *Cell* **175**, 1744-1755 e1715, doi:10.1016/j.cell.2018.10.028 (2018).

64 Mensali, N. *et al.* NK cells specifically TCR-dressed to kill cancer cells. *EBioMedicine* **40**, 106-117, doi:10.1016/j.ebiom.2019.01.031 (2019).

Chapter &

Nederlandse samenvatting

Dankwoord

Curriculum vitae

List of publications

Nederlandse samenvatting

De taak van het immuunsysteem is om binnenkomende micro-organismen die ons ziek maken, zoals bacteriën, virussen, en wormen, onschadelijk te maken. Het immuunsysteem grijpt in op de verschillen die bestaan tussen de eiwitten van het eigen lichaam en de ziekte verwekkers, om zo lichaamsvreemde binnendringers aan te vallen. Deze verdedigingslinie heeft ook een rol in kanker. Een elegant systeem, waarbij deze 'vreemde' stukjes eiwit, ook wel antigenen genoemd, worden gepresenteerd door cellen in MHC klasse I moleculen, en daarbij ervoor zorgt dat het immuunsysteem kan controleren of dit gaat om een gezonde cel, een of een kankercel. De belangrijke afweercellen die deze kankercellen kunnen vernietigen worden CD8 T cellen genoemd. Wanneer een CD8 T cel een kankercel herkent produceert deze allerlei stoffen met als doel de afweerreactie te versterken en de lichaamsvreemde cel te doden. Via verschillende mechanismen kunnen kanker cellen veranderen en daardoor ontsnappen aan het afweersysteem. Vervolgens wordt de kankercel minder of niet meer onderdrukt door het afweersysteem waardoor de tumor kan uitgroeien, en tot ziekte in de patiënt leidt. Het begrijpen van deze ontsnappingsmechanismen van kankercellen kan helpen om efficiëntere therapieën te ontwikkelen. Ook wel immunotherapie genoemd. In dit proefschrift worden verschillende ontsnappingsmechanismen beschreven, en de strategieën om dit tegen te gaan.

De balans tussen afweer activatie en suppressie is belangrijk om ervoor te zorgen dat een ontstekingsreactie niet te hoog oploopt. Om T cel reactiviteit te dempen zijn er regelmechanismen in het lichaam aanwezig, waaronder de interactie tussen receptoren en liganden op het oppervlak van de T cellen en weefsel cellen. Kankercellen maken hier goed gebruik van, bijvoorbeeld door het remmende ligand PD-L1 sterk tot expressie te brengen wanneer de kanker cel herkent wordt door het immuunsysteem. Het PD-L1 bindt dan vervolgens aan de PD-1 receptor op de T cellen, met als resultaat dat de functie van T cellen wordt geremd. Het blokkeren van deze PD-L1/PD-1 interactie heeft in de kliniek geleidt tot succesvolle behandeling van patiënten met kanker. Naast kankercellen kunnen andere witte bloedcellen, de afweer onderdrukkende leukocyten, PD-L1 expresseren. Dit kan, ook bijdragen aan de remming van een actieve afweerreactie. In **hoofdstuk 2** zoeken hebben we uitgezocht wat het effect was van PD-L1/PD-1 interactie blokkade wanneer het PD-L1 alleen geblokkeerd wordt op kankercellen of op afweercellen. We laten zien dat het blokkeren van PD-L1 op kanker cellen zorgt voor een verbeterde overlevingskans in muizen met tumoren. Als we vervolgens PD-L1 blokkerende therapie geven zien we een toegevoegd overlevingseffect. Dit geeft aan dat het blokkeren van PD-L1 op cellen anders dan kankercellen ook bijdraagt aan deze nieuwe vorm van behandeling.

Zoals beschreven in de eerste paragraaf van dit hoofdstuk, is het presenteren van antigenen in MHC klasse-I moleculen erg belangrijk voor de herkenning van kankercellen door CD8 T cellen. In tumoren vindt de presentatie van antigenen in MHC klasse-I in het algemeen plaats in een omgeving waar de toevoer en afvoer van voedingsstoffen en afvalstoffen erg lastig is. Meerdere mechanismen zijn beschreven die laten zien dat kankercellen de expressie van MHC klasse-I moleculen verlagen om er zo voor te zorgen dat ze niet herkent en opgeruimd worden door de CD8 T cellen. In **hoofdstuk 3** doen we onderzoek naar de effecten op antigeen presentatie in MHC klasse-I onder condities waar kankercellen een tekort aan glucose en zuurstof hebben. We laten zien dat onder deze omstandigheden de MHC klasse-I presentatie van antigenen sterk wordt beïnvloed wanneer kanker cellen een tekort hebben aan glucose en zuurstof. Dit kwam door een verandering in de activering van een PI3K-signaal transductie route in de kankercel. Deze observatie was alleen zichtbaar wanneer zowel glucose als zuurstof gelimiteerd waren, en niet wanneer alleen glucose of alleen zuurstof werden beperkt. Remming van de PI3K signaal transductie route zorgt voor een herstel van de herkenning van de kankercel door CD8 T cellen.

Een andere mogelijkheid voor kankercellen om MHC klasse-I expressie te verlagen is door het blokkeren van de peptidepomp, genaamd TAP, die in de cel ervoor moet zorgen dat de antigenen bij de MHC klasse-1 moleculen komen. Het uitschakelen van deze peptidepomp wordt vaak gebruikt door tumoren om herkenning door CD8 T cellen te voorkomen en zo onzichtbaar te worden voor het afweersysteem. In **hoofdstuk 4** geven we een overzicht van de bestaande literatuur over deze nieuwe categorie antigenen, welke verrassend genoeg alleen gepresenteerd wordt op kankercellen die de TAP functie verlagen of uitschakelen. Deze antigenen noemen wij TEIPP. In **hoofdstuk 5** gaan we dieper in op het identificeren van nieuwe humane TEIPP antigenen omdat deze een belangrijke rol kunnen spelen in de ontwikkeling van nieuwe immuuntherapieën voor aan de afweer ontsnapte kankercellen. In **hoofdstuk 6** hebben we voor één van de eerste TEIPP antigenen onderzocht hoe we die het beste kunnen aanbieden aan het afweersysteem om middels vaccinatie, de CD8 T cel reactie tegen dit antigeen te versterken. In **hoofdstuk 7** bediscussiëren we de impact van TEIPP antigenen op toekomstige ontwikkelingen van nieuwe immuun therapieën en strategieën om immuun-ontsnapte kanker cellen op te ruimen door middel van TEIPP antigenen.

In **hoofdstuk 8** wordt besproken hoe de in dit boek besproken kennis kan worden toegepast in toekomstige behandeling van kanker.

Dankwoord

Thorbald, ik kan me nog goed herinneren dat ik met jou het eerste sollicitatie gesprek voerde toen ik nog in Boston zat. Ik wist al snel dat ik graag op het TEIPP onderwerp wilde komen werken onder jouw supervisie, en hoefde geen moment na te denken om weer terug naar Nederland te komen toen ik hoorde dat ik de positie had gekregen. De afgelopen jaren heb je mij sterk gestimuleerd de onderzoeker te worden die ik nu ben. Daarvoor mijn dank!

Sjoerd, samen met Thorbald waren jullie voor mij de ideale combinatie als supervisors. Waar Thorbald mij erg stimuleerde mijn creatieve kant als onderzoeker te ontwikkelen, stimuleerde jij me om goed te focussen en pragmatisch te zijn. Dit heeft uiteindelijk geleid tot alle mooie publicaties die er nu zijn. Bedankt voor alles!

Lien, zonder jou zou menig geregel een stuk chaotischer verlopen. Bedankt dat ik voor alles bij je terecht kon!

Bart, al vanaf mijn eerste werkdag leek het alsof ik je al jaren kende. Deze start zorgde ervoor dat ik mij gelijk op mijn plek voelde. Binnen enkele weken vormde wij al een duo waar nu nog over gesproken wordt. Voornamelijk in combinatie met de woorden “quadrupple en DTIM”. Ik heb genoten van onze wetenschappelijke en niet-wetenschappelijke discussies en hoop dat je snel weer naar Nederland komt. Elien, de vrolijkheid die jij elke dag meebracht naar het lab maakte de duistere dagen in het lab altijd een stuk lichter. Jan-Willem, de 1000-en onnodige feitjes die je uitsprak in teveel verschillende talen maakte de gekte in de groep compleet. Een goed recept voor ontelbare gezellige avonden in “schommelen”. Bedankt!

Laura, jouw doorzettingsvermogen en vastberadenheid, waren essentiële eigenschappen om het TEIPP project tot een succes te brengen, en onmisbaar voor de mooie publicaties die eruit zijn gekomen. Bianca, Marten, Els, bedankt voor alle tips and tricks die jullie geven hebben voor de humane T cel kweken. Janis, Sophie, Febe, ik heb een hoop geleerd van jullie als begeleider voor jullie bachelor/master stage. Marjolein, bedankt voor al je ondersteuning en het werk wat je gedaan hebt voor het artikel. Elham, Ferenc, en Linda, zonder jullie geen heftige wetenschappelijk discussies en uitdagingen in ons kantoor. Bedankt! Verder dank aan iedereen van de afdeling medische oncologie die ik nu niet bij naam noem voor de gezelligheid/ borrels/ en ONCTI’s.

Tot slot, Marjolijn, de resultaten van onze “experimenten” zijn fantastisch. Het “gevoel” wat we thuis gecreëerd hebben, geeft mij elke dag genoeg energie om elk obstakel in het dagelijks leven te overwinnen.

Curriculum vitae

Koen Abraham Marijt was born on April 4, 1986 in Oegstgeest. After obtaining his HAVO degree in the year 2000 at the Bona Ventura College in Leiden, he started studying Biomedical laboratory sciences at the university of Applied Sciences in Leiden. He did an internship for 12 months in the department of Vascular and Medical diseases, Netherlands Organisation for Applied Scientific Research (TNO) in Leiden under supervision of Leonard Seghers in the group of Prof Dr Paul Quax. During this internship he investigated the role of NK-cells in the formation of new blood vessels. After obtaining his Bachelor degree in 2008, he started working in the department of Rheumatology in the Leiden University Medical Center under supervision of Dr Andree Ioan, in the group of Prof Dr Rene Toes. Here he explored the immunological characteristics of the Hoffa's fat pad in osteoarthritis. In 2008, Koen decided to continue his education by starting the research master Oncology at the VU university in Amsterdam. He did a 9 month internship in the angiogenesis department under supervision of Prof Dr Arjan Griffioen at the Cancer Center Amsterdam (CCA), exploring the effects on angiogenesis after discontinuation of sunitinib treatment in renal cell carcinoma patients. A second internship of 12 months was completed in the department of Tumor Biology at the Massachusetts General Hospital (MGH), Boston, USA under supervision of Prof Dr Rakesh Jain, where he worked on the dual inhibition of Ang-2 and VEGF receptor therapy in glioblastoma mouse models. Koen obtained his master's degree in 2012, after which he went back to MGH, Boston, USA where he was offered a position to continue his work of his internship project and started a new project on the effects of the secreted protein "serine protease leukocyte inhibitor" (SLPI) in metastatic breast carcinomas. In 2014 he returned to the Netherlands to start his PhD project described in this thesis, which was performed at the department of medical oncology at the Leiden University medical Center under supervision of Dr Thorbald van Hall and Prof Dr Sjoerd van der Burg. Currently, Koen continues working as a post-doc in this research group, exploring the impact of cancer metabolism on immune responses in the tumor microenvironment.

List of publications

1. **K.A. Marijt** and T. van Hall (2020) "To TAP or not to TAP: alternative peptides for immunotherapy of cancer". Curr Opin Immunol. - *In press*

2. Garrido G., Schrand B., Rabasa A., Levay A., D'Eramo F., Berezhnoy A., Modi S., Gefen T., **K.A. Marijt**, Doorduijn E., Dudeja V., van Hall T., Gilboa E. (2019). "Tumor-targeted silencing of the peptide transporter TAP induces potent antitumor immunity." Nat Commun. Aug 21;10(1):3773. doi: 10.1038/s41467-019-11728-2.

3. **K. A. Marijt**, M. Sluijter, L. Blijleven, S. H. Tolmeijer, F. A. Scheeren, S. H. van der Burg and T. van Hall (2019). "Metabolic stress in cancer cells induces immune escape through a PI3K-dependent blockade of IFNgamma receptor signaling." J Immunother Cancer 7(1): 152.

4. **K.A. Marijt**, S.H. van der Burg, T. van Hall (2019). "TEIPP peptides: exploration of unTAPped cancer antigens." Oncoimmunology 8:8, DOI: 10.1080/2162402X.2019.1599639.

5. Logtenberg, M. E. W., J. H. M. Jansen, M. Raaben, M. Toebes, K. Franke, A. M. Brandsma, H. L. Matlung, A. Fauster, R. Gomez-Eerland, N. A. M. Bakker, S. van der Schot, **K. A. Marijt**, M. Verdoes, J. Haanen, J. H. van den Berg, J. Neefjes, T. K. van den Berg, T. R. Brummelkamp, J. H. W. Leusen, F. A. Scheeren and T. N. Schumacher (2019). "Glutaminyl cyclase is an enzymatic modifier of the CD47-SIRPalpha axis and a target for cancer immunotherapy." Nat Med 25(4): 612-619.

6. van Montfoort, N., L. Borst, M. J. Korrer, M. Sluijter, **K. A. Marijt**, S. J. Santegoets, V. J. van Ham, I. Ehsan, P. Charoentong, P. Andre, N. Wagtmann, M. J. P. Welters, Y. J. Kim, S. J. Piersma, S. H. van der Burg and T. van Hall (2018). "NKG2A Blockade Potentiates CD8 T Cell Immunity Induced by Cancer Vaccines." Cell 175(7): 1744-1755 e1715.

7. **K. A. Marijt**, L. Blijleven, E. M. E. Verdegaal, M. G. Kester, D. J. Kowalewski, H. G. Rammensee, S. Stevanovic, M. H. M. Heemskerk, S. H. van der Burg and T. van Hall (2018). "Identification of non-mutated neoantigens presented by TAP-deficient tumors." J Exp Med 215(9): 2325-2337.

8. **K. A, Marijt**, E. M. Doorduijn and T. van Hall (2018). "TEIPP antigens for T-cell based immunotherapy of immune-edited HLA class I(low) cancers." Mol Immunol. pii: S0161-5890(18)30108-1. doi: 10.1016/j.molimm.2018.03.029.

9. Doorduijn, E. M., M. Sluijter, **K. A. Marijt**, B. J. Querido, S. H. van der Burg and T. van Hall (2018). "T cells specific for a TAP-independent self-peptide remain naive in tumor-bearing mice and are fully exploitable for therapy." Oncoimmunology 7(3): e1382793.

10. Kleinovink, J. W., **K. A. Marijt**, M. J. A. Schoonderwoerd, T. van Hall, F. Ossendorp and M. F. Fransen (2017). "PD-L1 expression on malignant cells is no prerequisite for checkpoint therapy." Oncoimmunology 6(4): e1294299.

11. Peterson, T. E., N. D. Kirkpatrick, Y. Huang, C. T. Farrar, **K. A. Marijt**, J. Kloepper, M. Datta, Z. Amoozgar, G. Seano, K. Jung, W. S. Kamoun, T. Vardam, M. Snuderl, J. Goveia, S. Chatterjee, A. Batista, A. Muzikansky, C. C. Leow, L. Xu, T. T. Batchelor, D. G. Duda, D. Fukumura and R. K. Jain (2016). "Dual inhibition of Ang-2 and VEGF receptors normalizes tumor vasculature and prolongs survival in glioblastoma by altering macrophages." Proc Natl Acad Sci U S A 113(16): 4470-4475.

12. Kroon, J., M. Puhr, J. T. Buijs, G. van der Horst, D. M. Hemmer, **K. A. Marijt**, M. S. Hwang, M. Masood, S. Grimm, G. Storm, J. M. Metselaar, O. C. Meijer, Z. Culig and G. van der Pluijm (2016). "Glucocorticoid receptor antagonism reverts docetaxel resistance in human prostate cancer." Endocr Relat Cancer 23(1): 35-45.

13. E. Yusuf, **K.A. Marijt**, G.J.V.M. van Osch, A. Zuurmond, V. Stoianovic-Susulic, R.E.M. Toes, M. Kloppenburg, A. Ioan-Facsinay (2011). "Immunological characterisation of hoffa's fat pad in osteoarthritis". Annals of the Rheumatic Diseases 2010;69:A48.